



ITQB NOVA

NOVA
NOVA SCHOOL OF
SCIENCE & TECHNOLOGY

NOVA
MEDICAL
SCHOOL

NOVA
UNIVERSIDADE NOVA
DE LISBOA

Ana Rita da Silva Bragança

Degree in Marine Biology and Biotechnology

**Microalgae for the Production of High-Value Compounds:
Evaluation of the Effect of Different Nitrogen and Carbon
Sources on the Production of Fucoxanthin in
*Phaeodactylum tricornutum***

Dissertation presented to obtain the Master's Degree in
Biochemistry for Health

Supervisor: Rita Sobral Moutinho Abranches, ITQB NOVA

July 2021



ITQB NOVA



Ana Rita da Silva Bragança

Degree in Marine Biology and Biotechnology

**Microalgae for the Production of High-Value Compounds:
Evaluation of the Effect of Different Nitrogen and Carbon
Sources on the Production of Fucoxanthin in
*Phaeodactylum tricornutum***

Dissertation presented to obtain the Master's Degree in
Biochemistry for Health

Supervisor: Rita Sobral Moutinho Abranches, Principal Investigator, ITQB NOVA

Advisor: Clélia Paulete Correia Neves Afonso, Professor, ESTM IPL

Júri:

Presidente: Doutor Pedro Manuel Henriques Marques Matias

Arguente: Doutor Francisco Xavier Inês Nascimento

Vogal: (a preencher)

**Instituto de Tecnologia Química e Biológica António Xavier
Universidade Nova de Lisboa**

July 2021

COPYRIGHT

Instituto de Tecnologia Química e Biológica António Xavier and Universidade Nova de Lisboa have the right, perpetual and with no geographic limits, to archive and publish this dissertation in printed copies reproduced in paper or digitally, or by any other known mean that may be invented, to disseminate it through scientific repositories and to admit its copy and distribution for educational or research, non-commercial purposes, as long as credit is given to the author and editor.

Ana Rita da Silva Bragança

Instituto de Tecnologia Química e Biológica António Xavier (ITQB NOVA)

Universidade Nova de Lisboa (UNL)

Esta dissertação é dedicada à minha família, que sempre lutaram para a educação se tornasse um dos maiores pilares da minha vida, que sempre acreditaram e nunca desistiram.
Que um dia possa retribuir tudo o que fizeram por mim.

ACKNOWLEDGMENTS

Desde já queria agradecer à minha orientadora Dr^a Rita Abranches, pela oportunidade, dedicação e apoio durante o tempo que fiz parte deste projeto. Foi um dos maiores desafios da minha vida e, claramente, sem a sua ajuda nada disto seria possível. Foi realmente uma honra enorme trabalhar no seu laboratório, dando oportunidade para estudar duas áreas que me fascinam: a biologia marinha e a saúde. Prezo a Dr^a Rita pela forma rigorosa, mas compreensiva como lida com as situações que foram decorrendo durante este tempo no laboratório. Por todas as oportunidades e ensinamentos, agradeço, do fundo do coração!

Também este projeto não seria possível sem a ajuda indispensável da Dr^a Clélia Afonso. Desde a licenciatura que a conheço e sempre a admirei, como pessoa, mas também como profissional. Transmitiu-me bases de biologia marinha importantíssimas para desenvolver este trabalho, mas também me motivou a seguir este caminho, dando-me a conhecer as áreas por explorar da biotecnologia. Foi uma honra enorme poder trabalhar consigo e poder crescer, tanto pessoal como profissionalmente. Não são as coisas boas que marcam a nossa vida, são as pessoas. E sem dúvida que a Dr^a Clélia foi uma delas, obrigada!

Quero agradecer também a todos os colegas do laboratório PCB. Todos deram um contributo importante para que este projeto fosse possível. À Bárbara, que sempre me orientou e ensinou durante o meu percurso neste projeto. Ajudou-me, não só a ter confiança a trabalhar no laboratório, mas também a estruturar um pensamento lógico sobre as adversidades que surgem nas experiências e tentar procurar o “porquê” dos resultados. À Tânia, que me ensinou a trabalhar a área da biologia molecular. Que se dedicou a ajudar-me a encontrar novas respostas para os problemas que estavam a acontecer. A admiração e o respeito são duas palavras talvez simples demais para demonstrar aquilo que o seu apoio representou para mim. Ao André, que sempre trocou ideias e sugestões para que este projeto corresse da melhor forma. Que se dedicou a ensinar-me algumas técnicas importantes para o meu futuro e sempre questionou diferentes abordagens de modo a seguir caminhos que levassem a um bom porto. À Francesca que me ajudou quando entrei para o laboratório e me “mostrou a casa” onde iria trabalhar por um ano e meio. Foi, certamente, uma honra trabalhar ao lado de pessoas tão dotadas, que dedicaram o seu tempo de trabalho para me ensinar algumas das muitas coisas que sabem e, a todos, o meu obrigada!

Não podia também deixar de agradecer a todos os técnicos de laboratório que me ajudaram neste projeto. À Cristina Leitão, Teresa Silva, entre muitos outros. Admiro aquilo que fazem e reconheço o valor do vosso trabalho. Agradecer também ao Daniel Pais, que sempre mostrou disponibilidade em me ajudar com o software Modde, que usei no meu trabalho. E a muitos outros investigadores que de uma maneira ou outra deram conselhos e prestaram apoio em tarefas de laboratório, tanto com material como com conhecimento. O meu enorme obrigada a todos!

Por último, gostaria de agradecer à minha família, que sempre lutaram para construir um futuro melhor, sem vocês esta jornada não seria possível. O poder da amizade é algo inexplicável e comigo trago aqueles que nunca duvidaram que eu fosse conseguir atingir este objetivo. Aos meus amigos de infância (Renata, Mauro, Franco, Cristiana, Pinheiro, Susana, Carlos, Ferreira), às minhas amigas da licenciatura (Clara, Patrícia, Rita), aos meus amigos do mestrado (Salomé, Gonçalo, Tiago, Oksana, Inês) e a muitos outros, o meu sincero e profundo obrigada!

Abstract

Phaeodactylum tricornutum is a model diatom used in studies of growth and production of photosynthetic pigments, with the particularity of its great capacity to produce fucoxanthin. Fucoxanthin is a high-value pigment with applications in the food, cosmetic and pharmaceutical industries, revealing in pre-clinical studies, antioxidant, anti-obesity, and anti-cancer activity. This xanthophyllous pigment plays an important role in microalgae, as its production occurs in response to abiotic stresses, allowing the cell to survive under less favourable conditions. Thus, it is possible to optimize the production of fucoxanthin by changing the growth conditions, in particular the composition of the culture medium.

In this thesis, changes in the culture medium composition were studied, through the modification of nitrogen and carbon sources in various concentrations. The results indicated that the conditions that most favoured the growth and production of fucoxanthin were achieved by increasing sodium nitrate by a factor of 10 to the f/2 medium supplemented with silica, which is used for maintenance of the diatoms growth. The increase in the concentration of sodium nitrate allowed to double the fucoxanthin production, in just 7 days of growth. Cell viability and behaviour under different light conditions were also investigated. Additionally, genetic expression studies were performed to evaluate the possible influence of N sources on the expression of target genes of the fucoxanthin synthesis pathway.

These results pave the way for further investigation on the mechanism of nitrogen regulation in the fucoxanthin synthesis pathway in microalgae, as well as introducing new data on the strategy for optimizing the production of photosynthetic pigments, with a view to large-scale production for use of these pigments in the health industry.

Keywords: *Phaeodactylum tricornutum*, Carotenoid Biosynthetic Pathway, Fucoxanthin, Nitrogen Sources, Photoperiod Cycle, Cell Viability

Resumo

Phaeodactylum tricornutum é uma diatomácea modelo usada em estudos de crescimento e produção de pigmentos fotossintéticos, tendo como particularidade a sua grande capacidade de produzir fucoxantina. A fucoxantina é um pigmento de alto valor com aplicações na indústria alimentar, cosmética e farmacêutica, tendo revelado em estudos pré-clínicos, atividade antioxidante, anti-obesidade e anticancerígena. Este pigmento xantófilo representa nas microalgas um papel importante, uma vez que a sua produção ocorre em resposta a stresses abióticos, permitindo a sobrevivência da célula em condições menos favoráveis. Assim, é possível a otimização da produção da fucoxantina através da alteração das condições de crescimento, em particular a constituição do meio de cultura.

Nesta tese foram estudadas alterações do meio através da modificação de fontes de azoto e carbono, em ensaios com diferentes concentrações. Os resultados indicaram que as condições que mais favorecem o crescimento e produção de fucoxantina foram alcançadas através da adição de nitrato de sódio num fator de 10 ao meio f/2 suplementado com sílica, usado para manutenção do crescimento de diatomáceas. O incremento da concentração de nitrato de sódio, permitiu produzir duas vezes mais fucoxantina em apenas 7 dias de crescimento. Testes de viabilidade e comportamento em diferentes condições de luz foram avaliados. Adicionalmente, estudos de expressão genética foram realizados para avaliar a possível influência das fontes de azoto na expressão de genes-alvo na via de síntese da fucoxantina.

Estes resultados abrem caminho para uma investigação mais aprofundada sobre o mecanismo de regulação do azoto na via de síntese da fucoxantina em microalgas, assim como introduz novos dados sobre a estratégia de otimização da produção de pigmentos fotossintéticos, tendo em vista uma produção em larga escala para utilização destes pigmentos na indústria da saúde.

Termos-chave: *Phaeodactylum tricornutum*, Via Biossintética de Carotenóides, Fucoxantina, Fontes de Azoto, Ciclo de Fotoperíodo, Viabilidade Celular

INDEX

1. INTRODUCTION.....	1
1.1. IMPORTANCE OF MICROALGAE AND THEIR COMPOUNDS IN HEALTH CARE ...	1
1.2. <i>Phaeodactylum tricornutum</i>	2
1.2.1. Morphology	3
1.2.2. Life Cycle.....	4
1.3. CAROTENOIDS.....	5
1.3.1. Legislation.....	6
1.3.2. Natural vs. Synthetic Carotenoids	7
1.3.3. Carotenoid synthesis pathways in microalgae.....	8
1.3.4. Fucoxanthin.....	10
1.3.4.1. Health Benefits of Fucoxanthin.....	11
1.3.4.2. Authorized Use of Fucoxanthin Rich Supplements	13
1.3.4.3. Regulation of Fucoxanthin Production: <i>PSY</i> and <i>LCYB</i> Genes.....	14
1.4. INFLUENCE OF ABIOTIC FACTORS ON CAROTENOID PRODUCTION	16
1.4.1. Cultivation System: Small scale vs. Industrial Scale	16
1.4.2. Culture Media.....	17
1.4.2.1. Nitrogen Source: Sodium Nitrate, Urea and Ammonia.....	17
1.4.2.2. Carbon Sources: Glycerol and Glucose.....	18
1.5. LIGHT.....	19
1.5.1. Light Intensity	19
1.5.2. Light Quality	19
1.5.3. Light/Dark Cycle.....	20
1.6. OBJETIVES	22
2. MATERIALS AND METHODS	23
2.1. Culture Conditions of <i>Phaeodactylum tricornutum</i>	23
2.1.1. Culture Characterization.....	23
2.1.2. <i>P. tricornutum</i> Growth Curve.....	23
2.1.2.1. Optical Density Reading at 595 nm.....	24
2.1.2.2. Cell Counting	24
2.1.2.3. Optical Density Reading at 750 nm.....	24
2.2. Modifications to the basal culture conditions.....	25
2.2.1. Screening of Carbon and Nitrogen sources: 6-well plate assay	25
2.2.2. Nitrogen Source: Scale-up to 50 mL of culture.....	27
2.3. Analysis of Photosynthetic Pigments	27
2.3.1. Extraction of fucoxanthin for chromatographic analysis	27

2.3.2.	Analysis of ethanolic extract by Thin Layer Chromatography (TLC)	28
2.3.3.	Quantification of fucoxanthin by High Pressure Liquid Chromatography (HPLC).....	28
2.3.4.	Relative Quantification of Fucoxanthin	28
2.3.4.1.	Correlation Cuvette vs. Microplate	29
2.3.4.2.	Extraction of fucoxanthin for formula application	30
2.4.	Bioinformatic Analyses	30
2.4.1.	Prediction Models for Medium Optimization – Modde® 12.1	30
2.4.2.	Statistical Analyses: Student’s t-test and Mann-Whitney’s test	31
2.5.	Light/Dark Photoperiod Assay	31
2.6.	Gene Expression Analysis	32
2.6.1.	Primer Design - Exon-Exon Junction Method	32
2.6.2.	Annealing Temperature Test	33
2.6.3.	DNA Extraction.....	34
2.6.4.	RNA Extraction.....	34
2.6.5.	RNA Precipitation	34
2.6.6.	Standard Polymerase Chain Reaction (PCR)	35
2.6.7.	cDNA Synthesis	35
2.7.	Semi-Quantitative Reverse Transcriptase Polymerase Chain Reaction (sqRT-PCR)	35
2.8.	Cell viability test	36
3.	RESULTS AND DISCUSSION	37
3.1.	Analysis of the ethanolic extract from <i>Phaeodactylum tricornutum</i>	37
3.2.	Screening of Carbon and Nitrogen Sources for Optimization of Growth and Fucoxanthin Production	40
3.2.1.	Nitrogen (N) Sources: Sodium Nitrate, Ammonium Chloride and Urea	40
3.2.2.	Carbon (C) Sources: Glucose and Glycerol	43
3.2.3.	Fucoxanthin Production	45
3.3.	Prediction of the interaction between N and C sources by “Design of Experiments” (DoE)	46
3.4.	Scale-up of the cultures supplemented with N source.....	50
3.4.1.	From N-free cultures to 10-fold NaNO ₃ supplementation	50
3.4.1.1.	Growth Curve	50
3.4.1.2.	Fucoxanthin Production.....	51
3.4.2.	From Basal to 40-fold NaNO ₃ Supplementation.....	52
3.4.2.1.	Cell Growth	53
3.4.2.2.	Fucoxanthin Production.....	55
3.5.	Ligh Assay.....	58
3.5.1.	Light/Dark Photoperiod Cycle	58
3.6.	Gene Expression Analysis.....	60
3.7.	Cell viability of the <i>P. tricornutum</i> culture	65

4.	CONCLUSIONS	68
5.	REFERENCES	70
6.	APPENDIX	76

FIGURE INDEX

Figure 1.1. Cell structure of the diatom <i>Phaeodactylum tricornerutum</i>	3
Figure 1.2. Cell morphologies from <i>Phaeodactylum tricornerutum</i>	4
Figure 1.3. MEP pathway.....	8
Figure 1.4. Hypothetical Carotenoid Biosynthetic Pathway.....	10
Figure 1.5. <i>all trans</i> -Fucoxanthin molecular structure.....	11
Figure 3.1. (A) Thin Layer Chromatography. (B) High Pressure Liquid Chromatography spectrum of the ethanol extract of <i>P. tricornerutum</i> (bottom) and absorption profile (top).....	38
Figure 3.2. HPLC spectra and respective absorption peak profiles of commercial standards.....	38
Figure 3.3. Growth curves for 7 days of growth, of the concentration range for each of the nitrogen sources.....	41
Figure 3.4. Microplates with cultures supplemented with sodium nitrate (A) and ammonium chloride (B), on the 7 th day of growth.....	42
Figure 3.5. Microplate with control cultures f/2+Si without N or C, on the 7 th day of growth.....	43
Figure 3.6. Microplates with cultures supplemented with urea, with a white background (A) and with a dark background (B), on the 7 th day of growth.....	43
Figure 3.7. Growth curves followed for 7 days, of the concentration range for each of the carbon sources.....	44
Figure 3.8. Microplates with cultures supplemented with glycerol (A) and glucose (B), on the 7 th day of growth.....	44
Figure 3.9. Fucoxanthin concentration for the range of concentrations in different sources of nitrogen and carbon, analysed by HPLC, on the 7 th day of the curve.....	45
Figure 3.10. The prediction plots of “Design of Experiment”.....	47
Figure 3.11. Response contour plots of factors interaction, showing effect of Optical Density ($\lambda = 595$ nm) and Fucoxanthin (mg/L).....	49
Figure 3.12. Growth curves of the 50 mL cultures supplemented with various concentrations of Sodium Nitrate.....	50
Figure 3.13. 50 mL culture flasks supplemented with various concentrations of Sodium Nitrate, on the 7 th day of growth.....	51
Figure 3.14. Fucoxanthin concentration of the cultures supplemented with f/2+Si medium modified with different concentrations of Sodium Nitrate, on 7 th day of growth.....	52
Figure 3.15. Growth curves of <i>P. tricornerutum</i> cultures supplemented with 0.882 (1-fold), 8.82 (10-fold), 17.64 (20-fold) and 35.28 (40-fold) mM of NaNO ₃	53
Figure 3.16. 50 mL cultures supplemented with 1, 10, 20 and 40-fold NaNO ₃ , on the day of inoculation (day 0), and on the 3 rd and 5 th day after the start of growth.....	55
Figure 3.17. Correlation between OD readings in cuvette (spectrophotometer) and in 96-well plate (Microplate Reader).....	56
Figure 3.18. Average fucoxanthin concentration in cultures supplemented with 0.882 (1-fold), 8.82 (10-fold), 17.64 (20-fold) and 35.28 mM (40-fold) of NaNO ₃	58
Figure 3.19. Variation of fucoxanthin concentration over the day/night cycle.....	59

Figure 3.20. 1.2% agarose gels from the reference genes with 25, 26 and 28 cycles. (A) <i>TATA Box Protein (TBP)</i> and (B) <i>Cyclin Dependent Kinase A (CDKA)</i>	62
Figure 3.21. 1.2% agarose gels from the target genes with 23 and 25 cycles. (A) <i>Phytoene Synthase (PSY)</i> and (B) <i>Lycopene β-cyclase (LCYB)</i>	63
Figure 3.22. Microscopic images at the 7 th day of growth, for <i>P. tricornutum</i> cultures supplemented with 0.882 mM (A), 8.82 mM (B), 17.64 mM (C) and 35.28 mM (D) of NaNO ₃	65
Figure 3.23. Microscopic images of cell aggregates at the 7 th day of growth, of <i>P. tricornutum</i> cultures supplemented with 35.28 mM of NaNO ₃	66

TABLE INDEX

Table 2.1. Composition of the 24 media prepared for screening on 6-well microplates from different sources of nitrogen (N) and carbon (C).....	26
Table 2.2. Primer sequences, annealing temperature, size of the amplicon and identification code for each gene on the NCBI database.	33
Table 3.1. Absorbance values of the media used with the various concentrations of NaNO ₃ , at wavelengths of 445, 663 and 750 nm.....	56
Table 6.1. Reaction Constituents of the GoTaq Flexi DNA Polymerase (M7805, Promega, USA)....	80
Table 6.2. Reaction Constituents of the ImProm II Reverse Transcriptase System (Promega, USA)..	80

Abbreviations and Acronyms

ASAE - Food and Economic Security Authority	LL - Low Light
BL - Blue Light (BL)	<i>LCYB</i> - Lycopene β -cyclase
CCAP - Culture Collection of Algae and Protozoa	<i>LCYE</i> - Lycopene ϵ -cyclase
C - Carbon	Mb – megabases
CDKA - Cyclin-Dependent Kinase A	MEP - methylerythritol 4-phosphate
CDS - Coding Sequence	mg – milligram
cDNA – complementary Deoxyribonucleic Acid	mL - millilitre
DNA - Deoxyribonucleic Acid	mm - millimetres
DHA - Docosahexaenoic Acid	N - Nitrogen
DMSO - Dimethylsulfoxide	NDIN - New Dietary Ingredient Notification
DOXP - 1-deoxy-D-xylulose 5-phosphate	nm - nanometres
DXS - 1-deoxy-D-xylulose 5-phosphate synthase	OD – Optical Density
DMAPP - Dimethylallyl Diphosphate	PDA - Photo Diode Array
DoE – Design of Experiments	<i>PSY</i> - phytoene synthase
e.g. - example	RL - Red Light
EFSA - European Food Safety Authority	RNA - ribonucleic acid
EC - European Commission	rpm – rotation per minute
EGT - Endosymbiotic Gene Transfer	ROS - reactive oxygen species
FDA - Food and Drug Administration	sqRT-PCR – semiquantitative Reverse Transcriptase – Polymerase Chain Reaction
g - gram	TBE - Tris-Borate-Ethylenediamine tetra acetic acid
G3P - Glyceraldehyde 3-Phosphate	TBP - TATA Binding Protein
GGPP - Geranylgeranyl Diphosphate	TLC – Thin Layer Chromatography
GL - Green Light (GL)	U.S. - United States
gDNA – genomic Deoxyribonucleic Acid	USA – United States of America
HL - high light intensity	UV - ultraviolet
HPLC – High Pressure Liquid Chromatography	VDE – Violaxanthin deepoxidase
IPP - Isopentenyl Diphosphate	ZEP - zeaxanthin epoxidase
Kg – kilograms	μ m – micromolar
LED – Light Emitting Diode	

Chemical Formulas

NO_3^- - Nitrate

NO_2^- - Nitrite

NH_4^+ - Ammonia

$\text{NaH}_2\text{PO}_4 \cdot 2\text{H}_2\text{O}$ - Monobasic Sodium Phosphate

$\text{Na}_2\text{SiO}_3 \cdot 9\text{H}_2\text{O}$ - Sodium Metasilicate

Na_2EDTA – Ethylenediaminetetraacetic acid disodium salt dihydrate

$\text{FeCl}_2 \cdot 6\text{H}_2\text{O}$ – Iron (III) chloride hexahydrate

$\text{CuSO}_4 \cdot 5\text{H}_2\text{O}$ – Copper(II) sulfate pentahydrate

$\text{ZnSO}_4 \cdot 7\text{H}_2\text{O}$ – Zinc sulfate heptahydrate

$\text{CoCl}_2 \cdot 6\text{H}_2\text{O}$ – Cobalt(II) chloride hexahydrate

$\text{MnCl}_2 \cdot 4\text{H}_2\text{O}$ – Manganese(II) chloride tetrahydrate

$\text{Na}_2\text{MoO}_4 \cdot 2\text{H}_2\text{O}$ – Sodium molybdate dihydrate

NaNO_3 - Sodium Nitrate

NH_4Cl - Ammonium Chloride

$\text{CH}_4\text{N}_2\text{O}$ - Urea

$\text{C}_6\text{H}_{12}\text{O}_6$ - Glucose

$\text{C}_3\text{H}_8\text{O}_3$ - Glycerol

Si – Silica

EtOH – Ethanol

1. INTRODUCTION

1.1. IMPORTANCE OF MICROALGAE AND THEIR COMPOUNDS IN HEALTH CARE

Microalgae are phytoplanktonic organisms, predominantly aquatic. From an evolutionary point of view, microalgae occupy two major domains, Eukaryota and Bacteria, including cyanobacteria, green, red, brown and dinoflagellate microalgae (Bowler & Falciatore, 2019). There are more than 41,000 described species and they are characterized by their morphology and production of compounds, such as photosynthetic pigments or lipids (reviewed in Marques, *et al.* 2013; Alam, *et al.* 2020).

Microalgae have several advantages compared to macroalgae. For example, many studies carried out show the potential of microalgae as a source of fucoxanthin production, as they demonstrate that the production of this pigment is much higher in microalgae than macroalgae. In macroalgae, the concentration of this pigment can reach values between 0.02 to 0.58 mg/g in fresh weight and 0.01 to 1.01 mg/g in dry weight. In contrast, in microalgae, it is possible to reach values between 2.24 to 18.23 mg/g in dry weight (reviewed in Xia, *et al.* 2013).

Other advantages are the high growth rate of microalgae, when compared to plants, since these microorganisms can grow much faster and have a high biomass production in a few days, unlike plants that can take several months or years (De Martino, *et al.* 2007; Koyande, *et al.* 2019). Another benefit is the low/cheap nutritional requirements (salt water and some basic nutrients), when compared to animal cell cultures that require expensive complex media and equipment suitable for cultivation under specific controlled conditions (De Martino, *et al.* 2007). Besides that, these microorganisms grow easily in solid or liquid cultures, and since they can grow in closed bioreactors under sterile conditions, they will be able to produce recombinant products or bioactive compounds of interest under controlled and required conditions according to the standards of good manufacturing practices (GMP) (Koyande, *et al.* 2019).

Due to the production of bioactive compounds, such as pigments and proteins, microalgae have been explored for their applicability to human health (reviewed in Marques, *et al.* 2013; Novoveská, *et al.* 2019; Alam, *et al.* 2020). For several centuries, traditional medicine has included nutraceuticals and natural supplements in diets, especially since many populations have a daily life characterized by excessive consumption of fats and high calorie foods. This lifestyle entails several health problems such as obesity, high blood pressure, diabetes, among others (Lane, *et al.* 2021). Faced with this problematic public health issue, multiple studies have shown the beneficial effects of consuming substances produced by microalgae, such as improving the immune system, pre- and probiotic effects, reducing viral infections and sugar levels (reviewed in Novoveská, *et al.* 2019).

The introduction of photosynthetic pigments in the food and pharmaceutical market has seen a huge increase. Initially, these pigments were introduced as food additives in aquaculture and due to their anti-inflammatory, antioxidant, and anticancer activity in the fish, they have been recommended to be tested

as additives for human health (reviewed in Pangestuti & Kim, 2011; Begum, *et al.* 2016; Chakdar & Pabbi, 2017).

For the large-scale production of these natural pigments and due to the high demand of these compounds on the market, model microalgae are being used (*Dunnaliella*, *Chlamydomonas*, among others.), however diatoms have shown to be a promising organism due to their evolutionary characteristics and ease of growth and transformation in the laboratory context (reviewed in Pulz & Gross, 2004).

1.2. *Phaeodactylum tricornutum*

Diatoms are unicellular phytoplanktonic organisms that belong to the eukaryotic domain, Class Bacillariophyceae (Bowler & Falciatore, 2019). This group of microalgae arose from a secondary endosymbiosis where, in a primary endosymbiosis, a cyanobacterium and a phagotrophic eukaryote united, giving rise to a red alga. Phagocytosis of this red alga by a eukaryote allowed the emergence of diatoms, initiating a new lineage known as Chromalveolata, which includes haptophytes, brown algae and dinoflagellates (Cavalier-Smith, 2003).

There are several organisms that belong to this kingdom, however *Phaeodactylum tricornutum* is one of the species that has been most used as a model organism to understand the biology of diatoms (reviewed in De Martino, *et al.* 2007).

Phaeodactylum tricornutum is a diatom that belongs to the Chromalveolata kingdom, superphylum Heterokonta, phylum Bacillariophyta, class Bacillariophyceae, order Naviculales and family Phaeodactylaceae. This organism was first described by Bohlin in 1897, and the most studied genotype was sequenced as CCAP1055/1, available from Culture Collection of Algae and Protozoa (CCAP) (Bowler & Falciatore, 2019). In terms of molecular biology, this diatom is used for several studies, due to its fully sequenced genome. The genome size is 27.4 Mb, with a total of 12,233 coding genes. It is a model organism due to its easy growth and genetic transformation in the laboratory, which can be done by electroporation or bombardment. The transformation of chloroplasts is also possible (Bowler & Falciatore, 2019).

Structurally, *P. tricornutum* is a simple microorganism and has a particularity, the external structure consisting of silica, called frustule (Figure 1.1.b). The frustule consists of two valves that resemble a Petri dish. This structure is composed by the hypotheca that fits into a larger valve called epitheca, which subsequently surrounds the living cell. The size of the frustule depends on the size of the cell (Francius, *et al.* 2008). Furthermore, the frustule is surrounded by extracellular polymers, mostly polysaccharides called sulphated glucomannans (Ford & Percival, 1965), which allow sessile adhesion, protection against drying and the formation of biofilms and endosymbiotic bacterial colonies (reviewed in Francius, *et al.* 2008).

Through atomic force microscopy was possibly to verify that, within the different morphologies that *Phaeodactylum* species can present, the silicified valves of the oval cells provide greater mechanical resistance than the valves of the other morphologies (reviewed in Whitmore, 2000).

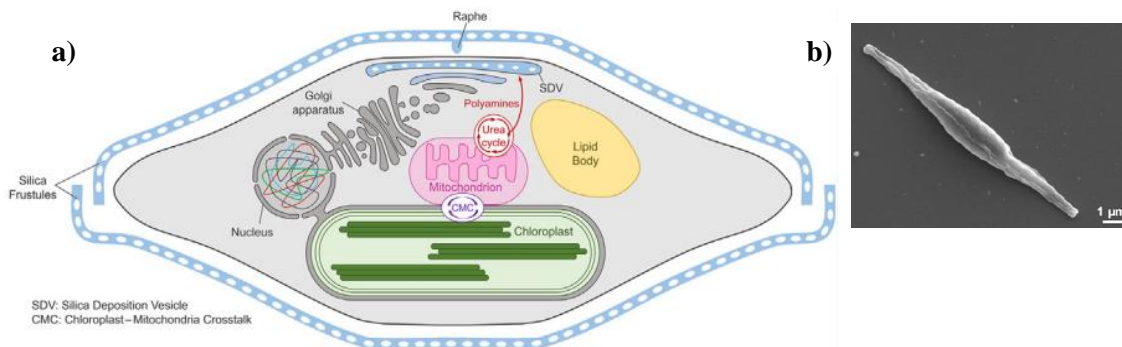


Figure 1.1. Cell structure of the diatom *Phaeodactylum tricornutum*: a) inner cell composition (Bowler & Falciatore, 2019) and b) external silica structure (Francius, *et al.* 2008)

1.2.1. Morphology

Several studies have verified over time that *P. tricornutum* is a pleiomorphic marine diatom, which implies that it has the ability to change morphology during its life cycle or when present in certain environmental conditions (De Martino, *et al.* 2011).

They may have three distinct morphologies: fusiform, triradiated or oval (Figure 1.2. a, b, c) (Bauer, *et al.* 2019). The occurrence of each of the morphologies is not yet fully known, however studies suggest that the morphogenesis in *P. tricornutum* is not genotype dependent but induced by environmental factors (He, *et al.* 2014).

It was found that fusiform morphology is more common throughout the world, however the triradiated morphology appears preferentially associated with alkaline environments. On the other hand, there is an increase in the occurrence of the oval shape in unfavourable conditions, of low salinity, temperature, or light, among others (Whitmore, 2000; He, *et al.* 2014). Furthermore, this oval shape demonstrated a greater ability to survive under conditions of nutritional deficiency, suggesting that this morphology may confer resistance to abiotic stress (reviewed in Tesson, *et al.* 2009).

In view of the commercial interest, the fusiform morphology tends to be the most advantageous since it shows a higher growth rate (1.4 greater) as compared with the oval and triradiate morphologies (Desbois, *et al.* 2010) and greater antibacterial activity (approximately 2-fold more) when compared to oval cells (Song, *et al.* 2020).

There is also a fourth morphology, called cruciform but its occurrence is considered extremely rare (Figure 1.2. d.). According to Bauer and his collaborators (2019), this morphology is able to transform into an oval shape by the degeneration of the arms that compose it. According to this study, the low temperature appears to have a beneficial role in the formation of the cruciform cell when there is a drop

from 25 °C to 10 °C. In addition to this rare typology, this form is characteristic for having a unique fatty acid composition and is, therefore, preferred morphology, when the goal is to produce biodiesel (Bauer, *et al.* 2019).

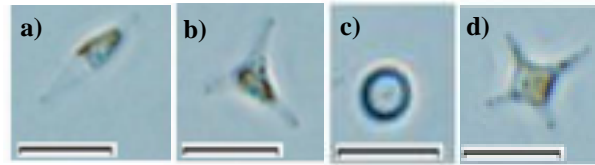


Figure 1.2. Cell morphologies from *Phaeodactylum tricornutum*: a) Fusiform, b) Triradiate, c) Oval and d) Cruciform. Scale bar = 10 μ m. Adapted from He, *et al.* (2014).

1.2.2. Life Cycle

P. tricornutum can have two lifestyles, planktonic and benthic. Given the physical and chemical characteristics of both lifestyles, *P. tricornutum* tends to adapt the fusiform and triradiated morphology in planktonic mode, and the oval type in the benthonic, since the latter has greater sedimentation capacity (De Martino, *et al.* 2011). In addition to this ability, the oval cell is also capable of secreting exopolymeric substances that support cell adhesion (De Martino, *et al.* 2011; Tesson, *et al.* 2009).

These unicellular microalgae reproduce via asexual mitotic division, and, to date, there is no evidence to prove that *P. tricornutum* undergoes sexual reproduction (Bowler & Falciatore, 2019; Borowitzka, 2018).

Studies developed by De Martino and co-workers (2011), demonstrated that during the lifecycle, *P. tricornutum* can present different morphologies considering the culture conditions. It was observed that the fusiform and triradiated forms occur during the exponential phase when the cultures are under agitation, optimal salinity level, and a temperature of approximately 19 °C. On the other hand, both morphologies can be converted directly or indirectly into oval forms, in response to low salinity and low temperatures. The same study also found the existence of dormancy cells formed as a consequence of changes in these last two abiotic factors. The authors identified these cells as “round cells”, which have several similarities with a “resting stage”, such as thicker cell walls or chloroplast disorganization (De Martino, *et al.* 2011).

However, it is possible to reverse all conditions except from fusiform to triradiate. The conversion from triradiate or fusiform to oval and, vice-versa, occurs by division or elongation, respectively (De Martino, *et al.* 2011). Although it appears that the existence of these “round cells” may be related with unfavourable growth conditions (Desbois, *et al.* 2010), only a few studies have shown effects when the temperature and salinity are changed, with no evidence for the formation of these aggregates in other abiotic conditions, such as pH or nutrients (Tesson, *et al.* 2009).

1.3. CAROTENOIDS

The macroalgae pigments have already been marketed, however, the biomass and pigments production systems of these organisms is still not profitable. Due to the advance of knowledge about diatoms, these organisms have been studied with the purpose to introduce their produced pigments, in the food industry, as supplements in human diets. In aquaculture, these microorganisms are used as feed additives for fish and molluscs in larval state. In the environmental level, diatoms are used for bioremediation of contaminated water and production of biofuels. Besides that, in the pharmaceutical industry, due to the various bioactive compounds produced, they have been thoroughly studied, since they have many beneficial health effects (reviewed in Marques, *et al.* 2013). Within the compounds produced by diatoms, especially by *P. tricornutum*, the pigments are the group of bioactive compounds that have shown promising results in health care, mainly the carotenoids (Bowler & Falciatore, 2019).

Carotenoids are photosynthetic pigments derived from tetraterpenes, consisting of eight isoprene units (C₅) comprising a 40-carbon structure. These compounds can be divided into two categories: xanthophylls that contain oxygen (e.g. astaxanthin and zeaxanthin) and carotenes that are pure oxygen-free hydrocarbons (e.g. beta-carotene and lycopene) (Mikami & Hosokawa, 2013).

These pigments, that occur in nature, are all-*trans* isomers, however *cis* isomers may occur as by-products resulting from abiotic factors, such as high temperatures and exposure to light. However, they do not have the same biological properties as the *trans* isomer (Britton, *et al.* 2016).

Although they are rigid molecules, carotenoid end groups may exhibit flexibility. These slight differences in molecular structures allow the biological function of these pigments to vary. The weight, the shape of the molecule and the functional groups are factors that determine their solubility and therefore the ability of the carotenoids to interact with other cell components (Britton, *et al.* 2016).

Carotenoids are fat-soluble pigments (hydrophobic) that absorb light at a wavelength between 400 and 550 nm, responsible for the yellow, orange, and red colours of various fruits and vegetables. The colour spectrum depends on the number of conjugated double hydrogen bonds. These pigments can only be obtained through food and cannot be synthesized by the human species, which promotes demand in the market and provides a greater need for large-scale production through biologically sustainable ways (Novoveská, *et al.* 2019; Goswami, *et al.* 2021).

For microalgal cells, carotenoids are divided into two categories: primary carotenoids, which are components of the functional and structural photosynthetic system (membranes) and are therefore essential to the cell survival (e.g. lutein); and secondary carotenoids, which are produced only when the cell is exposed to specific abiotic conditions, such as high light intensity, nutrient depletion/excess, among other factors (e.g. fucoxanthin) (Novoveská, *et al.* 2019). The latter category of carotenoids are located in lipidic vesicles in the plastid stroma or in the cytosol, however despite being synthesized in chloroplasts, they can be exported to the cytoplasm and, thus, be found throughout the cell (Gordon, *et al.* 1983).

In addition to the participation of carotenoids in photosynthesis, they also play an important role in light harvesting and photoprotection. When there is low light, the carotenoids capture the available light and transfer the energy to the chlorophyll molecules. On the contrary, when exposure to high light, carotenoids accept excessive light and dissipate it, protecting chlorophyll molecules from light damage (Novoveská, *et al.* 2019).

In human care, besides the carotenoids providing colour and nutrition to food, they also have a powerful antioxidant effect and are used to slow the oxidation process, as well as to reduce the degradation of food, acting as food preservatives. In cosmetics, carotenoids are used not only as a dye in tanning body lotions due to their naturally brown colour, but also in skin and hair care creams due to their antioxidant properties, providing protection to the skin from UV radiation damage. In the nutraceutical area, the sector is growing exponentially, as carotenoids neutralize free radicals and reduce oxidative stress in the cells. This imbalance in the normal functioning of cells can lead to disease, including degenerative pathologies. From this point of view, the antioxidant capacity of carotenoids is very important since it allows to slow down the aging process and reduces cells damage, also reducing the risk of inflammation, heart disease, cancer, type 2 diabetes, and chronic eye diseases (reviewed in Chakdar & Pabbi, 2017; Novoveská, *et al.* 2019).

1.3.1. Legislation

Between 1970 and 2003, the procedures for introducing a new natural bioactivity compound on the market were based on criteria developed by the Commission Directive 70/524/EEC (European Communities, 1970). However, in 2003, the directives were revised and published in Regulation (EC) No. 1831/2003 (EU 2003) (The European Parliament and the Council of the European Union, 2003). One of the procedures imposed in the new system is the independent safety assessment carried out by the European Food Safety Authority (EFSA), where the responsibility for approving or refusing product authorization lies with the European Commission (EC) assisted by the Standing Committee of the Food Chain and Animal Health. Authorized products can belong to three specific categories: sensory, nutritional or zootechnical additives. These products are listed in the EU Food Additives Register (EC 2016), which is regularly updated by the EC (The European Parliament and the Council of the European Union, 2003).

Carotenoids, according to this regulation mentioned above, belong to the category of "sensory additives", as a functional group of colourants that represents the substances that are added or that are used to restore colour in animal feed and all substances to which are added (e.g. bakery). When these colourants are supplied to animals, they give colour to feed of animal origin (The European Parliament and the Council of the European Union, 2003).

The introduction of carotenoids as food additives for colouring is also subject to regulation and any food containing these pigments should be labelled as a colourant and not as a nutrient (Begum, *et al.* 2016).

In Portuguese law and according to Law-Decree no. 55/2005 published in Diário da República no. 44/2005, Series I-A of 2005-03-03 emitted by Ministry of Agriculture, Fisheries and Forests, the use of mixed carotenes from plants or algae is authorized as dyes (<https://data.dre.pt/eli/dec-lei/55/2005/03/03/p/dre/pt/html>).

According to the Food and Economic Security Authority (ASAE) in Portugal, all compounds of a carotenoid nature, derived from plants, fungi, algae and cyanobacteria, belong to the dye category, being identified from E160a to f and E161b/g. (<https://www.asae.gov.pt/seguranca-alimentar/aditivos-alimentares/corantes.aspx>).

1.3.2. Natural vs. Synthetic Carotenoids

With the growing need to increase the production of carotenoids to meet the market demand, studies have been carried out to assess the best way to scale-up production. Bearing in mind that the amount of carotenoids naturally produced is relatively low, many companies have opted for the synthesis of these pigments (reviewed in Novoveská, *et al.* 2019).

Carotenoids can be synthesized faster with low-cost chemicals, without resorting to the presence of living organisms, thus avoiding the more complex extraction of the final product. Although synthesized carotenoids are faster and, generally, cheaper to produce compared to natural carotenoids, they have less health beneficial properties and are considered less valuable products, being undesirable for implementation in the food industry, leading to a greater investment in the natural production of these pigments (Novoveská, *et al.* 2019).

For example, the β -carotene pigment found in microalgae is a natural conjugation of all-*trans* and 9-*cis* isomers. On the contrary, synthetic β -carotene is only composed of all-*trans* isomers, having no beneficial health properties (Bogacz-Radomska & Harasym, 2018; Novoveská, *et al.* 2019).

In recent years, consumers have preferred the use of natural products over synthetics, due to the population's growing awareness of their health and the unwanted effects of non-natural products (reviewed in Novoveská, *et al.* 2019).

The European Union has standardized the restricted use of toxic products or additives (for example, dyes) that were obtained by chemical synthesis, in food, feed, cosmetics and nutraceuticals. In contrast to these synthetic dyes, natural carotenoids are a safe source and can be added to many products, such as juices, dairy, and bakery. Similarly, in aquaculture, these photosynthetic pigments are used to assign the desired colours to aquatic organisms through their diet, obtaining pink/red crustaceans, orange salmon, among others. In textile industry, natural dyes are used for colouring clothes, since several

people have developed, over time, allergic reactions to various colouring synthetic products (reviewed in Novoveská, *et al.* 2019).

Due to the increasing elderly population around the world, people are increasingly interested in their health and seeking to reduce the appearance of diseases related to the modern lifestyle, such as diabetes, hypertension, and obesity. To this end, a healthy diet, and the consumption of products of natural origin have shown to be the best solution to delay these problems, causing greater demand for these active principles (reviewed in Chakdar & Pabbi, 2017; Novoveská, *et al.* 2019).

1.3.3. Carotenoid synthesis pathways in microalgae

To produce carotenoids, diatoms have a very complex synthesis pathway. Initially, they use the non-mevalonate synthesis pathway for isoprenoid biosynthesis, also known as the methylerythritol 4-phosphate (MEP) plastidic pathway. MEP starts with glyceraldehyde 3-phosphate (G3P) and pyruvate from the Calvin cycle, which, when combined, give rise to 1-deoxy-D-xylulose 5-phosphate (DOXP), a reaction that is catalysed by 1-deoxy-D-xylulose 5-phosphate synthase (DXS). This enzyme and the intermediate products synthesized in the pathway, leads to the formation of isopentenyl diphosphate (IPP) and dimethylallyl diphosphate (DMAPP). After several steps, the interconversion between IPP and DMAPP giving rise to geranylgeranyl diphosphate (GGPP), also known as geranylgeranyl pyrophosphate (Figure 1.3.). Two GGPP molecules leads to the first step in the biosynthesis of carotenoids, catalysed by the enzyme phytoene synthase (*PSY*) forming a phytoene molecule (Figure 1.4.). This conversion is extremely important to obtain carotenoids since *PSY* is a limiting enzyme in this pathway. All carotenoids synthesized in the next steps with a C₄₀ structure are derived from phytoene, which make up a total of 90% of the carotenoids currently known (reviewed in Zhang, 2018; Khoroshyy, *et al.* 2018).

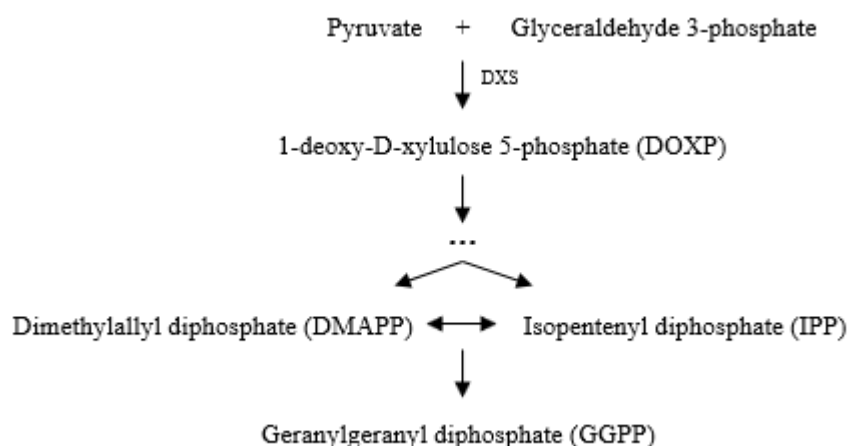


Figure 1.3. MEP pathway. Ellipsis indicates intermediate products (Adapted from Khoroshyy, *et al.* 2018)

The carotenoid biosynthesis pathway is not fully known, and many studies indicate putative pathways, considering the different compounds, the identified conversion enzymes and the different types of microalgae (brown, green and red). Different groups of microalgae produce different types of pigments. Figure 1.4. represents a hypothetical synthetic pathway to produce carotenoids in different microalgae groups (Zhang, *et al.* 2018).

As previously mentioned, carotenoids are divided into two categories: carotenes and xanthophylls. The first stage of carotenoid synthesis begins with the biosynthesis of carotenes from the phytoene molecule, which is the common precursor to all carotenoids. Within the group of carotenes, the first molecule to be converted is lycopene, produced from several dehydrogenation steps of phytoene. Therefore, lycopene is usually converted to α -carotene or β -carotene through lycopene cyclase (Lycopene ϵ -cyclase (*LCYE*) or Lycopene β -cyclase (*LCYB*)) (Khoroshyy, *et al.* 2018). When enzymatic reactions happen, such as hydroxylation or ketolation of these carotenes, xanthophyll synthesis occurs (Zhang, *et al.* 2018; Rebelo, *et al.* 2020).

In the brown box from Figure 1.4., pigments for brown microalgae, such as diatoms, are identified. They produce several common pigments with green microalgae (green box), yet the final product is mainly fucoxanthin. However, the enzymes responsible for converting of neoxanthin into fucoxanthin and diadinoxanthin are currently not known (Zhang, *et al.* 2018).

In plants, algae, fungi, and bacteria it is common to synthesize apocarotenoids, which are pigments derived from oxidation of carotenoids or other apocarotenoids through enzymatic cleavage. An example of an apocarotenoid is retinol, known as vitamin A, derived from β -carotene (Figure 1.4.) (Zhang, 2018; Khoroshyy, *et al.* 2018).

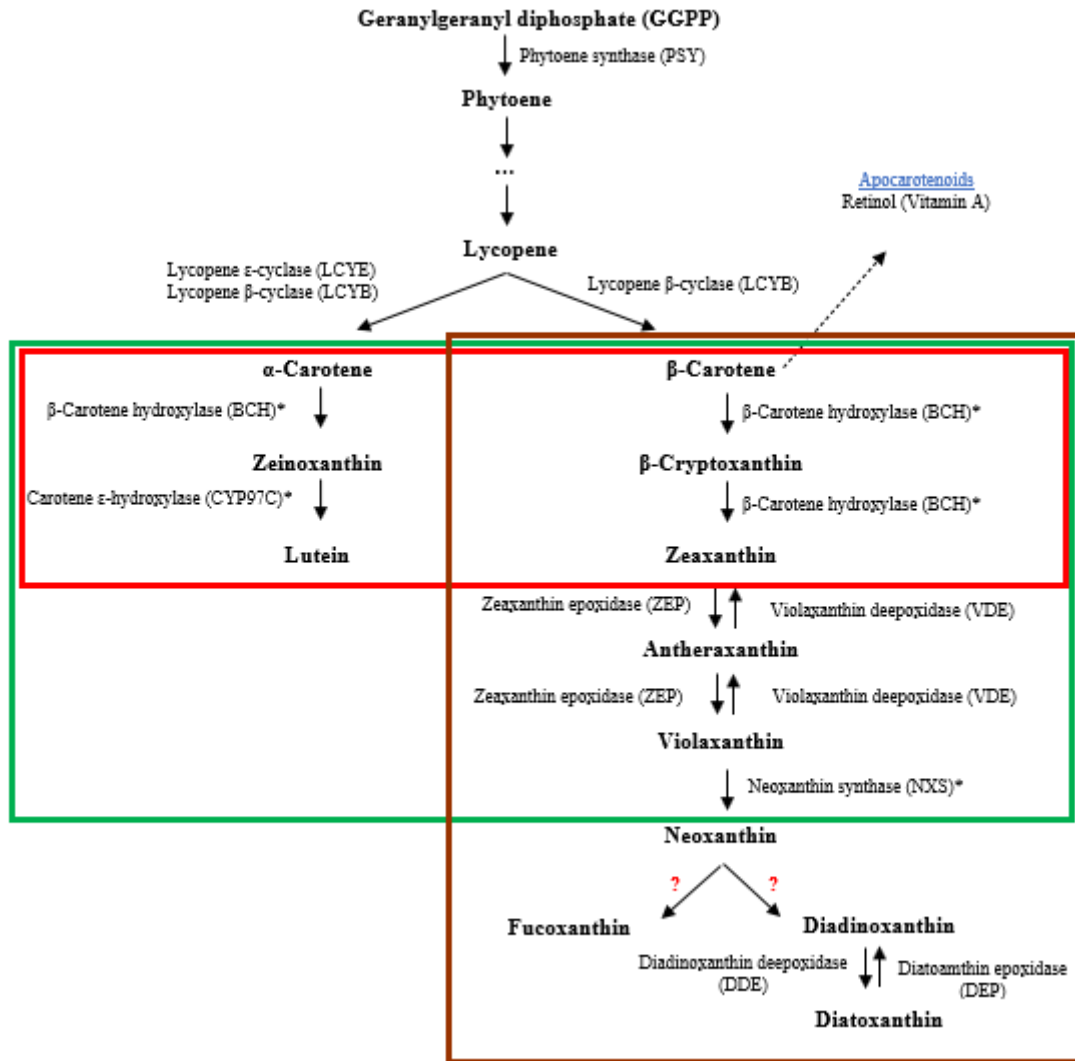


Figure 1.4. Hypothetical Carotenoid Biosynthetic Pathway. Red, green, and brown boxes indicate the pathway in red, green, and brown algae, respectively. Ellipsis indicates intermediate products. The symbol * indicates enzymes unidentified in algae. Red question marks reveal enzymes that have not yet been identified (Adapted from Zhang, *et al.* 2018).

1.3.4. Fucoxanthin

Fucoxanthin is a carotenoid pigment located in the chloroplasts on eukaryotic cells of brown macroalgae and unicellular microalgae, such as diatoms. It is responsible for the brown to yellow colours of the algae and masks the green chlorophyll *a* and *c* also produced by diatoms. This pigment was isolated from brown algae for the first time in Germany, in 1914 (Gupta, *et al.* 2017).

This pigment is a xanthophyll and shares the same physical and chemical properties with carotenes, being lipid-soluble and antioxidant. The presence of oxygen atoms in hydroxyl and epoxide group in the fucoxanthin structure allows it to be one of the most polar xanthophylls. In addition to its carbon skeleton, it is chemically structured by allelic bonds, an epoxide group and six oxygen atoms (Figure

1.5.). Due to its polar structure, industrially, it is easily extracted by organic solvents such as ethanol, methanol, DMSO, acetone, among others (reviewed in Gupta, *et al.* 2017).

In cells, fucoxanthin is stored in chloroplasts, inside membrane compartments called thylakoids. Within these organelles, fucoxanthin binds chlorophyll *a*, *c* and proteins, forming complexes that absorb light in the blue-green spectrum and transfer energy to the cell's metabolism. It is a pigment that has a wide absorption spectrum (445 and 540 nm), which increases the effectiveness of photosynthesis (Gupta, *et al.* 2017).

As previously mentioned, carotenoids can have *trans* and *cis* conformations, and fucoxanthin is no exception. However, the *trans* isomer of fucoxanthin is more chemically stable and has a greater antioxidant potential than its *cis* isomer. About 90% of fucoxanthin found in nature has a *trans* conformation, but geographic and seasonal variations may influence the content of these isomers, such as variations in salinity or light exposure (Gupta, *et al.* 2017).

In terms of legislation, fucoxanthin has few regulations. According to the European Food Safety Authority (EFSA), this pigment is considered a possible extract to be used as a food ingredient. The EFSA states that the allowed amount consumed is equivalent to 15 mg of pure fucoxanthin per day. However, to date, there is no evidence that could establish the amount needed to consume to maintain a normal body weight (Gupta, *et al.* 2017).

In the United States of America, the Food and Drug Administration (FDA) evaluates products derived by algae as a dietary supplement labelled "This product is not intended to diagnose, treat, cure or prevent any disease" (<https://www.fda.gov/consumers/consumer-updates/fda-101-dietary-supplements>). In Japan, the Ministries of Health, Labour and Welfare did not evaluate fucoxanthin as a functional or pharmaceutical food ingredient, however it is marketed as a food supplement (Gupta, *et al.* 2017). In Portugal, the regulatory authorities in the area do not present any information on the use of fucoxanthin, and the available information is for the groups of carotenes, being established as natural dyes and not food supplements (ASAE, consulted at 18/09/2020).

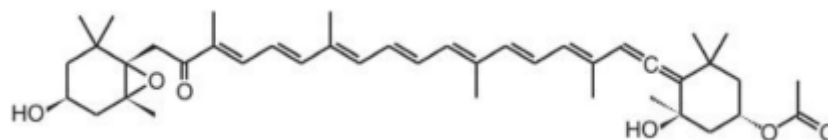


Figure 1.5. all *trans*-Fucoxanthin molecular structure (C₄₂H₅₈O₆) (Gupta, *et al.* 2017).

1.3.4.1. Health Benefits of Fucoxanthin

Although fucoxanthin was only introduced on the market as a dye or food supplement, with no apparent applicability in the health field, by regulatory authorities, this pigment has been the subject of study due to its beneficial effects on human health (Gupta, *et al.* 2017).

Clinically, fucoxanthin has been evaluated in the pharmaceutical area for its antioxidant power, since it inhibits the damage of free radicals in cells, among many other activities (reviewed in Gupta, *et al.* 2017).

In the treatment of obesity, fucoxanthin has demonstrated, in mice studies *in vivo*, an ability to mediate proteins from adipose tissue that allow the oxidation of fatty acids and heat production, reducing the white adipose tissue, which is responsible for the accumulation of fat (Gupta, *et al.* 2017).

Studies carried out in non-diabetic humans and diagnosed with obesity, allowed to check that a daily supplementation of 300 mg of brown algae extract with 2.4 mg of fucoxanthin, combined with essential oils, allowed to reduce weight on average 4.9 kg, after 16 weeks of ingestion (Abidov, *et al.* 2010). In Japan, studies have shown that the consumption of an extract with 3 % fucoxanthin, which was equivalent to 0.5-1 mg pure fucoxanthin per day, had a significant effect on blood parameters in metabolic syndromes (Oryza Oil & Fat Chemical, 2008).

For several years now, fucoxanthin has been investigated as a potential anticancer compound, however all tests developed to date have been *in vitro*, on cell lines, or *in vivo*, in mice. None of these studies have been developed in humans, so fucoxanthin activity is only hypothesized. Hosokawa and co-workers (1999) found that this pigment has the ability to induce apoptosis in human leukaemia cell lines, through the cleavage activity of tumour-inducing enzymes. Wang *et al.* (2014) reported the inhibition of the growth of human tumour cell lines using extracts containing fucoxanthin. Satomi and collaborators (2013) found that fucoxanthin extracts have a significant effect on the expression and enzymatic activity of xenobiotic metabolizing enzymes that activate pro-carcinogenic agents.

Regarding the antioxidant activity of fucoxanthin, it is known that this pigment has an unusual activity in relation to reactive oxygen species (ROS). ROS are known to have caused cellular damage, which directly implies the appearance of certain pathologies, such as type 2 diabetes, cardiovascular diseases, cancer, among others. In addition to fucoxanthin being tested only in cell lines and mice, there is ample evidence that it may have good antioxidant power, reducing the risk of oxidative stress in humans (reviewed in Britton, 2009).

In human fibroblast cell lines and in hairless mice, fucoxanthin has been successfully tested to protect the skin from cell damage caused by ultraviolet B exposure, and also has an antioxidant effect as anti-skin aging against free radicals (Gupta, *et al.* 2017). A study carried out by Shimoda, *et al.* (2010), which aimed to study the use of fucoxanthin in melanogenesis (melanin synthesis), which is catalysed by the enzyme tyrosinase. Evidence from this study demonstrates that fucoxanthin suppresses tyrosinase activity in UV irradiated guinea pigs and melanogenesis in UV irradiated rats. In addition, results in guinea pigs indicate that a treatment with daily small doses of fucoxanthin, may reduce skin pigmentation induced by ultraviolet radiation (Shimoda, *et al.* 2010). These results are very promising, since melanogenesis is known to have a regulatory role in the formation of melanomas (malignant skin cancer) (Slominski, *et al.* 2014), and these extracts may have the potential to reduce the risk of skin cancers.

Still within the world of cosmetics, studies indicate that extracts containing fucoxanthin show activity against acne, inhibiting the activity of bacteria (Renhoran, *et al.* 2017).

Several studies have been conducted to assess the toxicity of fucoxanthin. To date, no *in vivo* studies in mice have demonstrated toxicity or side effects of this compound (Maeda, *et al.* 2005; Beppu, *et al.* 2009; Zaragotá, *et al.* 2008). Some of these studies show that oral doses up to 2000 mg/kg of body weight do not reveal mortality or abnormal effects in various tissues, such as kidneys or liver (Beppu, *et al.* 2009; Zaragozá, *et al.* 2008). However, toxicity in humans needs to be studied, assessing toxic levels and daily dosage in order to evaluate the efficacy against the pathologies indicated above.

1.3.4.2. Authorized Use of Fucoxanthin Rich Supplements

Currently, few extracts containing fucoxanthin are used for healthcare applications. As mentioned earlier, there is strong legislation related to carotenoids and their applicability as therapeutic compounds, often due to the lack of scientific evidence that proves that the same effect observed in *in vivo* studies with mice, also occurs in humans.

However, there are two products that have had promising results:

- (1) FucoVital™ from Algatech (company located in Israel) is an extract with 3% fucoxanthin derived from the microalgae *Phaeodactylum tricornutum*. It was the first fucoxanthin extract to obtain New Dietary Ingredient Notification (NDIN) by the FDA and the first microalgae-derived fucoxanthin product on the market. It is recognized as a dietary supplement and targets the first stage of fatty liver, reducing the accumulation of fat in the liver (<https://www.algatech.com/algatech-product/fucovital/>). Studies developed in non-alcoholic fatty liver cell models *in vitro*, have shown that FucoVital™ is much more potent in preventing the accumulation of fat in liver cells than the best-selling supplement on the market, called Silymarin (Milk Thistle). The latter is one of the most worldwide used herbal supplements for liver problems (Jowers, 2019). The study performed by Dr. Joseph Tam, from the Faculty of Medicine of The Hebrew University in Jerusalem, found that low concentrations of FucoVital™ (13.2 µg/mL) protect the liver cells significantly inhibiting fat accumulation when compared to Silymarin (29.8 µg/mL) (Algatech, consulted at 10/02/2021). Given the promising results of Dr. Tam's study, Algatech started in 2018, a clinical trial in patients diagnosed with elevated liver enzymes and excess liver fat. To date, the results of these tests have not yet been published (Clinical Trial FucoVital, consulted at 10/02/2021).
- (2) BrainPhyt™ from Microphyt (company located in France) is a fully characterized natural extract of *Phaeodactylum tricornutum*. It has a composition of phycoprostanes, xanthophylls (including fucoxanthin), omega-3 fatty acids, sterols, among others (<https://microphyt.eu/brainphyt/>). In 2019, Microphyt received FDA's New Dietary Ingredient

Notification (NDIN) for BrainPhyt™, which allows this nutritional ingredient, supported by patented efficacy data in cognitive applications, to be sold in the U.S. dietary supplement market. BrainPhyt™ aims to prevent the effects of cognitive decline, especially loss of spatial and short-term memory. It has been evaluated in 7 pre-clinical studies and has shown greater effectiveness in mice compared to Docosahexaenoic Acid (DHA) and *Ginkgo biloba* extract, both recognized as references for improving and maintaining brain function.

1.3.4.3. Regulation of Fucoxanthin Production: *PSY* and *LCYB* Genes

In an attempt to manipulate the synthesis of metabolites, it is necessary to modulate the enzymes that are part of their metabolic synthesis pathways. Commonly, the overexpression of these enzymes can make it possible to redirect the pathway to the desired product (Saini, *et al.* 2020). For example, in an attempt to overexpress a desired product, the regulation process can occur by gene regulation, silencing/overexpressing of specific genes, or by indirect regulation of abiotic factors, in which a cell regulates its own metabolism in response to stress (Huang & Daboussi, 2017). However, active knowledge of the pathway's mechanism and the enzymes involved may allow us to assess whether the pathway is capable of being controlled, to overexpress the product of interest.

Tran and co-workers (2009) took available sequences from various genes from the carotenoid biosynthesis pathway, within which they highlighted the gene encoding *phytoene synthase (PSY)*. This gene was analysed in higher plants and algae, building phylogenetic trees in order to group the organisms from the evolutionary point of view. From the results obtained, the authors state that the *PSY* gene of the algae was inherited from cyanobacteria via endosymbiotic gene transfer (EGT). They also claim that in algae, an ancestral gene has possibly undergone duplication, giving rise to two classes of *PSY* (I and II). Green algae, called Chlorophytes and higher plants, retain only class I, while red and brown algae (Ochrophyta, Haptophyta and Cryptophyta) have class II *PSY* genes. Although different groups have different classes of *PSY*, the authors observed, by aligning the various versions of the gene, that both classes have similar regions of substrate-Mg²⁺-binding site and catalytic residues, and the major differences between the various sequences occur in regions that are not associated with the normal functioning of the enzyme (Tran, *et al.* 2009).

During the evolutionary process, independent duplication of genes and consequently divergence, gave rise to the *LCYB* and *LCYE* genes (Cui, *et al.* 2011), molecules formed from *LCY* to which β - and ϵ - rings were added, respectively (Zhang, *et al.* 2018). Through the phylogenetic tree built by Cui and co-workers (2011), based on *LCY* sequences, it was found that the *lycopene cyclase* genes came from cyanobacteria and all the algae that arose from a secondary endosymbiosis with rhodophytes (e.g. Ochrophyta (taxonomic group where diatoms belong)), acquired the gene *LCYB* with the loss of *LCYE* gene, which justifies the fact that these organisms only produce β -carotenoids (Cui, *et al.* 2011). In contrast, red macroalgae have *LCYE* and *LCYB*, allowing the production of α - and β -carotenoids,

respectively. This last evidence obtained from the duplication of the ancestral gene may have happened before secondary endosymbiosis, because the gene was transferred from the phagocyte organism to the nucleus of the host cell (Cui, *et al.* 2011).

Thus, the hypothesis arises that these gene duplications, both for the *PSY* and *LCY* gene, are the result of algae responses to stress conditions, promoting the flexibility and adaptability of carotenoid synthesis pathway in order to assure the survival of the species (Tran, *et al.* 2009).

Several studies demonstrated a regulatory role of the *PSY* gene in the carotenoid synthesis pathway. This evidence hypothesized that *PSY* is a rate-limiting enzyme and alterations in this pathway may be due to the variation of its expression and activity (Arango, *et al.* 2014; Kadono, *et al.* 2015; Maass, *et al.* 2009; Meier, *et al.* 2011; Rodríguez-Villalón, *et al.* 2009). Furthermore, it is suggested that the increase or decrease in downstream metabolites may modulate *PSY*, being able to regulate positively or negatively their protein levels and, consequently, the concentration of carotenoids in order to maintain the homeostasis of these compounds (Arango, *et al.* 2014). A study carried out by Kadono *et al.* (2015), demonstrates, using genetic engineering tools, that the overexpression of *PSY* in *P. tricornutum* cells increased 1.45-fold the fucoxanthin content when compared to the wild-type. Knowing that *PSY* expression levels may be direct indicators of the carotenoid biosynthesis pathway behaviour (Kadono, *et al.* 2014; Maass, *et al.* 2009; Eilers, *et al.* 2016), makes this gene a target to assess the impact of abiotic effects on the production of fucoxanthin.

As for *LCYB*, there are few studies that demonstrate the regulatory role of this gene in the synthesis pathway. However, when it comes to assessing the content of fucoxanthin this is the most viable gene to be used since it is the first enzyme responsible for the synthesis of fucoxanthin in brown algae (brown box in Figure 1.4.), which converts lycopene into β -carotene, being successively converted until the final product of the synthesis, fucoxanthin (Zhang, *et al.* 2018). A study carried out by Ramos *et al.* (2008), revealed that when the microalgae *Dunaliella salina* is exposed to stress conditions such as salinity, high light intensity and nutrient depletion, the mRNA levels of the *LCYB* gene and the levels of carotenoids are increased. On the other hand, studies indicates that the overexpression of the *LCYB* gene allows an increased production of β -carotene (reviewed in Saini, *et al.* 2020).

Although there is extensive literature for *P. tricornutum* in which the authors make modifications to this diatom in order to increase the production of lipids, there are few articles that carry out this same analysis seeking to increase the production of fucoxanthin (Kadono, *et al.* 2015; Eilers, *et al.* 2016; Lavaud, *et al.* 2012). To this end, there are several strategies that can be used, such as the introduction of heterologous DNA or the overexpression of endogenous genes (Huang and Daboussi, 2017).

However, the use of genetically modified organisms may not be the ideal solution, due to the great reluctance of the public towards products obtained by these methods, associated with the concern of companies due to strict legislation that involves their use. Thus, the opportunity arises to study the

environmental factors that can increase the expression of several genes, with the advantage that *P. tricornutum* is one of the diatoms with a fully sequenced genome (Bowler & Falciatore, 2019).

Consequently, there are several abiotic factors that can have a great impact on diatoms, like the cultivation type (batch, fed batch or continuous), agitation, salinity, temperature, nutrients use mode (autotrophic, heterotrophic or mixotrophic), light intensity/quality and nitrogen source (Arora & Philippidis, 2021). Some of these factors and their impact on carotenoid production will be further discussed.

1.4. INFLUENCE OF ABIOTIC FACTORS ON CAROTENOID PRODUCTION

1.3.1. Cultivation System: Small scale vs. Industrial Scale

P. tricornutum is capable of growing under photoautotrophic and mixotrophic conditions, both indoors and outdoors, in open or closed systems (Garcia, *et al.* 2005).

Currently, on an industrial scale, the most common cultivation system to produce photosynthetic pigments, mainly carotenoids, is in photoautotrophic conditions, in outdoor culture systems that include glass bottles, cylinders or horizontal panels, in a batch system. Batch cultures consist of a single inoculum of cells, unique addition of culture media and natural light, followed by growth from 3 to 18 days, reaching the maximum biomass peak typically on the seventh day. During this period, the carotenoids content, mostly fucoxanthin, shows a higher production rate between the end of the exponential phase and the beginning of the stationary phase (Garcia, *et al.* 2005; Fernandez & Galvan, 2007). However, in photoautotrophic outdoor cultivation, the intensity and quality of the light is not adequate, since it depends on the sunlight, that is not always constant throughout the day. Regardless the high biomass productivity, when it comes to producing pigments that are light-dependent, like fucoxanthin, the production yield is very low, therefore it is not a sustainable and profitable production system for companies (De Martino, *et al.* 2007). Another factor that can be a disadvantage in these systems is the temperature, since it has a great influence on photorespiration. When the temperature increases, the respiration and carbon flow through the Calvin cycle also increase, reducing the efficiency of photosynthesis. This condition can affect cell cultures mainly in the context of photoautotrophic systems when the temperature is not controlled and can vary dramatically between day and night (Márquez-Rocha, *et al.* 2019).

In a laboratory context, the cultivation of diatoms is mixotrophic, which means that there is an artificial supplementation of nutrients in the cultures, instead of using simple wastewaters without nutrient addition, like in autotrophic systems. Mixotrophic cultivation is characterized by the addition of organic sources of carbon (glycerol, mannose, fructose, etc.) and/or nitrogen (sodium nitrate, urea, ammonia), essential compounds for the growth and production of pigments. It is a cultivation where the light energy is artificial and can be adapted in lamps of different types (fluorescent or non-fluorescent),

different wavelengths, emitting various shades of colour (green, blue, red) and that allow microalgae to produce different pigments (Fernandez & Galvan, 2007).

These conditions enable the production of compounds with a higher degree of sterility, regulating their production and composition, promoting a more controlled growth than in photoautotrophic systems. However, they are more expensive due to the need to use supplemented culture media and equipment (Garcia, *et al.* 2005).

Mixotrophic cultivation has been an approach to be used for growth of *P. tricornutum*, both in wild type and in mutants, but the optimization of the production of photosynthetic pigments is still underway. This optimization may lead to a greater control of production conditions, reducing the cost of cultivation and, consequently, the cost of the final product, attending only the needs that these diatoms require to produce the compound of interest (Fernandez & Galvan, 2007).

1.3.2. Culture Media

It is known that the growth rate and biochemical composition of microalgae varies depending not only on the culture media but also on other conditions (light, temperature, etc.). However, not only the chemical composition of the culture medium in nutritional terms is important for the cultivation of microalgae, but also the source of nitrogen (N) and carbon (C) (Fernandez & Galvan, 2007), the available CO₂ and the pH of the medium, can influence the growth and production of bioactive compounds (reviewed in Alam, *et al.* 2020).

In a study carried out by Guzmán-Murillo *et al.* (2007), several types of media were tested, with the control typically used, f/2 medium. Within all these media, the variant corresponded mainly to the type of supplemented N source (urea, ammonium nitrate, etc.). The results show that the simple fertilized media containing organic or inorganic N, can efficiently support the growth of *P. tricornutum*, compared to the standard f/2 medium. However, it was observed that some of these media promote an early death phase in the cultures, when compared to the control (Guzmán-Murillo, *et al.* 2007). One possible explanation may be that these fertilized media do not contain silica. This is an important compound for diatoms, since silica allows to maintain the integrity of the cell wall (Francius, *et al.* 2008). Since silica is not part of the constitution of these media or its presence in small amounts, the growth curve tends to be shorter (Guzmán-Murillo, *et al.* 2007; Francius, *et al.* 2008). Evidence allows to conclude that f/2 medium supplemented with silica is one of the most suitable media for the growth of this diatom (Guzmán-Murillo, *et al.* 2007).

1.3.2.1. Nitrogen Source: Sodium Nitrate, Urea and Ammonia

Nitrogen (N) is one of the main nutritional requirements in cell growth for the majority of the organism, and its absence or excess can cause stress to organisms in culture. When this stress is applied, microalgae reduce cell division, since N is essential for normal cell metabolism. However, in addition to reducing cell growth, N also influences pigment synthesis (Couso, *et al.* 2012).

Sodium nitrate, urea and ammonia are the most frequently used sources of inorganic N to support the growth of *Phaeodactylum* species (Alipanah, *et al.* 2015).

The assimilation of inorganic N consists of two separate steps, the first being in the cytoplasm (Nitrate (NO_3^-) \rightarrow Nitrite (NO_2^-)) and the second in the chloroplast (Nitrite (NO_2^-) \rightarrow Ammonia (NH_4^+)). NH_4^+ is then incorporated into the carbon skeletons via glutamine synthase/glutamate synthase, two enzymes that play an essential role in the carbon metabolism (Alipanah, *et al.* 2015).

A studied carried out by Glibert and co-workers (2016) demonstrated that diatom cultures supplemented with nitrate and urea, showed greater cell growth when compared to cultures supplemented with ammonia, which did not grow.

Therefore, one of the biggest challenges for any microalgae production, in order to provide the optimum conditions for growth and production, is to choose the best N source. The problem with urea and ammonia remains on the fact that urea metabolism releases ammonia which is toxic to the cells and inhibits cell growth. At low concentrations, urea is a good N source for growth, however at high concentrations it has a negative effect due to the toxicity of products derived from the urea cycle (Gupta, *et al.* 2017).

When cells are present in an environment rich in NH_4^+ or NO_3^- , they assume a greater preference for NH_4^+ . This occurs because the cells spend less energy transporting NH_4^+ by the cell membrane than NO_3^- , under optimal growth conditions. However, under conditions where NH_4^+ exceeds optimal values (more than 10 μM), growth can be inhibited by the toxicity associated to this compound (Gupta, *et al.* 2017).

Besides that, light plays an important role and can have an opposite effect to that played by nitrogen. The interaction between light and nitrogen may affect the concentration of pigments and the increase or decrease of these concentrations is related to the photosynthetic capacity (Ramlov, *et al.* 2011; Parjikolaei, *et al.* 2013). To evidence that pigments are directly influenced, not only by light, but also by the nitrogen availability, Pereira (2012) indicates that in the months of less sunlight and higher nitrogen concentration, the pigment concentration is highest.

1.3.2.2. Carbon Sources: Glycerol and Glucose

As previously mentioned, diatoms such as *P. tricornutum* have the ability to grow in both photoautotrophic and mixotrophic systems (reviewed in Garcia, *et al.* 2005). However, the photoautotrophic system adopted for production on an industrial scale, has a biomass productivity limited by the self-shading of cells when cultures reach high cell density (Ceron, *et al.* 2006).

Thus, a mixotrophic cultivation can be introduced as an alternative. This type of growth is characterized by the combined interaction of light and an organic carbon source, which promotes the growth and increase the biomass production (Ceron, *et al.* 2006; Garc, *et al.* 2000; Liu, *et al.* 2009; Garcia, *et al.* 2005). This type of cultivation requires low light intensities, which in itself is an advantage, given the reduction of the cost with energy (Sevilha, *et al.* 2004).

The most used carbon sources are glycerol, glucose and acetate (Hayward, 1968; Garcí, *et al.* 2000; Garcia, *et al.* 2005; Ceron, *et al.* 2006; Liu, *et al.* 2009; Villanova, *et al.* 2017). In a study carried out by Liu and co-workers (2009), it was found that the addition of these three carbon sources significantly increased the culture growth rate. However, the same study observed that this same addition led to a reduction in the content of chlorophyll *a* and carotenoids, when compared to the photoautotrophic cultivation. This hypothesis may be justified by the fact that these carbon sources have an important impact on the energy metabolism of cells, such as respiration and photosynthesis, and not on pigment synthesis. The same authors observed that when organic carbon sources are added to the cultures of *P. tricornutum*, the parameters associated with photosynthetic efficiency, such as photosynthetic oxygen evolution rate, pigment content, among others, were reduced. These carbon sources significantly increased respiration rates, enhancing the biomass content (Liu, *et al.* 2009).

The addition of carbon sources to microalgal cultures does not seem to favour the production of photosynthetic pigments, as this type of supplementation allows to increase the production of lipids and fatty acids. One of the major applications of this system is the production of biofuels by algae, such as biodiesel, bioethanol and biohydrogen, with different microalgal species producing different high-value products (reviewed in Márquez-Rocha, *et al.* 2019). However, other conditions such as light intensity (He, *et al.* 2015; Nzayisenga, *et al.* 2020) and nitrogen-limiting cultivation also influenced lipid accumulation (Juergens, 2016).

1.5. LIGHT

1.5.1. Light Intensity

Photosynthetic organisms such as microalgae tend to adopt protection strategies against the stress factors to which they are exposed in their natural habitat, being the light one of the stresses that strongly influence pigment production (Garcia, *et al.* 2005). Knowing that pigments have a photoprotective role, these organisms have the ability to regulate their pigment amount in a short time as light intensity change (Garcia, *et al.* 2005). For example, some studies have shown that with high light intensity (HL), there is an increase in photoprotective carotenoids and a decrease in fucoxanthin, the opposite occurs when cells are exposed to low light intensities (LL) (Stolte, *et al.* 2000; Falkowshi & Chen, 2003; Nymark, *et al.* 2009).

1.5.2. Light Quality

Diatoms can adopt two different ways of lifestyle: pelagic state, where they circulate freely in the water column; or benthic, being found sessile at the bottom of the sea (Garcia, *et al.* 2005). Different habitats have different characteristics, and therefore cells tend to adapt their morphology and physiology to survive in these conditions (Garcia, *et al.* 2005; Lavaud, *et al.* 2004). Thus, different diatoms stages

of life may be subject to different light intensities and light spectra, considering the depth at which they are found in the water column (Kuczynska, *et al.* 2015).

Yang and co-workers (2020) demonstrate in *P. tricornutum* that with the induction of blue light (BL) it is possible to increase the production of fucoxanthin. However, for cell growth better results were obtained when there is a mixture of red and blue (6:1). Jungandreas *et al.* (2014) found that the change from BL to red light (RL) results in a slight decrease in the growth rate in 48 hours, while the change from RL to BL caused a total growth inhibition for 24 hours. It also demonstrates that the first response of diatoms to a change in light conditions is carbon allocation, that is, a reorganization of the distribution of carbon in the cells (Jungandreas, *et al.* 2014). This evidence occurs when is switch RL to BL. In this situation, the carbon is directed towards protein synthesis, and when the opposite happens, BL to RL, occurs the accumulation of carbohydrates, thus hypothesizing that changes in the spectrum of light promote a metabolic reorganization of cells (Jungandreas, *et al.* 2014).

In addition to the light quality affecting cells in the cellular context, it also has the ability to change at the molecular level. According to Coesel *et al.* (2008b), BL can control the expression of several genes in the carotenoid synthesis pathway, especially *PSY*. Valle and co-workers (2014) demonstrates in *P. tricornutum*, that genes associated with the synthesis of fucoxanthin such as *LCYB* have a higher level of transcripts when exposed to green light (GL) and RL. In the same study, it was concluded that GL and RL are strong inducers of genes associated with light-harvesting proteins and photosynthetic electron transport (Valle, *et al.* 2014). BL, on the other hand, seems to be a strong inducer of genes linked to cell photoprotection, such as light damage repair genes and genes associated with ROS scavenging (Valle, *et al.* 2014). This evidence reveals that the spectral quality of light can have a great influence on the regulation of the expression of genes involved in cell protection and pigment synthesis (Coesel, *et al.* 2008a).

1.5.3. Light/Dark Cycle

The day and night cycle, is a natural phenomenon in all habitats on Earth and it is possible to assume that most organisms on the planet can regulate their metabolic activities, considering the variation of the diurnal cycle (Ragni & d'Alcalà, 2007).

The organisms, from animals to plants, tend to individually respond to the diurnal rhythms and the genes that control the endogenous clock are different, conferring changes at the level of transcription, translation and post-translation (Ragni, 2005; Ashworth, *et al.* 2013). The existence of these rhythms in cyanobacteria supports the evidence that the circadian cycle had followed the evolution of species since the ancestral organism, and algae may have assumed this evolutionary component during secondary endosymbiosis (Ragni, 2005).

Many marine microorganisms, such as phytoplankton, have been studied by the diel cycle in metabolic processes, such as pigment content (Fábregas, *et al.* 2002; Ragni & d'Alcalà, 2007), cell division (Ragni & d'Alcalà, 2007; de Winter, *et al.* 2017) and nitrogen assimilation (Fábregas, *et al.*

2002; Clark, *et al.* 2002). The majority of these studies used cycles of artificial lighting in order to simulate the daily variations of light in the ocean.

As mentioned above, light is a very important factor in the production of pigments. Ragni & d'Alcalà (2007) found, in *P. tricornutum* cultures, a continuous increase in the intracellular concentration of pigments during the light period, with a decrease during the dark phase. In addition to the increase in pigments during the light phase, this is accompanied by an increase in the cell growth rate, which tends to be constant or decrease during the dark period, indicating a possible control of the light on the cell cycle progression (Fábregas, *et al.* 2002; Kromkamp & Claquin, 2005; Ragni & d'Alcalà, 2007; de Winter, *et al.* 2017).

Ragni and d'Alcalà (2007) believe that the decreased efficiency of the use of light for growth and production of pigments, is a consequence that can occur when cells are transferred to continuous light systems (removal of the dark phase), which makes it difficult to organize the metabolic pathways that are synchronized with day and night, also decreasing the efficiency of the cells' response to stress.

In addition to the influence of the photoperiod on cell growth and pigment synthesis, its action on nitrogen assimilation has also been studied (Fábregas, *et al.* 2002; Clark, *et al.* 2002; Kromkamp & Claquin, 2005).

As previously mentioned, cells assume a preference for certain nitrogen sources depending on the energy cost of membrane nitrogen transport (Gupta, *et al.* 2017). Thus, it can be assumed that when the cell reduces its metabolism, it opts for the use of nitrogen sources that require less energy expenditure (Gupta, *et al.* 2017). This evidence indicates that nitrate transport and its consequent reduction to ammonia at the intercellular level appear to be limiting steps and are under rigid internal regulation (Clark, *et al.* 2002).

Clearly, the light/dark cycle has an important role in the modulation of the response by the diatoms, and the cells tend to adapt their metabolisms as a consequence of the induced stress and the culture conditions to which they were exposed (Clark, *et al.* 2002; Ragni & d'Alcalà, 2007).

1.6. OBJETIVES

In this thesis project, the main objective is to evaluate the effect of various N and C sources on cell growth, fucoxanthin production and cell viability in cultures of the model diatom *Phaeodactylum tricornutum*. These parameters will be evaluated by performing optimizations of the culture medium with different sources and concentrations of N and C, from microscale assays to 50 mL cultures, using tools for design of experiments (DoE). Additionally, a chromatographic characterization of the ethanol extract of *P. tricornutum* by TLC and HPLC will be performed. Preliminary studies of the day/night cycle will be carried out to follow the variation of fucoxanthin during a 24h photoperiod, where cultures will grow with different concentrations of N, in order to understand the role of N and light, simultaneously, in the synthesis of this pigment. Furthermore, genetic expression studies will be performed by semi-quantitative RT-PCR, which will allow to observe the possible influence of N concentration and cell growth curve on the expression of target genes (*LCYB* and *PSY*) of the fucoxanthin synthesis pathway. To assess the cell viability of cultures when exposed to different concentrations of N, observations will be made by optical microscopy, using the Neutral Red staining technique.

2. MATERIALS AND METHODS

2.1. Culture Conditions of *Phaeodactylum tricornutum*

2.1.1. Culture Characterization

The strain *Phaeodactylum tricornutum* CCAP 1055/1 used in this work was acquired from the Culture of Collection of Algae and Protozoa (CCAP), Scottish Association for Marine Science Laboratory.

The non-axenic *P. tricornutum* culture was maintained at a constant temperature of $19.5\text{ }^{\circ}\text{C} \pm 1\text{ }^{\circ}\text{C}$ under a cycle of 16 hours of light and 8 hours of darkness, with a light intensity of approximately $30\text{ }\mu\text{mol photons m}^{-2}\text{ s}^{-1}$, under continuous agitation in an incubator (Agitorb 200IC, Aralab, Portugal) at 110 rpm. The cultures were grown in 250 ml Erlenmeyer flasks with biological replicates, with the culture volume corresponding to 1/5 of the Erlenmeyer volume. Cultivation was done in f/2 medium supplemented with silica (hereinafter referred as “basal medium”) (Guillard R.R.L., 1975). The medium was prepared by adding Instant Ocean salts (Aquarium Systems, France), monobasic sodium phosphate ($\text{NaH}_2\text{PO}_4 \cdot 2\text{H}_2\text{O}$), sodium metasilicate ($\text{Na}_2\text{SiO}_3 \cdot 9\text{H}_2\text{O}$), trace elements (Na_2EDTA , $\text{FeCl}_2 \cdot 6\text{H}_2\text{O}$, $\text{CuSO}_4 \cdot 5\text{H}_2\text{O}$, $\text{ZnSO}_4 \cdot 7\text{H}_2\text{O}$, $\text{CoCl}_2 \cdot 6\text{H}_2\text{O}$, $\text{MnCl}_2 \cdot 4\text{H}_2\text{O}$ and $\text{Na}_2\text{MoO}_4 \cdot 2\text{H}_2\text{O}$), vitamins (Cyanocobalamin, Thiamine and Biotin) to bidistilled water (concentration of each component is described in Appendix 1). The nitrogen or carbon sources, changed according to the experimental setting as described below.

To proceed to the subculture, 25 % of inoculum and 75 % of fresh medium were added to an Erlenmeyer flask, in sterile conditions, in a biological safety laminar flow hood (Faster Bio48, UK). For all cultures to be tested with different concentrations of nitrogen or carbon sources, the initial inoculum came from a culture with a basal sodium nitrate (NaNO_3) concentration (0,882 mM).

2.1.2. *P. tricornutum* Growth Curve

The growth curves of *P. tricornutum* were generated using three distinct methods for different assays. In a first assay, the screening of several nitrogen and carbon sources was carried out in 6-well plates, using optical density (OD) reading at 595 nm to establish the growth curves. Then, after selecting the best nitrogen and carbon sources, for scale up to 50 mL Erlenmeyer cultures, the curves were generated by cell counting under the optical microscope (first scale up test) and OD readings at 750 nm (following scale up tests). The different assays are further described below.

2.1.2.1. Optical Density Reading at 595 nm

In the 6-well plate assay (see subchapter 2.2.1.), growth curves were established by reading the OD at a wavelength of 595 nm. The cultures were followed up for 7 days, with readings in all days, with independent triplicates for each experimental set.

The readings were performed on the FLUOstar OPTIMA microplate reader (BMG Labtech, Thermofisher, USA). The absorbance readings were the result of the average of three automatic direct readings for each well.

2.1.2.2. Cell Counting

Growth curves were established for the microalgae *Phaeodactylum tricornutum*. In a preliminary assay of NaNO₃ concentrations from 0 mM to 8.82 mM, 50 mL Erlenmeyer cultures were initiated, with biological duplicates for each test condition. The counts were performed on days 0, 2, 5, 6 and 7.

A volume of 20 µL was taken from each culture and used for counting. The number of cells in each aliquot was counted in the hemacytometer or Neubauer chamber (Hirschmann, Germany), with 16 small squares of 0.25mm x 0.25mm each, creating a large square with the total area of 1 mm² and a depth of 0.1 mm. The chamber was filled with 10 µL of culture on each side, and the samples were observed under a microscope (Leica DM6 B, Germany). When necessary, the samples were diluted with medium to maintain physiological conditions of the cells.

To calculate the number of cells per mL, the following formula was used:

$$N^{\circ} \text{cells/mL} = \frac{\text{Mean number of cells} \times 1000 \text{ mm}^3}{0,1 \text{ mm}^3}$$

Note:

1000 mm³, represent the volume of 1 mL (1 mL = 1000 µL = 1000 mm³).

0.1 mm³, represent the volume of one large square (Volume (0.1 mm³) = Depth (0.1 mm) x Area (1 mm²))

2.1.2.3. Optical Density Reading at 750 nm

An assay to establish growth curves for *P. tricornutum* grown with NaNO₃ concentrations from 0.882 mM to 35.28 mM was performed by using triplicates for each experimental set. A volume of 600 µL of each culture was centrifuged at 10,000 g for 3 minutes (Centrifuge 5425, Eppendorf, Germany). The supernatant was discarded, and the pellet resuspended in 600 µL of the respective growth medium (corresponding to the different NaNO₃ concentrations). The OD readings at 750 nm were performed on

a 96-well microplate in the microplate reader (EPOCH2, BioTek, USA), with three independent readings of 200 μ L per well. Readings were taken every two days for 20 days, including day 0. When necessary, the samples were diluted with growth medium to maintain physiological conditions of the cells. OD values at 750 nm should vary between 0.1 and 0.8 (Wang, *et al.* 2018).

To obtain the exact OD value of the culture, the value obtained by the microplate OD reading on the equipment, must be substituted in the equation of the correlation line at 750 nm. This equation represents the correlation between the microplate and the cuvette. This conversion is important since the values obtained from the OD reading are representative of a cuvette reading, however the reading performed in our case occurred in a microplate. By replacing the y-value of the equation by the OD value, the real value in microplate will be obtained (see subchapter 2.4.1.) (Wang, *et al.* 2018).

2.2. Modifications to the basal culture conditions

2.2.1. Screening of Carbon and Nitrogen sources: 6-well plate assay

In order to understand how the sources of nitrogen and carbon may influence the growth and production of fucoxanthin in cultures of *P. tricornutum*, an initial screening of 6-well plates with a total volume of 5 mL of culture was performed, with an initial inoculum of 25 %. The nitrogen sources tested were sodium nitrate (0.183, 0.441, 0.882, 3.528 and 8.82 mM), ammonium chloride (0.183, 0.441, 0.882, 3.528 and 8.82 mM) and urea (5, 10, 20, 40 and 80 mM). The carbon sources were glucose (3, 6, 30 and 60 mM) and glycerol (25, 50, 75 and 100 mM). As a control, cultures growing in f/2 medium supplemented with silica without nitrogen or carbon source were used. Each concentration was done in triplicate. The different media are described in Table 2.1.

Table 2.1. Composition of the 24 media prepared for screening on 6-well microplates from different sources of nitrogen (N) and carbon (C). The type of medium was the same for all (f/2+Si), changing only the concentrations of N or C. Control represents f/2 medium supplemented with silica, without N or C source (hereinafter referred as “f/2+Si without N or C”). The symbol * represents the basal concentration of NaNO₃ for *P. tricornutum* growth (hereinafter referred as “basal concentration”).

		Type of medium	[Nitrogen] mM	[Carbon] mM
Nitrogen Sources	Sodium Nitrate	<i>f/2+Si</i>	0.183	-
			0.441	-
			0.882*	-
			3.528	-
			8.82	-
	Ammonium Chloride	<i>f/2+Si</i>	0.183	-
			0.441	-
			0.882	-
			3.528	-
			8.82	-
	Urea	<i>f/2+Si</i>	5	-
			10	-
			20	-
			40	-
			80	-
Carbon Sources	Glycerol	<i>f/2+Si</i>	-	25
			-	50
			-	75
			-	100
	Glucose	<i>f/2+Si</i>	-	3
			-	6
			-	30
			-	60
			-	-
Control	<i>f/2+Si</i>	-	-	

In order to ascertain the effect of each source of nitrogen or carbon and the respective concentrations, the cultures were grown with only one source, with no combination of two distinct sources (no interaction between nitrogen-nitrogen or nitrogen-carbon). The different concentrations of each source were achieved using stock solutions described in Appendix 1. The initial inoculum of *P. tricornutum* originated from a single culture of 50 mL growing in a basal medium (f/2 medium supplemented with silica and 0.882 mM of sodium nitrate).

On the 7th day of the cultures, the biomass was collected and fucoxanthin was extracted for analysis by High Pressure Liquid Chromatography (extraction and analysis method described in subchapters 2.3.1. and 2.3.3, respectively).

2.2.2. Nitrogen Source: Scale-up to 50 mL of culture

In this work, various concentrations of NaNO₃ were tested in *P. tricornutum* cultures in order to evaluate the effect on growth and production of fucoxanthin. For that, different concentrations of sodium nitrate (0, 0.183, 0.220, 0.441, 0.882, 1.176, 3.528, 7.056, 8.82, 17.64 and 35.28 mM) were used, in addition to the concentration of 0.882 mM, the basal concentration, which was considered as a basis for comparison. The type of medium for all cultures was f/2 supplemented with silica, with no changes to any of the remaining constituents. The final NaNO₃ concentration of each culture was achieved using a 50 mM NaNO₃ stock solution (Appendix 1).

In a preliminary assay, cultures with NaNO₃ concentrations from 0 mM to 8.82 mM were followed only for 7 days of the growth curve, by counting the cells. After the results of this initial test, cultures with NaNO₃ concentrations from 0.882 mM to 35.28 mM were assessed every 2 days during 20 days of growth, by reading the OD at 750 nm.

2.3. Analysis of Photosynthetic Pigments

2.3.1. Extraction of fucoxanthin for chromatographic analysis

First, the cells were separated from the culture medium by centrifuging at 3,000 g for 15 minutes (Allegra X-12R Centrifuge, Beckman Coulter, USA), and discarding the supernatant. Then, the cells were resuspended in 500 µL of distilled water to wash the salt residues of the culture medium. Cells were centrifuged at 3,000 g for 15 minutes and the pellet was frozen in liquid nitrogen, to promote cell lysis. The frozen cells were weighed, and 100% ethanol (Carbo Erba, Spain) was added in a 1:30 ratio (fresh weight in mg: µL EtOH). After adding the solvent, the samples were placed in the water bath at 45 °C for 2 hours in the dark, with vortex homogenization every 30 minutes. Finally, the samples were centrifuged at 3,000 g for 15 minutes and filtered using a 0.22 µm nylon syringe filter (VWR, USA). Eppendorf's with ethanolic extract were sealed with parafilm and stored at -80 °C to prevent evaporation of the solvent, until analysis.

2.3.2. Analysis of ethanolic extract by Thin Layer Chromatography (TLC)

As a preliminary indication, a TLC was performed in order to verify the presence of pigments that constitute the ethanolic extract of *P. tricornutum*.

A 7x7 cm silica gel plate (TLC Silica Gel 60 F₂₅₄, Merck Milipore, Germany) was used on which a 1 cm wide baseline was drawn. Points were scored on the line for the application of commercial standards and samples. The standards of neoxanthin, violaxanthin, lutein, beta-carotene and fucoxanthin (Sigma-Aldrich, USA) were used.

For the separation of the pigments, a mobile phase consisting of hexane and acetone (70:30% v/v) was used. The compounds were observed, under natural light, when the front of the eluent reached the line drawn 1 cm from the top of the silica plate.

2.3.3. Quantification of fucoxanthin by High Pressure Liquid Chromatography (HPLC)

The extracts described above were analysed with an Alliance 2695 HPLC System equipped with a Photo Diode Array (PDA) 2996 detector (Waters Corporation, USA) using a C18 reverse phase column with 5 µm particle size, 150x3.9 mm (Delta PAK, Portugal). The HPLC equipment was programmed to compose a mobile phase with a solvent A of milli Q water and a solvent B of acetonitrile (Sigma-Aldrich, USA). The gradient starts with 80% B and 20% A over 1 minute, changes to 100% B in 8 minutes and maintains for 3 minutes. In 2 minutes, it returns to the initial conditions (80 B:20 A gradient) and equilibrates for 6 minutes, at a flow rate of 0.5 mL per minute. The chromatogram was recorded using the PDA detector at 445 nm. The column temperature was 24°C and the sample was 4°C, in order to avoid evaporation of the solvent. A volume of 10 µL of sample was injected.

A fucoxanthin standard (ref 16337-1MG, Sigma-Aldrich, USA) was used to perform a calibration curve in a concentration range from 1.87 mg/L to 30 mg/L (1.87, 3.75, 7.5, 15, 30 mg/L), using a stock solution of 1 mg/mL.

The automated integration software Empower 3 was used for data processing. Results were then expressed as mg of fucoxanthin per litter.

2.3.4. Relative Quantification of Fucoxanthin

Wang and co-workers (2018) developed a method to assess the concentration of fucoxanthin in ethanolic extracts of *P. tricornutum*. This is a spectrophotometric method in which the concentration of fucoxanthin in algae cells is determined by measuring the absorbance of the cell culture at 750 nm, discarding the background noise of the optical density of the cells and other pigments. The ethanolic extract was measured at 445 and 663 nm, maximum absorption for fucoxanthin and chlorophyll *a*, respectively.

The formula was created for analysis of cell culture or extract in cuvette, however the authors created a correlation between cuvette and microplate. The use of a microplate allows the simultaneous measurement of 96 samples, reducing the amount of plastic to use, the cost, solvents volume and cell culture, as well as the time spent on readings. Nevertheless, the authors recommend that the correlation between cuvette and microplate needs to be adapted to the laboratory conditions of each study. The authors also refer that this spectrophotometric method has an error of less than 5%, compared to HPLC analysis, and has the advantage of being faster, user-friendly and less costly.

$$[\text{Fucoxanthin}] \text{ mg/L} = 6.29 \times A_{445} - 5.18 \times A_{663} + 0.312 \times A_{750} - 5.27$$

Note:

This formula was used for the relative quantification of fucoxanthin on all the tests carried out afterwards, as described below, since these assays had a large number of samples to analyse.

2.3.4.1. Correlation Cuvette vs. Microplate

The cultures used to monitor the production of fucoxanthin during the growth curve contained different concentrations of NaNO₃ (0.882, 8.82, 17.64 and 35.28 mM). Because of that it was necessary to verify whether the absorbance at wavelengths 445, 663 and 750 nm, varied according to the concentrations of NaNO₃ added, in order to apply the formula described by Wang and co-workers (2018). For this purpose, the three absorbance values of the different media were measured in a 96-well microplate. As the absorbance values at the various wavelengths did not show clear differences, only a culture of 50 mL of *P. tricornutum* was initiated with the basal concentration of NaNO₃ (0.882 mM). The culture was followed for 9 days, with measurements at day 0 (day of inoculation), 1, 3, 5, 7 and 9, thus following the entire growth curve that includes the log, exponential and stationary phase.

To carry out the measurements, 3.6 mL of culture were collected into two 15 mL tubes. The culture was centrifuged at 3,000 g for 5 minutes (Allegra X-12R Centrifuge, Beckman Coulter, USA) and the supernatant was discarded. One of the pellet's was resuspended with a basal concentration of NaNO₃ medium, with equal (3.6 mL) or higher volume, if necessary, to dilute. The absorbance values at 445 nm and 663 nm must be between 0.2 and 1, while for 750 nm between 0.1 and 0.8 (Wang, *et al.* 2018). If the values did not belong to the indicated intervals, it would be necessary to dilute. In the other tube, the pellet was resuspended with equal (3.6 mL) or higher volume, if necessary to dilute, of 100% ethanol. Both tubes were vortexed for 1 minute and the tube with the cell suspension in ethanol was wrapped in aluminium foil to protect the pigments against light degradation.

From each tube, a 3 mL volume was taken for cuvette reading on the spectrophotometer (NanoDrop2000C, Thermofisher, USA) with three independent readings of 1 mL per cuvette, and 600 µL for reading on a 96-well microplate in the microplate reader (EPOCH2, BioTek, USA), with three independent readings of 200 µL per well. In both for cuvette and microplate, absorbance at 750 nm was

measured for the cell suspension in medium and absorbance at 445 nm and 663 nm for the cell suspension in ethanol. For the same wavelengths, blanks were measured, at 750 nm the medium with basal NaNO₃ concentration and at 445 nm and 663 nm, 100 % ethanol.

After the measurements, a graph was created where a linear equation was adjusted ($y = mx + b$) for each wavelength. The first point of each line was normalized, corresponding to the first measurement of the cell suspension at 750 nm. The ordinate at the origin (b) of the linear equation was discarded, given that the calibration coefficient is the essential factor (slope of the line: $y = mx$).

2.3.4.2. Extraction of fucoxanthin for formula application

To measure the fucoxanthin concentration of the samples to be tested, the same procedure described above was performed, however readings were only performed on a 96-well microplate.

Volumes of 600 μ L of each culture were taken into 2 mL Eppendorf tubes (VWR, USA). After centrifugation, the supernatant was discarded, and the pellet resuspended in 600 μ L of medium (corresponding to the different NaNO₃ concentrations) or 600 μ L of absolute ethanol. Cell suspensions were vortexed for 1 minute. A volume of 200 μ L, of each Eppendorf tube, was transferred to three wells and 200 μ L of each of the blanks (medium and ethanol). The absorbance was read at 445 nm, 663 nm and 750 nm, as indicated above.

To calculate fucoxanthin concentration, the calculation method to apply the formula is described in Appendix 2.

2.4. Bioinformatic Analyses

2.4.1. Prediction Models for Medium Optimization – Modde® 12.1

In order to better understand the data obtained on the 6-well plate assay and find the best concentration and source of nitrogen or carbon to grow the cells and produce fucoxanthin, the data collected from the optical density at 595 nm and the concentration of fucoxanthin obtained by HPLC, were introduced in the software Modde® 12.1 (Sartorius, Germany). This software is a design of experiments (DoE) software that allows to optimize the experimental set and observe the interactions between different factors, predicting the best result, based on the data obtained experimentally. Considering the experiments carried out, each response was fitted using the Partial Least Squares (PLS) method. This is a method that builds predictive models, developing a linear regression model where the predicted and observed variables are projected, in a new space. Thus, models were made for each of the nitrogen and carbon sources individually, and for the interactions between the nitrogen and carbon sources.

2.4.2. Statistical Analyses: Student's t-test and Mann-Whitney's test

Data regarding the growth and fucoxanthin production were analysed between cultures growing with the control condition, on each assay, and cultures with the f/2+Si medium modified with different N and C sources. The differences between the conditions were tested using the Real Statistics software as a Microsoft Excel 2016 Supplement (Microsoft Corporation, Redmond, Washington, EUA). The normal distribution of independent samples was analysed using the Shapiro-Wilk's test, whereas the homogeneity of variances was assessed using the Levene's test. When the assumption of homogeneity of variances was not accomplished, a correction was performed using the Welch's t-test. $p < 0.05$ was considered as a statistically significant difference.

When the assumption of normal distribution was not accomplished for the independent samples, the Mann-Whitney's test was used, instead the student's t-test. $p < 0.05$ was considered as a statistically significant difference.

2.5. Light/Dark Photoperiod Assay

In order to evaluate how the concentration of fucoxanthin and cell growth varies during the photoperiod, triplicates of the cultures of *P. tricornutum* grown in medium with the basal concentration (0.882 mM) and 10-fold sodium nitrate (8.82 mM) were started. The initial inoculum of all cultures under study, came from a single culture growing at basal medium. The cultures were all grown at the same time, under the same conditions of temperature, light and agitation. There was no prior adaptation of cultures to dark or continuous light. The assay was carried out for 24 hours between the 4th and 5th days of the cultures, allowing to evaluate the effect of sodium nitrate during the exponential phase. In a photoperiod of 16h light and 8h dark, samples were extracted every two hours under sterile conditions, for a total of seven points in the first light phase, four points in the dark phase and two points in the second light phase, with a total duration of 24 hours. During the dark phase, it was necessary to turn off all the artificial lights to prevent any cells' response to light. In order to enable the sampling, a LED lamp with absorption in the green region was used during this period. The spectral light has a major influence on the chloroplast of photosynthetic organisms such as algae, with red and blue light playing a key role in activating pigment synthesis. Thus, the green light was used to prevent this activation to occur in the dark period of the assay.

The absorption spectrum of the lamp was previously analysed using the lighting detector Spectral PAR Meter PG100 N (UPRTek, Taiwan).

The analysis procedure of fucoxanthin is described in subchapter 2.3.4.2.

2.6. Gene Expression Analysis

2.6.1. Primer Design - Exon-Exon Junction Method

When performing Reverse Transcriptase Polymerase Chain Reaction (RT-PCR) analysis, one of the most relevant problems is contamination with genomic DNA. The presence of this contaminant in the samples can lead to overestimation of the RNA, reduction of the specificity of the primers or even false-positive results (Apte & Daniel, 2009). Thus, one of the strategies to adopt when is doing RT-PCR is to design specific primers for cDNA sequences in which the gDNA is not amplified. One of these methods is called exon-exon spanning (Apte & Daniel, 2009). These primers are designed for one half of the primer to hybridize at the 3' end of an exon and the other half at the adjacent exon, in genes that contain introns. These primers have the unique feature of binding to cDNA and not gDNA, eliminating any amplification by contamination with gDNA. In this method, only one of the primers needs to be designed covering the exon-exon junction, and the other primer can be designed entirely on top of a single exon (Apte & Daniel, 2009).

Siaut and co-workers (2007) conducted a study on *P. tricornutum* where they identified the best reference genes from which the *Cyclin-Dependent Kinase A (CDKA)* and *TATA Binding Protein (TBP)* gene were selected for this work. As the primers (*CDKA* and *TBP*) designed by Siaut and co-workers (2007) were not built with the exon-exon junction method, the reference of both genes was used for the design of new primers. In our study, the primers for the target gene *Lycopene β -cyclase (LCYB)* were designed with this method, while the primers for the target gene *Phytoene Synthase (PSY)* were designed by Skehan (2019) with same strategy.

The primers design was based on the mRNA sequences from the National Center for Biotechnology Information database (NCBI <https://www.ncbi.nlm.nih.gov/>). Using the NCBI ORF Finder tool (<https://www.ncbi.nlm.nih.gov/orffinder/>), the initiation codon (ATG) and the stop codon (TGA) of the DNA sequence of each gene were located, identifying the coding sequence (CDS). The gDNA sequence for each of the genes was taken from two different databases, NCBI and JGI PhycoCosm (<https://phycocosm.jgi.doe.gov/phycocosm/home>). The CDS and gDNA taken from the two databases were aligned in the Multiple Sequence Alignment Clustal W tool (<https://www.genome.jp/tools-bin/clustalw>), in order to confirm the homology of the sequences in both databanks and to check where the introns were located. Using the Primer 3 software (<https://bioinfo.ut.ee/primer3-0.4.0/>) the primers were designed, selecting the target region of the exon-exon junction. To observe the specificity of the primers, NCBI Primer Blast software (<https://www.ncbi.nlm.nih.gov/tools/primer-blast/>) was used, using the Primer Pair Specificity Checking Parameters tool with RefSeq mRNA and for the species *Phaeodactylum tricornutum* CCAP 1055/1.

The primers were synthesized by Eurofins Genomics' service from NZYTech, Lda - Genes and Enzymes (Portugal) and the primers details are described in Table 2.2.

Table 2.2. Primer sequences, annealing temperature, size of the amplicon and identification code for each gene on the NCBI database.

Primer	Primer Sequence	T _a ⁵ (°C)	Size ⁶ (bp)	Gene ID Code	Reference
<i>CDKA</i> ¹	Fwd: TTAACGGGAGTGGCGTATTG Rev: CTGGCTAAACCGAAATCTGC	57	116	XM_002180023.1	Adapted from Siaut, <i>et al.</i> (2007)
<i>TBP</i> ²	Fwd: CACACGGCTGGATTTAAAGAA Rev: TAGCACGGGGTTCACGTAAT	57	104	XM_002186285	Adapted from Siaut, <i>et al.</i> (2007)
<i>LCYB</i> ³	Fwd: GCAACGTAGACAACGCCATC Rev: TCCATTGGAATGTCAAACGAT	58	80	<u>XM_002176576.1</u>	-
<i>PSY</i> ⁴	Fwd: CGTTGCAGGCACAGTAGGATTG Rev: AGTGACAGTGCTGGTTCTCTTGC	58	93	XM_002178740	Skehan (2019)

¹ *Cyclin-Dependent Kinase A*; ² *TATA Binding Protein*; ³ *Lycopene β-cyclase*; ⁴ *Phytoene Synthase*; ⁵ Annealing Temperature; ⁶ Product Size (Amplicon)

2.6.2. Annealing Temperature Test

In order to assess the optimal annealing temperature for each pair of primers, a standard Polymerase Chain Reaction (PCR) was performed with Taq Supreme NZYTaq II 2x Green Master Mix (MB36001, NZYTech, Portugal), with the final primer concentration of 0.25 μM. To test the new primers, cDNA (dilution 1:10) and gDNA from *P. tricornutum*, grown with the basal concentration of NaNO₃, were used. The use of gDNA allowed to evaluate if the primers work correctly with the exon-exon junction method. The PCR cycle was as follows: initial denaturation at 95°C, for 5 minutes, followed by 35 cycles of denaturation at 95°C for 30 seconds, annealing at 57°C for *CDKA* and *TBP*, at 58°C for *LCYB* and *PSY*, for 30 seconds, extension at 72°C for 40 seconds and final extension at 72°C for 10 minutes, with a final reaction volume of 15 μL. After the PCR reaction, all samples were run onto a 1.2% agarose gel in 0.5x TBE (Appendix 3) at 90V for 40 minutes and the NZY Ladder III molecular weight marker (NZYTech, Portugal) was used. The result of the gel was developed under UV light, using a DocEZ Gel Documentation System Gel (BioRad, USA).

2.6.3. DNA Extraction

The DNA was extracted from biomass of *P. tricornutum*. First, the cells were centrifuged at 1,500 g for 10 minutes at room temperature (Allegra X-12R Centrifuge, Beckman Coulter, USA). The supernatant was discarded, and the collected cells were immediately frozen in liquid nitrogen. The fresh weight of the frozen biomass was recorded. Then, extraction was performed with the NZY Plant/Fungi gDNA isolation kit (NZYtech, Portugal), following the manufacturer's instructions. The concentration of extracted DNA was determined by spectrophotometry using NanoDrop2000C (ThermoFisher, USA) at 260 nm. Its quality was analysed by electrophoresis in 0.8% agarose gel in 0.5x TBE (Appendix 3). Finally, the DNA was stored at -20°C for future use.

2.6.4. RNA Extraction

P. tricornutum cultures were centrifuged at 3,000 g for 5 minutes at room temperature (Allegra X-12R Centrifuge, Beckman Coulter, USA). After discarding the supernatant, the cells were resuspended in 1 mL of medium and the cell suspension transferred to a sterile Eppendorf tube, centrifuging at 10,000 g for 3 minutes (Centrifuge 5425, Eppendorf, Germany). The supernatant was discarded, and the weight of the fresh biomass was recorded. For subsequent procedures, the biomass was adjusted to be between 80 and 100 mg. The samples were frozen in liquid nitrogen.

Since *P. tricornutum* has a silica frustule difficult to break, before starting RNA extraction, it was necessary to carry out some cell lysis procedures. For this, the cells were frozen in liquid nitrogen for 5 minutes and thawed at room temperature for 5 minutes. This step was repeated three times. Then, 100 µL of milli Q water, autoclaved twice, was added, in order to induce osmotic pressure lysis. The suspension was allowed to incubate for 5 minutes. In the fume hood, 300 µL of NZYol (NZYTech, Portugal) were added, vortexed for 20 seconds and incubated for 5 minutes. The cell suspension was centrifuged at 12,000 g for 15 minutes and the supernatant was transferred to a new tube. An equal volume of 100% ethanol was added to the tube and homogenized vigorously by pipetting. The RNA was extracted using the Direct-Zol RNA Extraction Kit (Zymo Research, USA), according to the manufacturer's instructions. For the treatment with DNase in column, the RNeasy Plant Mini kit (Qiagen, Germany) was used.

The RNA was subjected to a second purification using the TURBO DNA-free kit (Invitrogen, USA) to remove the residual genomic DNA (gDNA). The procedure was performed according to the manufacturer's instructions. The treated RNA was used for precipitation.

2.6.5. RNA Precipitation

To the purified RNA, 5 µL of 3M Sodium Acetate at pH 5.2 (0.1 volume) and 125 µL of 100% ethanol (2.5 volume) were added. The solution was incubated overnight at -20 °C. After incubation, the solution was centrifuged at 10,000 g, 30 minutes at 4 °C (Centrifuge 173OR Gyrozen, Korea). The

supernatant was removed and 500 μL of cold 70 % EtOH on ice was added. It was centrifuged for another 5 minutes, the supernatant was discarded, and the pellet was allowed to dry for 15 minutes. Then, the pellet was resuspended in 20 μL of milli Q water. The concentration of extracted, treated, and purified RNA was determined by spectrophotometry using NanoDrop2000C (ThermoFisher, USA) at 260 nm. Its quality was analysed by electrophoresis in 1.2% agarose gel in 0.5x TBE (Appendix 3).

Finally, the RNA was frozen in liquid nitrogen and stored at $-80\text{ }^{\circ}\text{C}$ for future applications.

2.6.6. Standard Polymerase Chain Reaction (PCR)

In order to assess the quality of RNA purification and the existence of possible contamination with genomic DNA, a PCR reaction was performed with the *CDKA* primer (Table 2.2.), using the GoTaq Flexi DNA Polymerase (M7805, Promega, USA). The PCR cycle was the following: initial denaturation at $95\text{ }^{\circ}\text{C}$ for 2 minutes, followed by 35 cycles of denaturation at $95\text{ }^{\circ}\text{C}$ for 1 minute, annealing at $57\text{ }^{\circ}\text{C}$ for 30 seconds, extension at $72\text{ }^{\circ}\text{C}$ for 10 minutes seconds and final extension at $72\text{ }^{\circ}\text{C}$ for 10 minutes, with a final reaction volume of 10 μL . The final concentration of the different components of the reaction is described in Table 6.1. in Appendix. After the PCR reaction, all samples were run onto a 1.2 % agarose gel in 0.5x TBE (Appendix 3) at 90V for 40 minutes and the NZY Ladder III molecular weight marker (NZYTech, Portugal) was used. The result of the gel was developed under UV light, using a DocEZ Gel Documentation System Gel (BioRad, USA).

2.6.7. cDNA Synthesis

The PCR process via reverse transcriptase was performed, following the protocol ImProm II Reverse Transcriptase System (Promega, USA). The RNA was normalized to all samples at 200 ng. The RNA was added to the mixture of 0.5 μL of oligo dTs, 0.5 μL of random primers and water was added until the final volume was 5 μL . This solution was placed at $70\text{ }^{\circ}\text{C}$ for 5 minutes and quickly transferred to ice, where it was incubated for 5 minutes. For a total reaction of 20 μL , the reaction constituents were added according to the manufacturer's instructions. The final concentration of the different components of the reaction is described in Table 6.2. in Appendix. In the T100 TM thermocycler (Bio-Rad, Portugal), the solution was incubated at $25\text{ }^{\circ}\text{C}$ for 5 minutes, $42\text{ }^{\circ}\text{C}$ for 1 hour and $70\text{ }^{\circ}\text{C}$ for 15 minutes. The complementary DNA (cDNA) synthesized was stored at $-20\text{ }^{\circ}\text{C}$ for future use.

2.7. Semi-Quantitative Reverse Transcriptase Polymerase Chain Reaction (sqRT-PCR)

In order to analyse the variation of the target genes expression (*PSY* and *LCYB*) during the growth curve, biomass samples were taken from cultures of 50 mL of *P. tricornutum* growing with basal concentration (0.882 mM) and 10-fold (8.82 mM) NaNO_3 . Samples were collected on day 4, 7, 11 and 18 of the curves. The RNA was extracted and treated. The cDNA was synthesized as mentioned above. The cDNA was diluted 10 times and 4 μL was used as template for the sqRT-PCR. The GoTaq Flexi DNA Polymerase (M7805, Promega, USA) was used, and in the T100 TM thermocycler (Bio-Rad,

Portugal) the following thermal cycling conditions were performed: initial denaturation at 95 °C for 2 minutes, followed by denaturation (95 °C for 1 minute), annealing (57 °C for *TBP* and *CDKA*; 58 °C for *PSY* and *LCYB*, for 30 seconds), extension (72 °C for 1 minute) and final extension of 72 °C for 10 minutes. Different number of cycles were used (25, 26 and 28 cycles for *TBP* and *CDKA*; 23 and 25 cycles for *PSY* and *LCYB*). As previously mentioned, to avoid gDNA amplification, primers designed with the exon-exon junction method were used (Table 2.2.). The *TBP* and *CDKA* genes from *P. tricornutum* were used as reference genes. The PCR product was loaded onto a 1.2% agarose gel (Appendix 3) and the gel was visualized on Gel Doc™ EZ (Bio-Rad, USA). The areas of the bands visible on the gel were analysed by the image processing package Fiji-Image J (<https://imagej.net/Fiji>). The relative density was calculated using the ratio of the target gene/ reference gene area.

2.8. Cell viability test

To observe the effects caused by different concentrations of NaNO₃ in the cultures of *P. tricornutum*, a cell viability test was performed with the dye Neutral Red 0.2 %. A volume of 20 µL of each culture (cells grown with 0.882, 8.82, 17.64 and 35.28 mM of NaNO₃) was collected, to which 2 µL of dye was added and incubated for 20 minutes, at room temperature, in the dark. A volume of 10 µL of the stained culture was placed on a glass slide with a cover glass (VWR, USA) and observations were made under an optical microscope (Leica DM6 B, Germany). Photographs to document the observations were taken using the colorDMC4500 camera integrated into the microscope and processed using Leica LAS X software.

3. RESULTS AND DISCUSSION

3.1. Analysis of the ethanolic extract from *Phaeodactylum tricornutum*

To determine the composition of the ethanolic extract of *P. tricornutum*, initially, a TLC was performed, which allowed the preliminary assessment of the extract pigments. In addition, HPLC analysis was carried out with the same extract, to assess the presence of any compounds not detectable by TLC, as well as the identification of the pigments considering their retention time and peak co-chromatography with the respective commercial standard.

On the TLC, the pigments were separated using hexane and acetone (described in subchapter 2.3.2. on Materials and Methods), and several commercial standards for visual identification (Neoxanthin, Violaxanthin, Fucoxanthin, Lutein and β -carotene) were used.

The TLC (Figure 3.1.A) showed three distinct pigments in concentrations high enough to be visually detected. Band A1 can possibly be identified as fucoxanthin, as it has a similar retention factor (Rf) to the fucoxanthin standard (FUC), however confirmation by HPLC is needed for correctly identify the pigment. Band A2 appears to be violaxanthin, as it has Rf similar to the second band of the corresponding standard (VIO), however it is not possible to identify it correctly. Band A3 has a green colour. Regardless the lack of commercial standard, studies previously performed in our laboratory demonstrate that this pigment detected is part of the chlorophylls group, however, with this technique it was not possible to identify the class of chlorophylls to which it belongs (chlorophyll *a* or *c*).

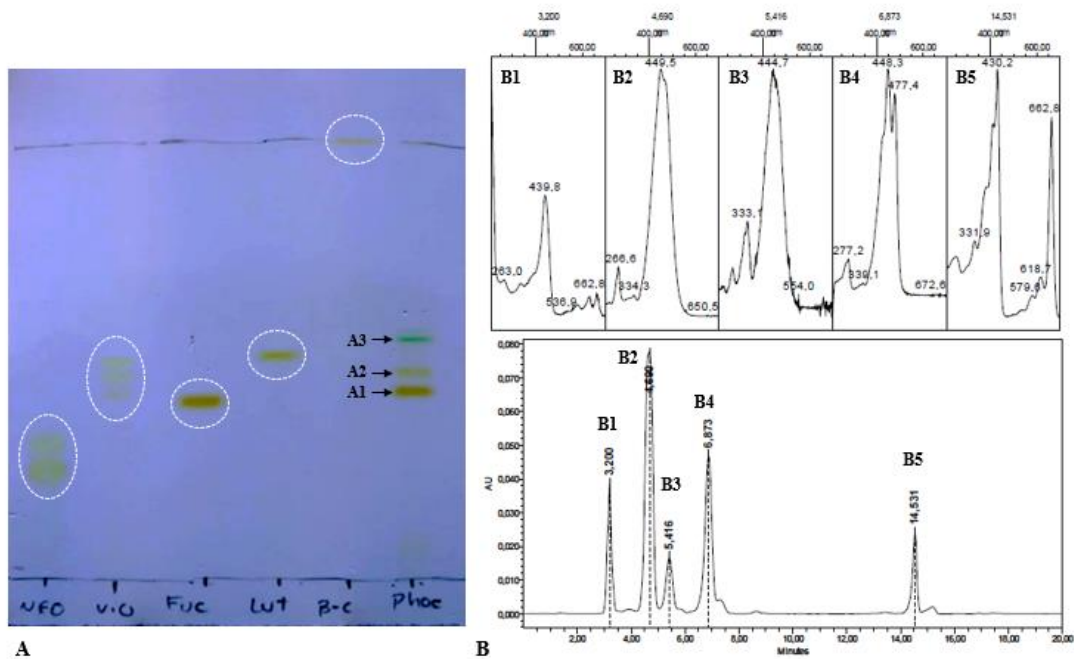


Figure 3.1. (A) Thin Layer Chromatography. White dashed line circles represent the bands of the commercial patterns. A1, A2 and A3 represent the bands of the ethanolic extract under analysis. Commercial Standards: NEO- Neoxanthin, VIO- Violaxanthin, FUC- Fucoxanthin, LUT- Lutein, β -C- β -Carotene. PHAE - ethanolic extract of *P. tricornutum*.

(B) High Pressure Liquid Chromatography spectrum of the ethanolic extract of *P. tricornutum* (bottom) and peak absorption profile (top). (B1) Chlorophyll *cl+c2*, (B2) all-*trans* fucoxanthin, (B3) *cis*-fucoxanthin, (B4) Diadinoxanthin and (B5) Chlorophyll *a*. The peaks B1, B4 and B5, require confirmation with commercial standard.

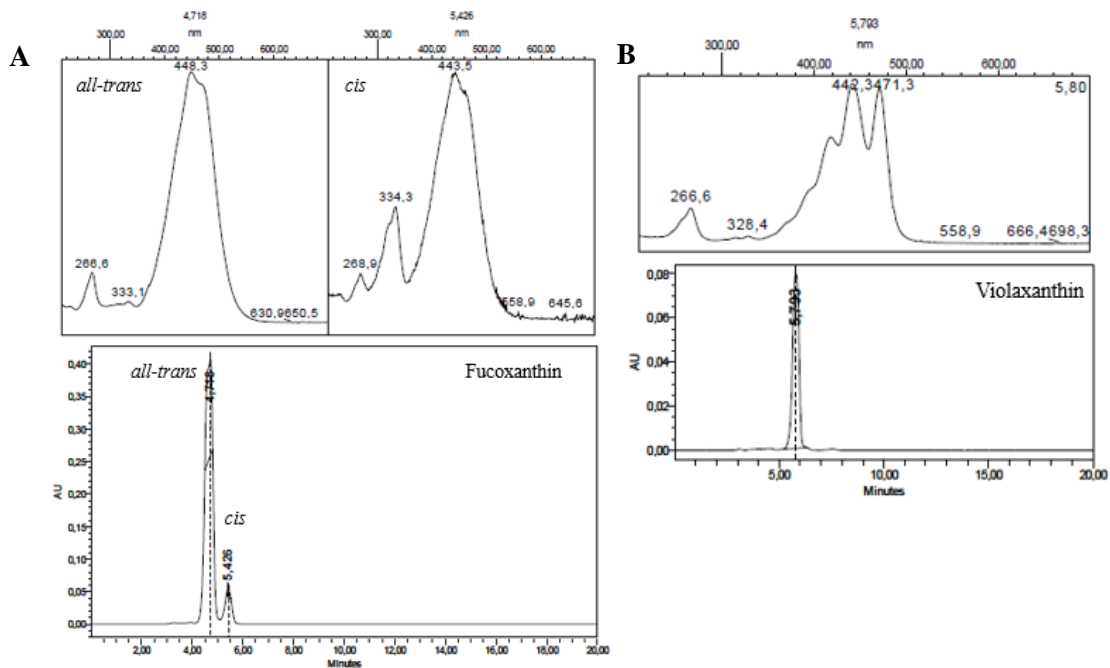


Figure 3.2. HPLC spectra and respective absorption peak profiles of commercial standards. Wavelength- 445 nm. (A) all-*trans* and *cis* isomers of fucoxanthin; (B) Violaxanthin.

The same extract from the TLC was run on HPLC (Figure 3.1.B). In this analysis, a C18 reverse phase column was used in the HPLC equipment coupled to a PDA system (conditions described in subchapter 2.3.3. on Materials and Methods). The PDA system allows the visualization of the peak profiles, observed in Figure 3.1.B on the top. These profiles enable the analysis of the absorption peaks that characterize the compounds.

There are few articles describing pigments that compose the extract of diatoms (Kraav, *et al.* 1992; Lohr & Wilhelm, 1999; Zapata, *et al.* 2000; Kosakowska *et al.* 2004). These reports describe different cultivation methods (light intensity/quality, nutrient supplementation, etc.) which can influence the pigment production. Nonetheless, in all studies the prevailing pigments are chlorophylls and fucoxanthin. In our ethanolic extract, peak A is a non-identified peak. Lohr & Wilhelm (1999) and Kosakowska *et al.* (2004), both observed a peak of a very polar pigment that appeared before the characteristic peak of fucoxanthin, which they identified as chlorophyll *c1+c2*. Observing the peak B1 absorption profile in our sample (Figure 3.1.B on top), it was possible to distinguish two absorption peaks at wavelengths around 440 and 663 nm, a typical profile of chlorophyll *c* (Yacobi, 2012).

Peak B2 and B3 were identified as all-*trans* and *cis* fucoxanthin isomers, respectively. These were both identified by the commercial standard (Figure 3.2.A). Peak B2 has a higher peak area, which presupposes a higher concentration of the compound in the extract, being this also visible in the TLC (band A1 in Figure 3.1.A). The *cis*-fucoxanthin isomer, on the other hand, has a low concentration, being neither visible in the extract of *P. tricornutum* nor in the commercial standard on the TLC plate. Kuznestsova and co-workers (2017) demonstrates that this isomer shows a characteristic absorption peak at 330 nm, being clearly distinguished by its absorption profile compared to the *trans* isomer.

Peak B4 may correspond to TLC band A2. The TLC technique does not detect low concentrations of pigments, so it may be assumed that when bands are detected on the TLC plate, it like corresponds to a high concentration of those pigments in the extract used, as observed for band A2 with an expressive peak in the HPLC (Peak B4 in Figure 3.1.B). This compound could be violaxanthin, by visual comparison with the given standard on the TLC, however, the retention times in HPLC differ. Although the violaxanthin pattern (Figure 3.2.B) and peak B4 (Figure 3.1.B) both have a double absorption between 440 and 480, the retention times are 5.79 and 6.87 minutes, respectively. Thus, it can be concluded that peak B4 is not violaxanthin. In a study carried out by Lohr & Wilhelm (1999), the authors observed a peak after the fucoxanthin peak, which was identified as the pigment diadinoxanthin. This is a more non-polar compound than fucoxanthin due to the absence of the carbonyl group, and derived from neoxanthin, as well as fucoxanthin (Figure 1.5.). Therefore this peak could be diadinoxanthin, however confirmation with the appropriate standard is required.

Peak B5 may correspond to band A3 of the TLC. From the HPLC peak profile (Peak B5 in Figure 3.1.B), could be suggested that this pigment is chlorophyll, namely chlorophyll *a*, since *P. tricornutum* does not produce chlorophyll *b*. This evidence is supported by the HPLC peak profile, which demonstrate two characteristics peak absorbances of chlorophyll, at 430 and 663 nm (Figure 3.1., B5 on

top). The same peak was observed for different diatoms in the studies carried out by Lohr & Wilhelm (1999) and Kosakowska *et al.* (2004) for *P. tricornutum* and Zapata, *et al.* (2000) for *Skeletonema costatum*.

Xia and collaborators (2013) also observed the same pattern of pigments produced for another diatom (*Odontella aurita*).

3.2. Screening of Carbon and Nitrogen Sources for Optimization of Growth and Fucoxanthin Production

In this work, a 6-well microplate screening was performed, with biological triplicates, for various sources of nitrogen and carbon, in order to evaluate the effect of these compounds on cell growth and production of fucoxanthin by *P. tricornutum*. A concentration range of each of the nitrogen and carbon sources was used. Once the original f/2+Si medium developed by Guillard R.R.L. (1975), does not contain any carbon source, only the N source was removed from the original recipe in order to use as a control in this microplate assay. Thus, the control used was a modified f/2+Si medium without addition of N or C sources, in order to exclude any influence of both sources in growth and fucoxanthin production. The *P. tricornutum* cells used, were not subjected to any previous adaptation to the different media formulation, growing only with f/2+Si medium supplemented with silica and basal concentration of NaNO₃, according to Guillard R.R.L. (1975). It is known that the pigments produced by this diatom are carotenoids that absorb between 440 and 480 nm, and chlorophylls *a* and *c*, which have two absorption maxima between 430-440 and 663 nm. Therefore, to follow the cell growth, the wavelength used to read the optical density was 595 nm, where there is no absorption of any of the compounds produced. The same wavelength was used by Huete-Ortega (2018), who developed a study with *Nannochloropsis oceanica* and *Phaeodactylum tricornutum*, to assess cell growth.

3.2.1. Nitrogen (N) Sources: Sodium Nitrate, Ammonium Chloride and Urea

In order to assess the effect of the different N sources tested, cell growth was followed for 7 days through OD readings at 595 nm.

Figure 3.3. shows the growth curves of the cultures growing in f/2+Si medium with different concentrations of sodium nitrate (NaNO₃), ammonium chloride (NH₄Cl), urea (CH₄N₂O) or in control conditions (f/2+Si without N or C source).

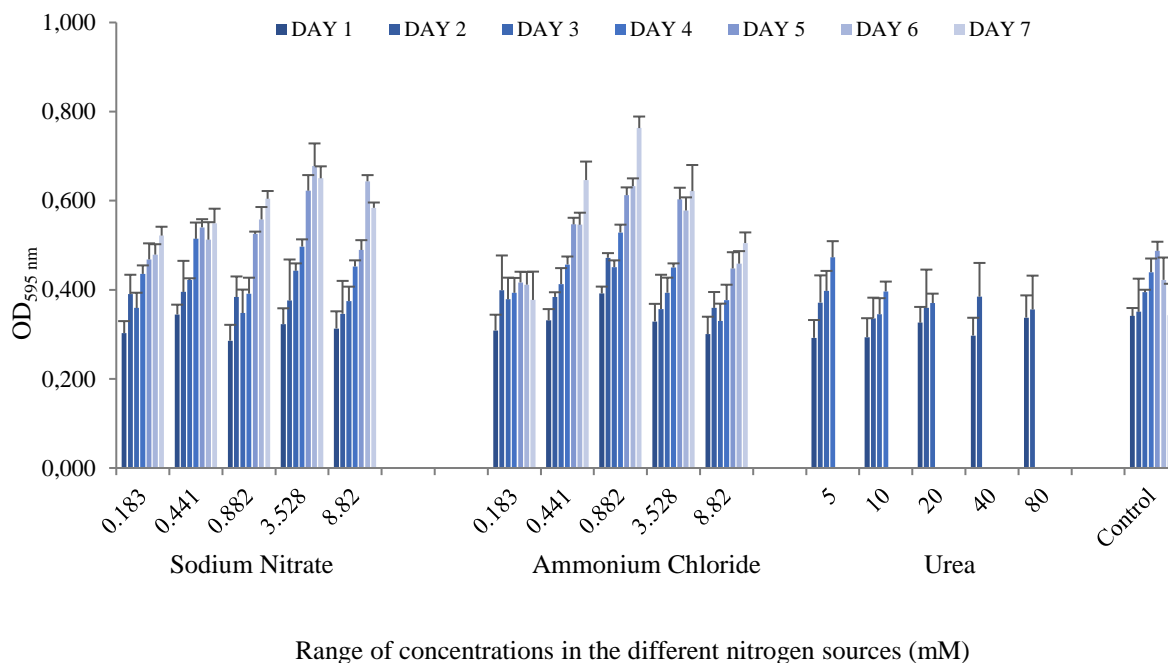


Figure 3.3. Growth curves for 7 days of growth, of the concentration range for each of the nitrogen sources. Control represents cultures that have grown in modified f/2+Si medium, without N or C. ($n = 3$)

For NaNO_3 and NH_4Cl media, as the concentration of these two nitrogen sources increases, the optical density gradually increases, with the maximum OD achieved at the concentrations of 3.528 mM to NaNO_3 and 0.882 mM to NH_4Cl , in the last days of the curve.

These results are very similar, and it is difficult to draw conclusions on which of the nitrogen sources maximize cell growth. It is noteworthy that these results may not be the same as when the cultures are grown in flasks (Haire, *et al.* 2018). Therefore, it is necessary to confirm these results, scaling up the cultures under analysis. However, it is possible to state that the addition of both sources of nitrogen favoured cell growth. On the 7th day, the t-test for independent samples showed that differences in cell growth were statistically significant when was added the concentration of 3.528 mM of nitrate to cultures (nitrate concentration with higher growth), compared to the control ($t_{(4)}=13.69$; $p < 0.001$). However, for the concentration of 0.882 mM of ammonia (ammonia concentration with higher growth), the t-test for independent samples indicated that the differences were not significant compared to the cultures without N, besides the beneficial effect in growth ($t_{(4)} = 2.28$; $p = 0.08$). These results indicate that the cultures may have a greater capacity for assimilation of nitrate, compared to ammonia.

Urea can decompose when exposed to heat sources, becoming one of the problems associated with its use for cultivation of microalgae. Urea must be added aseptically after sterilization (Andersen, 2005; Podevin, *et al.* 2015). Urea is converted to bicarbonate and ammonium by enzymatic conversion.

White deposits appeared at the bottom of the wells (Figure 3.6.B), which compromised the reading of the optical density. This is probably due to the fact that the f/2+Si medium was autoclaved with urea.

Thus, it was not possible to assess the effect of urea on cell growth. However, a study developed in our laboratory by Fontebasso (2021), who added sterile urea after the f/2+Si medium was autoclaved, observed that the growth of *P. tricornutum* was not enhanced by the addition of 1x urea, compared to the commercially used basal medium (f/2+Si medium supplemented with 1x nitrate) (unpublished data).

After 7 days of growth, the microplates were photographed in order to observe the colour variation of the cultures supplemented with different types and concentrations of N sources (Figure 3.4.-3.6).

The browner cultures correspond to the ones supplemented with 3.528 mM and 0.882/3.528 mM of nitrate and ammonia, respectively (Figure 3.4.). The addition of any of the concentrations under study from both sources had a positive effect on the cultures when compared to the control (Figure 3.5.). As for cultures supplemented with urea (Figure 3.6.), it was possible to observe that, after 7 days, the densest cultures correspond to the lowest concentrations (5 and 10 mM). This evidence may be justified by the fact that the urea metabolism releases ammonia into the medium, becoming toxic to cells, inhibiting the growth (Glibert, *et al.* 2016). Thus, higher concentrations (more than 10 mM) of urea induce a negative effect on cultures.

In addition, it was possible to observe that at the highest concentrations of ammonium chloride and urea, on the 7th day, which could be cell aggregates or cell debris (Figures 3.4.B and 3.6.). This may be a response of the cultures to the toxic conditions of growth, forming cell aggregates in an attempt to survive on the environment where they are growing or a process of cell lysis.

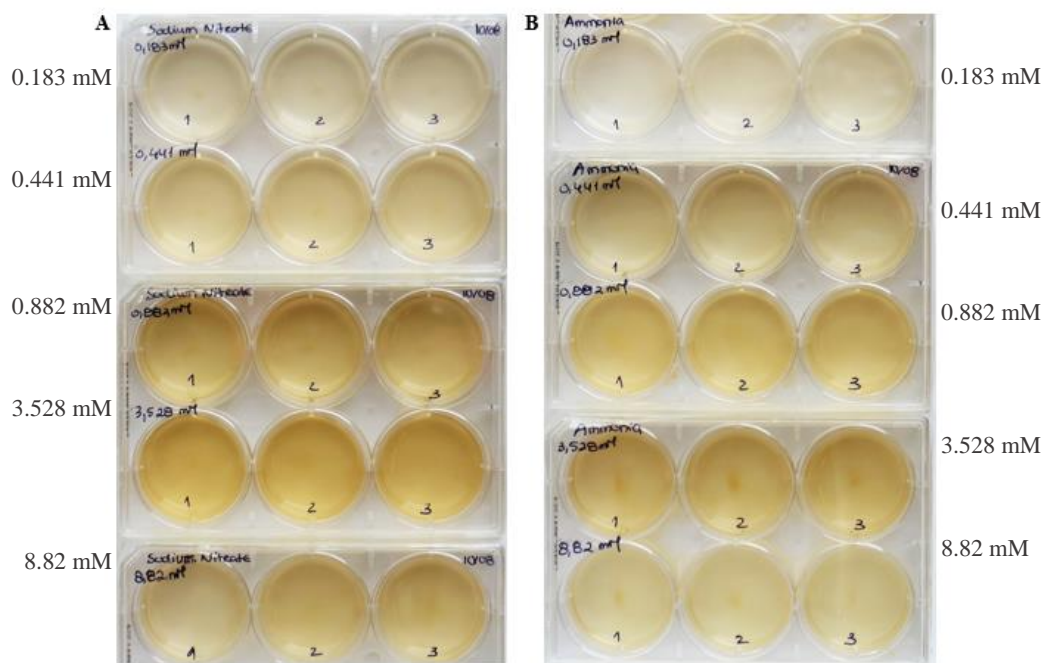


Figure 3.4. Microplates with cultures supplemented with sodium nitrate (A) and ammonium chloride (B), on the 7th day of growth. Concentrations are in ascending order, from top to bottom (0.183, 0.441, 0.882, 3528 and 8.82 mM, for both N sources).

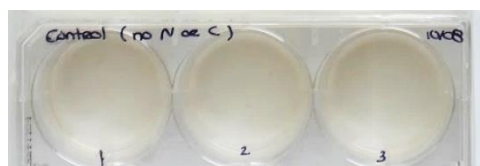


Figure 3.5. Microplate with control cultures f/2+Si without N or C, on the 7th day of growth.

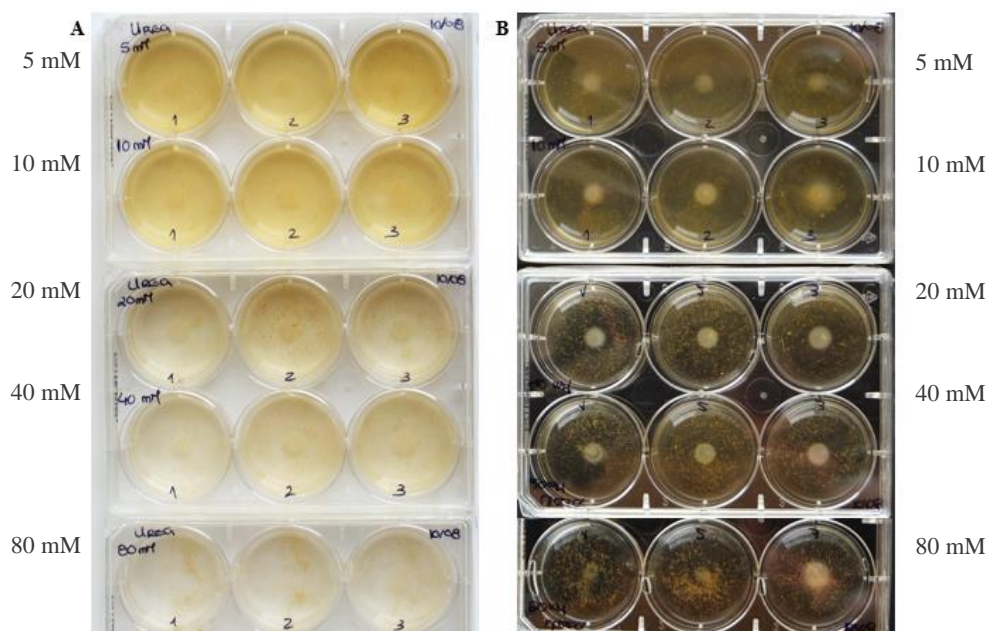


Figure 3.6. Microplates with cultures supplemented with urea, with a white background (A) and with a dark background (B), on the 7th day of growth. Concentrations are in ascending order, from top to bottom (5, 10, 20, 40, 80 mM).

3.2.2. Carbon (C) Sources: Glucose and Glycerol

In order to assess the effect of the different carbon sources tested, cell growth was followed for 7 days through OD readings at 595 nm.

Figure 3.7. shows the growth curves in f/2+Si medium modified with a concentration range tested for glycerol (C₃H₈O₃) or glucose (C₆H₁₂O₆).

The results obtained in Figure 3.7. indicate that the addition of carbon sources in N-deprived cultures do not favour the cell growth, compared to the control cultures. It also was possible to observe that over the 7 days, there was a slight increase in OD, however the addition of C sources does not represent a visibly positive effect on growth, in general. On 7th day of growth, the t-test for independent samples demonstrated that none of the glycerol concentrations added to the cultures, resulted in significant differences in growth compared to the control. However, for glucose, on the 7th day of growth, the t-test demonstrated the effect of glucose addition in the culture growth, compared to control, except for the concentration of 60 mM where the differences were not significant ($t_{(4)}=2.52$; $p = 0.06$). It is also

observed that higher concentrations of glycerol (> 50 mM) tend to inhibit the growth. This evidence is noted in Figure 3.8A., in which the cultures have a very light colour, similar to the control (Figure 3.5.).

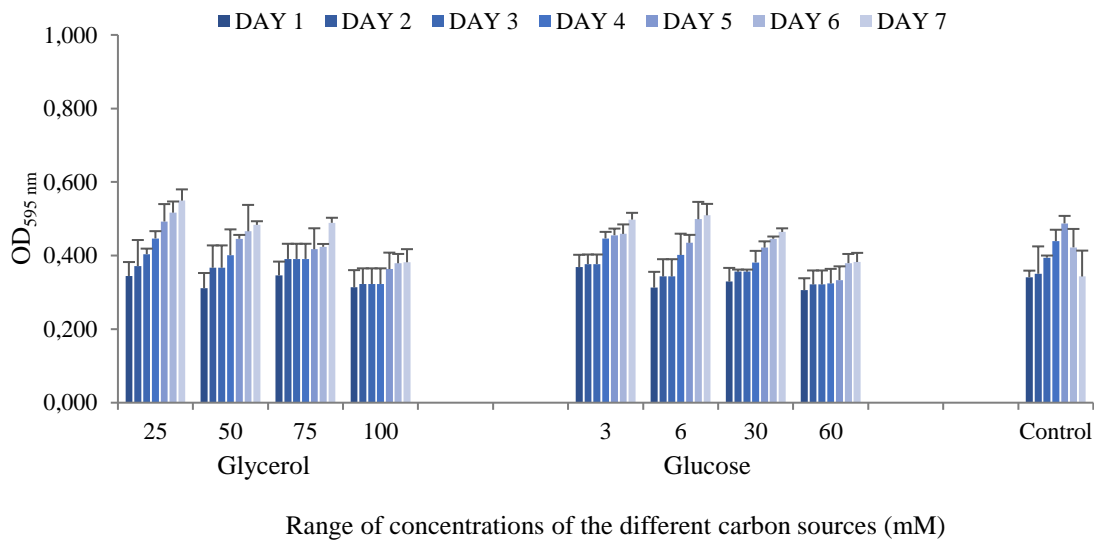


Figure 3.7. Growth curves followed for 7 days, of the concentration range for each of the carbon sources. Control represents cultures that have grown without any source of nitrogen or carbon. ($n = 3$)

Other studies demonstrated that the addition of glycerol stimulates growth of *P. tricornutum*, compared to the cultures in photoautotrophic regimen, without addition of nutrients (Ceron, *et al.* 2006), which indicates that the use of a nutrient rich environment is an optimization strategy to grow diatoms. However, the authors noted that high concentrations of glycerol (> 100 mM) inhibited growth (Ceron, *et al.* 2006; Huete-Ortega, *et al.* 2018).

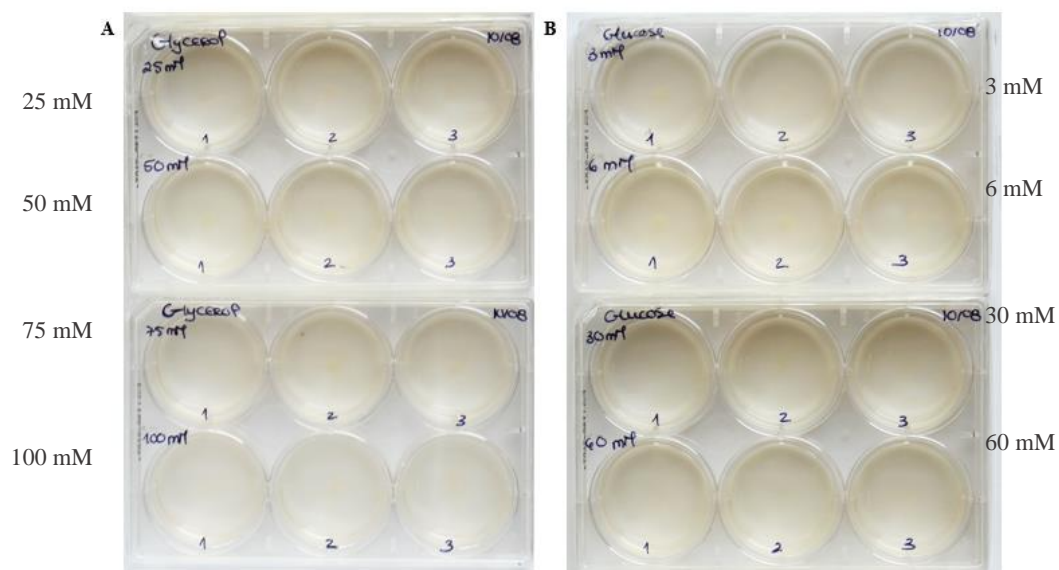


Figure 3.8. Microplates with cultures supplemented with glycerol (A) and glucose (B), on the 7th day of growth. Concentrations are in ascending order, from top to bottom (glycerol: 25, 50, 75 and 100 mM; glucose: 3, 6, 30 and 60 mM).

3.2.3. Fucoxanthin Production

On the 7th day of the growth curve, an ethanolic extract was prepared for the cultures growing with the various sources of nitrogen (Sodium Nitrate and Ammonium Chloride) and carbon (Glycerol and Glucose), using biological triplicates for each condition. Cultures growing at f/2+Si without nitrogen or carbon (Control) were also evaluated. Cultures supplemented with urea were discarded, given the circumstances mentioned above.

The ethanolic extracts were analysed by HPLC and the commercial standard of fucoxanthin was used to identify the pigment of interest. The results are shown in Figure 3.9., in mg of fucoxanthin per litter of culture (mg/L).

By analysing Figure 3.9., it was possible to observe that the cultures with higher concentration of fucoxanthin correspond to the cultures that also show the highest cell growth rate (Figure 3.3.), and consequently a more intense brown colour (Figure 3.4.), which correspond to the concentrations of 3.528 and 0.882 mM nitrate and ammonia, respectively. Similar results were reported by García, *et al.* (2005), who suggest that the increase in pigment content is dependent on the increase of biomass concentration. For both nitrogen sources, it is possible to notice that the concentration of fucoxanthin increases proportionally with the concentration of nitrogen, until 3.528 and 0.882 mM with sodium nitrate and ammonium chloride, respectively, decreasing afterwards. On the 7th day of growth, the t-test for independent samples demonstrated that the addition of either of the two N sources, regardless the concentration, always had beneficial effects on fucoxanthin production as compared to the control. In contrast, the independent addition of the two C sources, regardless the concentration, did not lead to differences in fucoxanthin production when compared to the control.

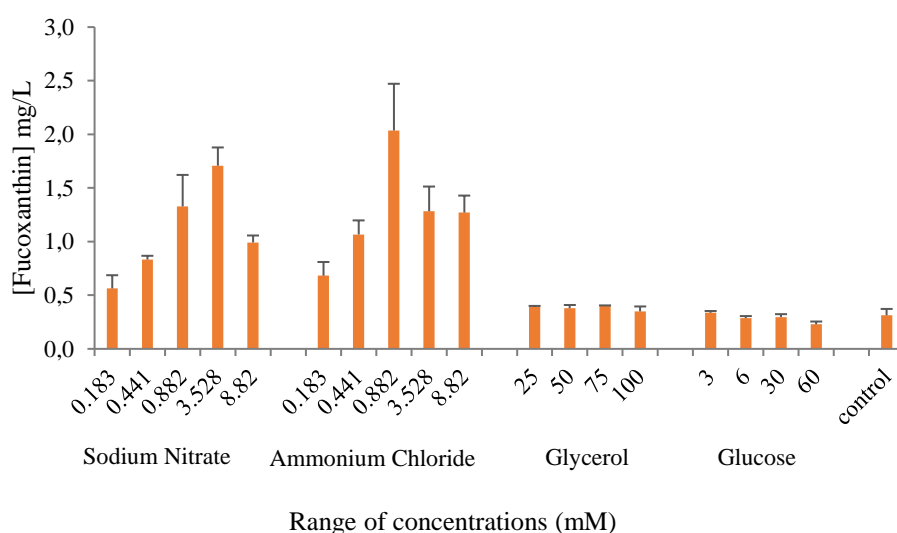


Figure 3.9. Fucoxanthin concentration for the range of concentrations in different sources of nitrogen and carbon, analysed by HPLC, on the 7th day of the curve. Standard deviation represents the analysis of three biological replicates. Concentration of Fucoxanthin represented in mg of fucoxanthin per litter of culture. Control represents cultures that have grown in f/2+Si without N or C sources. ($n=3$)

This evidence is consistent with other studies. For example, in a study carried out by McClure and co-workers (2018), it was observed that the increase in nitrate supplementation in the f/2 medium, significantly increases the concentration of fucoxanthin produced, as a response of cells to the availability of nitrate. The same authors also demonstrated that the addition of 10-fold in phosphate did not promote the production of this pigment, indicating that the nitrogen source may be limiting for the production of pigments by algae (McClure, *et al.* 2018).

As observed in Figures 3.5. and 3.8., which show the photographs of microplates of the cultures growing with f/2+Si without N or C and the cultures supplemented with glycerol and glucose, respectively, the cultures have a very light colour, consistent with reduced cell growth (Figure 3.7.) and low fucoxanthin production (Figure 3.9.).

In the absence of N, the proteins associated with the light harvesting complexes are poorly expressed and their downregulation promotes a low absorption of light. The decrease in photosynthetic activity inhibits carbon fixation, and the assimilation of carbon is compensated by the high accumulation of lipids (Yang, *et al.* 2014). This evidence indicates that the N starvation does not favour the production of pigments but promotes the production of lipids, being an advantage for the production of biodiesel.

Thus, it is evident that in order to increase the production of fucoxanthin in *P. tricornutum* cultures it is crucial to consider two factors: the type N source and the concentration added, since very high concentrations may become toxic to the cells and low concentrations do not enhance pigment production.

3.3. Prediction of the interaction between N and C sources by “Design of Experiments” (DoE)

To predict the interaction between the N and C sources of biological screening systems in microplates, the “DoE” approach using Modde® v.13 software (Sartorius) was used. The optical density at 595 nm and the fucoxanthin concentration (mg/L) were used as response parameters for the predictive models.

Figure 3.10. represents the prediction plots for each one of the sources of N (Sodium Nitrate and Ammonium Chloride) and C (Glycerol and Glucose), individually, in the two responses analysed. With the increase in the concentration of N sources (Figure 3.10. A and B), the models do not predict perceptible changes in the concentration of fucoxanthin, however a gradual increase in OD was observed with the increase in N concentration, showing the effect of N in cell growth. On the contrary, the models predict, for both C sources, a similar pattern of a decrease in the concentration of fucoxanthin and the OD, as the concentration of the C sources increases (Figure 3.10. C and D). It is necessary to emphasize that, in order to have an optimization model, it would be necessary to find, experimentally, the concentration limits that respond as extremes for biological systems, where the objective is to reach a solution in which the response is within the specification limits (minimum and maximum limits), so that the models could robustly predict the response, and whose predictions can be applied to maximize both growth and fucoxanthin.

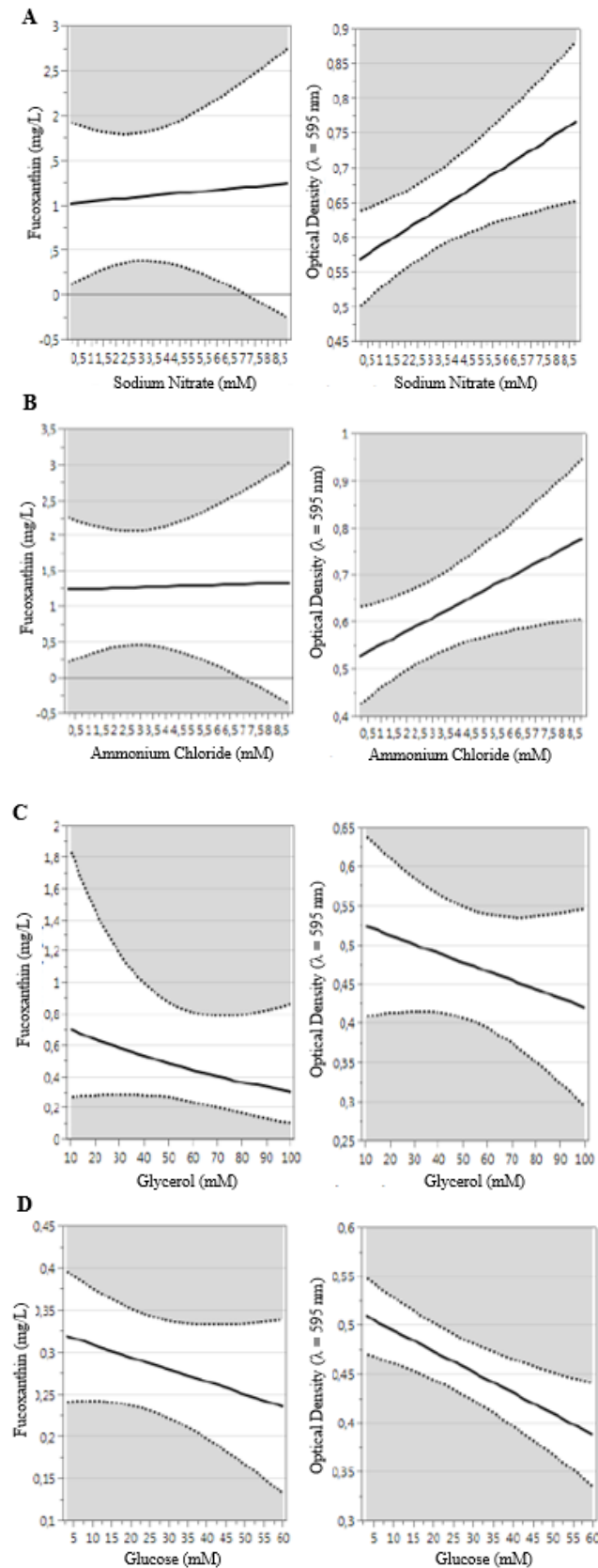


Figure 3.10. The prediction plots of “Design of Experiment”. The solid line represents the predicted value, while the dashed line represents the upper and lower limits of the confidence interval (95%). Predicted responses of Fucosanthin (mg/L) and Optical Density ($\lambda = 595$ nm) for (A) Sodium Nitrate, (B) Ammonium Chloride, (C) Glycerol, (D) Glucose.

Figure 3.11. demonstrates the contour plots of factor interaction (N versus C sources) and the prediction of responses when both factors interact. The colour system represents the predicted response when the interaction of factors occurs. A beneficial interaction is considered the red colour. Blue colour represents values in which the interaction has a negligible effect. In all plots, the model's behaviour is similar and demonstrates that in order to obtain high OD and fucoxanthin values, high concentrations of N sources and low concentrations of C sources will be necessary. For example, Garcí (2000) noted that when a N source is added to cultures growing with a C source, such addition favours growth, much more than the cultures growing only with carbon source.

Thus, the prediction models analysed allow us to conclude that the addition of glycerol or glucose does not contribute positively to cell growth and fucoxanthin production by *P. tricornutum* cells. Given the results obtained, the scale up tests were performed for N source.

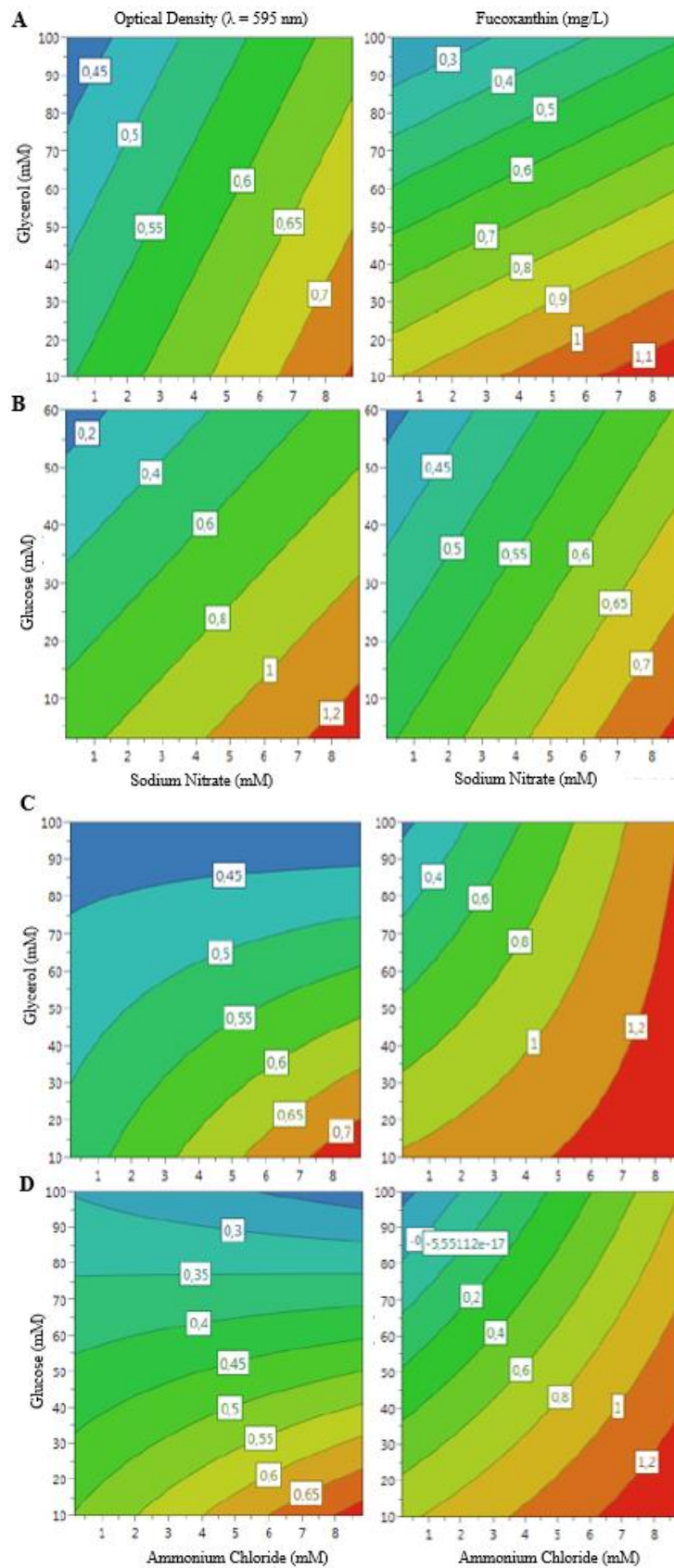


Figure 3.11. Response contour plots of factors interaction, showing effect of Optical Density ($\lambda = 595$ nm) and Fucoxanthin (mg/L). (A) Glycerol and Sodium Nitrate, (B) Glucose and Sodium Nitrate, (C) Glycerol and Ammonium Chloride, (D) Glucose and Ammonium Chloride, (D) Glucose and Ammonium Chloride.

3.4. Scale-up of the cultures supplemented with N source

By analysing the models of each of the N sources (Figure 3.10. A and B), it is not clear which is the best source to choose. Differently, it would be advantageous to choose NH_4Cl because the best results were obtained with a lower concentration (0.882 mM), compared to NaNO_3 (3.528 mM), reducing the associated costs. As previously mentioned, NH_4^+ is preferentially assimilated by cells as compared to NO_3^- (Glibert, *et al.* 2016). On the contrary, it is not evident that supplementation of one or another source of N will be energetically beneficial for the increase in biomass (Grobbelaar, 2004). Thus, the nitrogen source chosen for the following tests was sodium nitrate, since it is already one of the constituents of the f/2 medium for the cultivation of diatoms. Different concentrations of this nitrogen source were used to scale up the cultures for 50 mL.

3.4.1. From N-free cultures to 10-fold NaNO_3 supplementation

3.4.1.1. Growth Curve

The scale-up assay for *P. tricornutum* cultures in 250 mL flasks was performed using biological duplicates from a wide range of concentrations, from N-free cultures (0 mM) to cultures supplemented with 10-fold NaNO_3 (8.82 mM). Like in the microplate assay, the growth of the cultures was followed over 7 days, establishing growth curves by counting the number of cells under the microscope (Figure 3.12.). In this study, the growth was evaluated through cell counting, to minimize the culture harvesting in order to perform further extractions of fucoxanthin for HPLC, at the end of the growth period (7th day). The initial inoculum for all cultures came from a single culture growing under basal conditions (0.882 mM of NaNO_3), with the average initial number of cells at day 0 being $3.04 \times 10^6 \pm 2.91 \times 10^4$ cells/mL for all cultures.

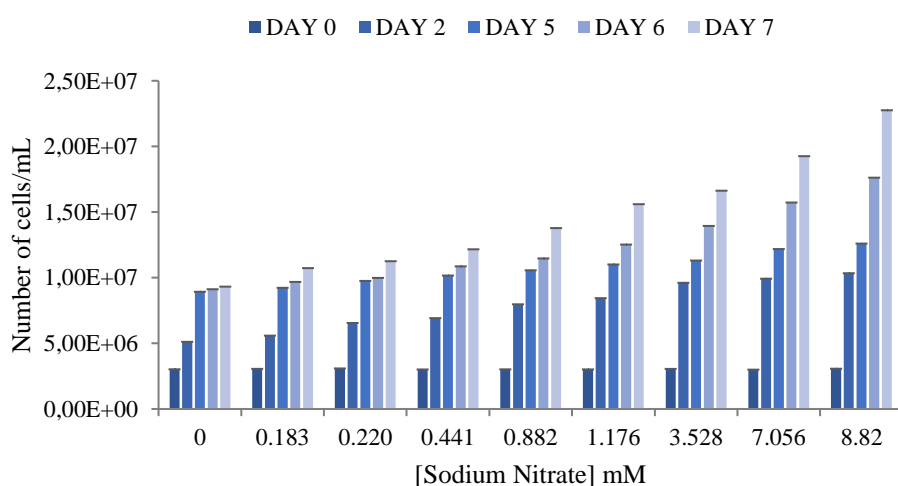


Figure 3.12. Growth curves of the 50 mL cultures supplemented with various concentrations of Sodium Nitrate. Curves were followed at day 0, 2, 5, 6 and 7, after inoculation. The number of cells is represented in cells per millilitre. ($n=4$)

It was possible to observe that cultures not supplemented with NaNO₃, presented a relatively short growth curve, ceasing growth from day 5. As predicted in the model of Figure 3.10.A for the OD, the higher the concentration of NaNO₃, the greater is the cell growth. The addition of NaNO₃ tends to show an acceleration of cell growth early on the curve. When the NaNO₃ concentration is higher, it was observed that the number of cells is greater in the first days at the growth. For example, on day 2, cultures with 10-fold NaNO₃ had approximately 2-fold cells (1.03×10^7 cells/mL) than cultures without supplementation of this nutrient (5.12×10^6 cells/mL).

The basal concentration of NaNO₃ in the f/2 medium is 0.882 mM. It is a concentration that allows to maintain cell growth without this nutrient becoming a limiting factor for the cells, for 7 or 8 days of growth. After this time, due to lack of available nutrients, the cell division will be reduced, and the number of dead cells will increase (McClure, *et al.* 2018). It was observed that on the 7th day, cultures with 10-fold nitrate (8.82 mM), approximately doubled in number of cells ($2.28 \times 10^7 \pm 2.76 \times 10^5$ cells/mL), compared to the cultures growing with 0.882 mM of NaNO₃ ($1.38 \times 10^7 \pm 7.93 \times 10^4$ cells/mL). The t-test for independent samples showed that, on the 7th day, the growth in these two types of supplementations is statistically different ($t_{(6)}=62.62$; $p < 0.001$). Thus, in the range of concentrations studied, it is evident that the greater the availability of N in the medium, the more favoured is the growth. This evidence can also be observed in Figure 3.13., which represents the cultures on the 7th day.

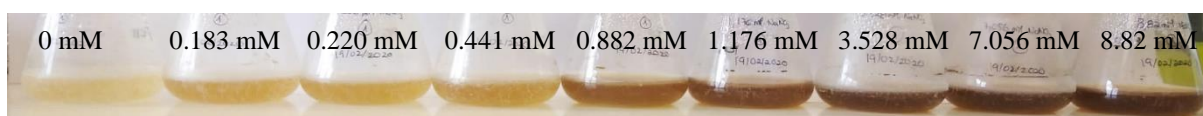


Figure 3.13. 50 mL culture flasks supplemented with various concentrations of Sodium Nitrate, on the 7th day of growth. Concentrations are in ascending order, left to right, from 0 mM to 8.82 mM.

3.4.1.2. Fucoxanthin Production

On the 7th day, the above-mentioned cultures were subjected to ethanol extractions to quantify fucoxanthin by HPLC. The results are shown in Figure 3.14. Xia and collaborators (2013) demonstrated that one of the best organic solvents for extracting fucoxanthin is ethanol, in a ratio of 30 μ L to 1 mg of algal biomass. The same authors observed that, for a greater increase in yield, extraction should be carried out at 45°C for more than 60 minutes (Xia, *et al.* 2013). Thus, in this study the same procedures were adopted, in order to maximize the extraction of fucoxanthin.

It was possible to observe that as the NaNO₃ concentration increase, the concentration of fucoxanthin also gradually increases. The concentration of this pigment was relatively low (around 1 mg/L) at lower NaNO₃ concentrations, when compared to fucoxanthin produced by cultures with the nitrate concentration of 0.882 mM (basal concentration) (Figure 3.14.). An interesting fact is that the cultures with 10-fold NaNO₃ produced, on average, 2 times more fucoxanthin than cultures with 1-fold NaNO₃

concentration, with a fucoxanthin productivity on day 7 of 1.23 and 0.59 mg/L/day, respectively. This clear increase in production was also observed in a bioreactor study by McClure and co-workers (2018), who evaluated the role of different media in the production of fucoxanthin in *P. tricornutum*. The authors observed that fucoxanthin productivity at day 7 was much higher for cultures growing with 10-fold nitrate (2.16 mg/L/day) than a basal concentration f/2 medium (0.64 mg/L/day). The same study demonstrates that the increase of other factors such as light intensity and/or the concentration of carbon dioxide, did not contribute to the increase in the production of fucoxanthin, being the most influential factor the high addition of nitrate to the cultures (McClure, *et al.* 2018).

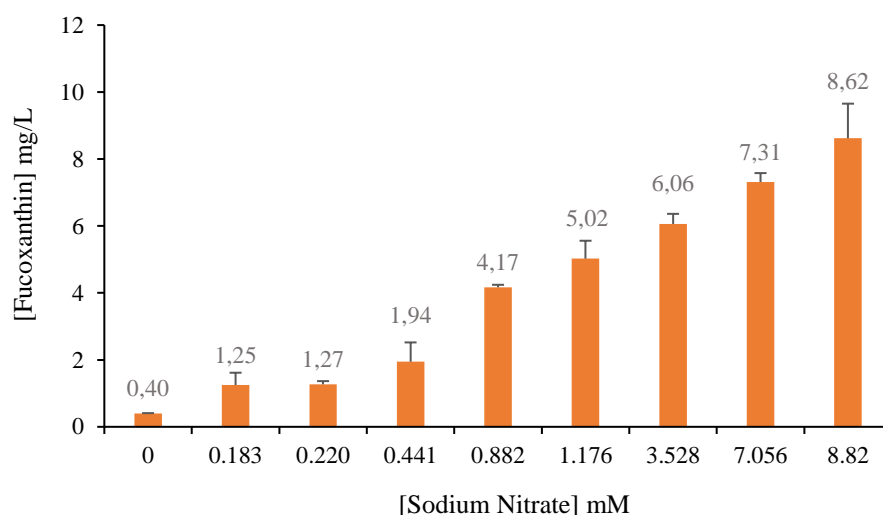


Figure 3.14. Fucoxanthin concentration of the cultures supplemented with f/2+Si medium modified with different concentrations of Sodium Nitrate, on 7th day of growth. The concentration was quantified by HPLC using a standard curve with a pure fucoxanthin standard. Fucoxanthin expressed in mg of Fucoxanthin per liter of culture. ($n=2$)

3.4.2. From Basal to 40-fold NaNO₃ Supplementation

Nitrate concentrations higher than 10-fold (8.82 mM) were also tested. Biological triplicates were used for each experimental condition, and the growth curves were followed for 20 days, in order to reach the stationary phase. In this assay, the growth curves were followed by reading the OD at 750 nm, with three independent readings of 200 μ L for each well, on a 96-well plate. The OD readings were performed at 750 nm in order to follow the growth curves and to calculate the fucoxanthin produced using the formula described by Wang, *et al.* 2018 (see subchapter 2.3.4. in Materials and Methods).

3.4.2.1. Cell Growth

Figure 3.15. shows the growth curves over 20 days, for cultures with high concentrations of NaNO₃. All cultures started growth with an average OD of 0.657 ± 0.03 (which corresponds approximately to $1.92 \times 10^6 \pm 9.23 \times 10^4$ cells/mL).

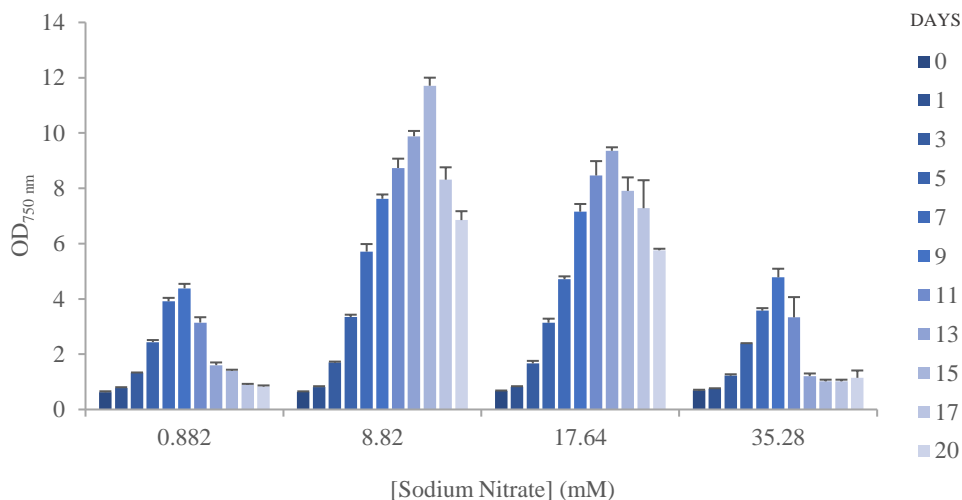


Figure 3.15. Growth curves of *P. tricornutum* cultures supplemented with 0.882 (1-fold), 8.82 (10-fold), 17.64 (20-fold) and 35.28 (40-fold) mM of NaNO₃. Curves followed for 20 days by reading OD at 750 nm. ($n=9$)

As shown by McClure *et al.* (2018), the concentration of 0.882 mM NaNO₃ in cultures of *P. tricornutum*, only allows growth for 8 days, with a decline in the availability of nutrients, cell growth is no longer supported. Our results demonstrated that after 9 days, cultures with the basal concentration of NaNO₃, entered the cell death phase, with a gradual decrease in OD, until the 20th day. On day 9, when OD at 750 nm was maximum for cultures supplemented with the basal concentration of nitrate (0.882 mM), the t-test for independent samples showed that there was an effect on growth when 8.82 mM (10-fold) of nitrate was added to the cultures, compared to the addition of 0.882 mM (1-fold) of nitrate ($t_{(16)}=14.23$; $p < 0.001$). Cultures with 10-fold nitrate grow, approximately, two times more (day 9, OD_{750 nm} (8.82 mM) = 7.62 ± 0.57) when compared to cultures with 1-fold nitrate (day 9, OD_{750 nm} (0.882 mM) = 4.38 ± 0.37).

Cultures supplemented with 8.82 mM (10-fold) and 17.64 mM (20-fold) of NaNO₃, obtained the greatest cell growth rate, and cultures with 10-fold nitrate, obtaining the highest OD values. Cultures supplemented with these concentrations showed a significant increase in cell growth over the days, reaching the stationary phase at day 15 and 13, for concentrations of 8.82 mM and 17.64 mM, respectively. Comparing the two concentrations, it may be suggested that the concentration of 17.64 mM, 20-fold nitrate, showed an apparent toxicity in the culture, given that it reached the stationary phase earlier, however further studies are necessary to confirm this hypothesis. The t-test for independent samples showed that there were differences in cell growth between cultures supplemented with concentrations of 8.82 mM and 17.64 mM of nitrate, at 15th of growth, the day when the OD was

maximum for the concentration of 10x nitrate ($t_{(16)}=15.18; p < 0.001$). Cultures with 10-fold nitrate have, on average, 1.5 times more cell density ($OD_{750\text{ nm}}(8.82\text{ mM}) = 11.71 \pm 0.46$), when compared to cultures with 20-fold nitrate ($OD_{750\text{ nm}}(17.64\text{ mM}) = 7.91 \pm 0.59$). Thus, becomes evident the clear beneficial effect of adding a concentration of 8.82 mM nitrate to *P. tricornutum* cultures to optimize cell growth.

The cultures supplemented with 40-fold nitrate (35.28 mM) showed a behaviour similar to the cultures with basal concentration. However, in cultures with 40-fold nitrate, the response given by the decrease in OD will not be due to the total consumption of nitrate in the medium but may be due to the excess of toxic metabolites produced by N metabolism. This evidence may be justified by the fact that nitrate is assimilated, converted to nitrite and later to ammonia (Alipanah, *et al.* 2015), which in high concentrations is inhibitory to cell growth (Glibert, *et al.* 2016). By working with a concentration of 35.28 mM NaNO_3 , we are supplementing 3 g/L of N to the cultures, inducing toxicity and possibly causing physiological stress to the cells.

Other studies have been performed to evaluate the role of other sources of N in cell growth. For example, Fontebasso (2021) carried out a study, in our laboratory, where cultures of *P. tricornutum* were supplemented with different N sources. The authors observed no differences in the growth of cultures when supplemented with 1-fold nitrate, 1-fold urea or 1-fold ammonium carbonate. As for cultures supplemented with nitrate, greater growth was observed when cells were supplemented with 10-fold nitrate, compared to 1-fold nitrate (unpublished data), corroborating also the results obtained in this thesis.

On days 0, 3 and 5, photographs were taken of the flasks containing 50 mL of culture, in the various experimental conditions. In Figure 3.16., it was possible to observe the brown colour intensification in the cultures and the clear differences between the various concentrations. On the 5th day it was found that the first and last flasks, which correspond to 0.882 mM and 35.28 mM, respectively, have a similar colour, with a parallel behaviour in the growth curves (Figure 3.15.). The concentrations of 10 and 20-fold nitrate (2nd and 3rd flasks) resulted in darker colours in the cultures, showing similar results both in colour (Figure 3.16.) and in cell growth (Figure 3.15.).

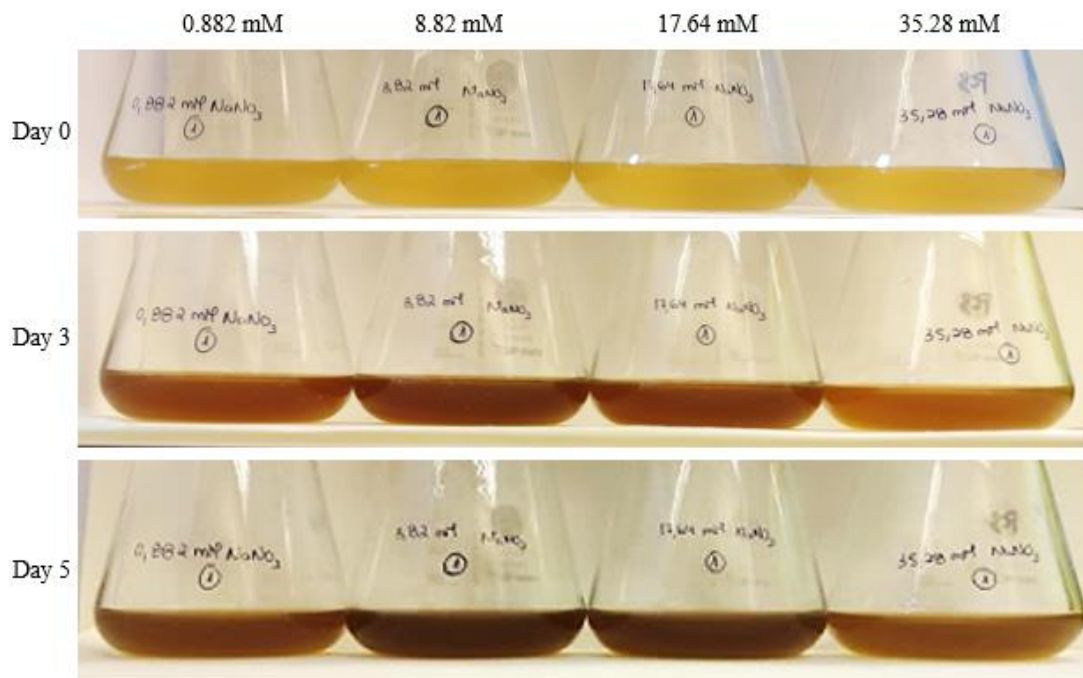


Figure 3.16. 50 mL cultures supplemented with 1, 10, 20 and 40-fold NaNO_3 , on the day of inoculation (day 0), and on the 3rd and 5th day after the start of growth.

3.4.2.2. Fucoxanthin Production

Along the growth curve, the relative concentration of fucoxanthin produced by the cultures under analysis was evaluated. For this, the method described by Wang and co-workers (2018) was used, which developed a formula specially designed for the quick and easy quantification of fucoxanthin in diatoms. The formula developed by the authors is applied to absorbance readings in cuvette for the wavelengths at 445, 663 and 750 nm. In order to facilitate the readings of several different experimental conditions, the authors developed a correlation between cuvette readings on a spectrophotometer and plate readings on a microplate reader. The same study draw attention to the fact that there is a need to optimize this correlation for each study and the material to be used. For this purpose, in our study, a correlation was made between 1 mL cuvette's and 96-well plates, adapted to the material and equipment in the laboratory. Since the samples to be analysed contained media with different constitutions (more specifically the concentrations of NaNO_3), it was necessary to read the absorbance in the three wavelengths indicated above, for the different media. The results are displayed in Table 3.1. The absorbance values of the various media were quite similar, and therefore, it was decided to perform only one correlation, using the concentration of 0.882 mM NaNO_3 , following the curve for 9 days, which is equivalent to adaptation, exponential and stationary phases.

Table 3.1. Absorbance values of the media used with the various concentrations of NaNO₃, at wavelengths of 445, 663 and 750 nm. 200 μL were added to a 96-well plate. Readings (n =2) performed on the EPOCH 2 microplate reader (BioTek). Mean ± Standard Deviation.

Wavelength	[NaNO ₃]			
	0.882 mM	8.82 mM	17.64 mM	35.28 mM
445 nm	0.089 ± 7.07E-04	0.090 ± 7.07E-04	0.090 ± 2.83E-03	0.089 ± 7.64E-04
663 nm	0.080 ± 2.12E-03	0.081 ± 0.00E+00	0.081 ± 1.41E-03	0.081 ± 8.66E-04
750 nm	0.084 ± 1.41E-03	0.086 ± 7.07E-04	0.085 ± 2.12E-03	0.085 ± 7.64E-04

The correlation between cuvette versus microplate readings is shown in Figure 3.17. The correlations for each wavelength were normalized to the 1st point of the 750 nm correlation, which corresponds to the OD reading at 750 nm, on day 0 of the culture. The ordinate at the origin was discarded as it was not essential to assess the correlation. Through the observation of Figure 3.17., it was possible to verify that there is a good correlation between the values ($R^2 > 0.9$), with the calibration coefficients of 0.605, 0.724 and 0.288 for Abs445, Abs663 and Abs750 nm, respectively.

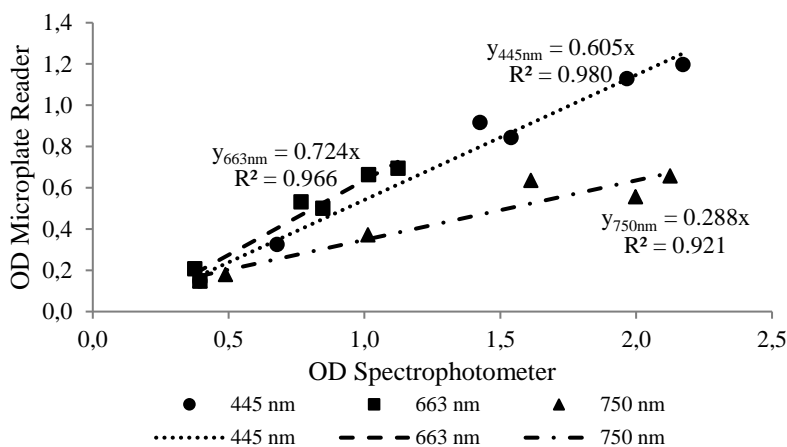


Figure 3.17. Correlation between OD readings in cuvette (spectrophotometer) and in 96-well plate (Microplate Reader). The symbols “●”, “■”, “▲” represent the wavelengths of 445, 663 and 750 nm, respectively.

The concentration of fucoxanthin for each sample under analysis was calculated as indicated in Appendix 2 and the results are shown in Figure 3.18. Negative values obtained by calculating the formula were concentrations of fucoxanthin not detectable by this method, which were equivalent to values less than 2 mg/L, in our study. For this reason, the concentration of fucoxanthin only started to be detected from day 3 of growth, for all cultures. It stopped being detected on day 11 and day 13 of cultures supplemented with basal concentration and 40-fold nitrate, respectively.

Similar to what was observed in the previous test (Figure 3.14.), on day 7 of growth, the day when fucoxanthin concentration reaches a maximum for cultures supplemented with the basal concentration of nitrate (0.882 mM), the t-test for independent samples showed that there is an effect on fucoxanthin production when 8.82 mM (10-fold) of nitrate is added to the cultures, compared to the addition of 0.882 mM (1-fold) nitrate ($t_{(16)}=13.73$; $p < 0.001$). Cultures with 10-fold nitrate produce, on average, 2-fold fucoxanthin ($[\text{fucoxanthin}]_{8.82 \text{ mM}} = 15.45 \pm 1.65 \text{ mg/L}$) when compared to cultures with 1-fold nitrate ($[\text{fucoxanthin}]_{0.882 \text{ mM}} = 7.16 \pm 0.74 \text{ mg/L}$). However, the day of maximum production corresponded to day 13 of the cultures supplemented with 10-fold NaNO_3 (29.69 mg/L). The t-test for independent samples showed that there were differences in fucoxanthin production between cultures supplemented with concentrations of 8.82 mM (10-fold) and 17.64 mM (20-fold) of nitrate, on the 13th day of growth, the day when production is maximum for both the concentrations ($t_{(16)} = 2.15$; $p = 0.047$). Cultures with 10-fold nitrate had higher fucoxanthin production ($[\text{fucoxanthin}]_{8.82 \text{ mM}} = 29.69 \pm 2.97 \text{ mg/L}$), when compared to cultures with 20-fold nitrate ($[\text{fucoxanthin}]_{17.64 \text{ mM}} = 27.38 \pm 1.25 \text{ mg/L}$). However, there were no differences, during cell growth, in the production of fucoxanthin between cultures supplemented with concentrations of 0.882 mM and 35.28 mM of nitrate, except for day 11, when the differences were significant between both types of supplementations. Since the concentration of 0.882 mM nitrate, on day 11, did not follow a normal distribution, the Mann-Whitney non-parametric test for independent samples was performed. The test showed that there were significant differences between cultures supplemented with 1 and 40-fold ($U=11$; $p = 0.007$). Cultures with 40-fold nitrate had, approximately, 2 times more fucoxanthin ($[\text{fucoxanthin}]_{35.28 \text{ mM}} = 4.44 \pm 0.77 \text{ mg/L}$) on this day, compared to 1-fold nitrate cultures ($[\text{fucoxanthin}]_{0.882 \text{ mM}} = 2.50 \pm 0.96 \text{ mg/L}$).

Using the same method developed by Wang, *et al.* (2018) to quantify the relative concentration of fucoxanthin, Fontebasso (2021) observed that different sources of N contribute differently to the production of fucoxanthin. In cultures of *P. tricornutum*, the author found that the highest concentrations of this pigment were obtained in cultures supplemented with 10-fold NaNO_3 , on the 12th day of growth, for a total of 18 days. On day 8, the fucoxanthin concentration of these cultures was 1.5-fold higher than cultures with basal NaNO_3 concentration, similar to the observations in our study. As stated for cell growth, the addition of other N sources (urea and ammonium carbonate) does not benefit the production of this pigment (unpublished data).

The observed OD and fucoxanthin results indicate that optimization of growth and fucoxanthin production is possible when nitrate is added in a factor of 10 to cultures, suggesting which may be a toxic effect of higher concentrations of this N source in both responses evaluated.

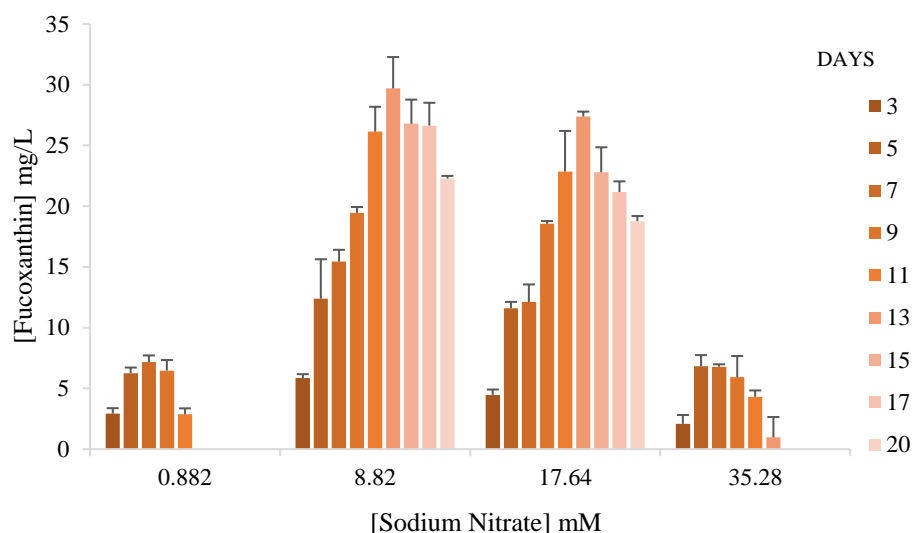


Figure 3.18. Average fucoxanthin concentration in cultures supplemented with 0.882 (1-fold), 8.82 (10-fold), 17.64 (20-fold) and 35.28 mM (40-fold) of NaNO₃. Concentration calculated using the formula developed by Wang, *et al.* 2018. Fucoxanthin represented in mg of fucoxanthin per liter of culture. (*n*=9)

3.5. Light Assay

It is known that light strongly affects diatom cultivation not only the presence or absence of light is important, but also its quality and intensity. Guo and collaborators (2016) demonstrated the effects of light intensity on the production of fucoxanthin and cell growth. The best results for fucoxanthin were obtained with low intensities of 10 to 30 $\mu\text{mol}/\text{m}^2/\text{s}$, however none of the light intensities studied had significant effect on the cell growth. Yang & Wei (2020) also found that the intracellular content of fucoxanthin decreases when the light intensity exceeds 30 $\mu\text{mol}/\text{m}^2/\text{s}$. Considering these reported results, the reference limit (30 $\mu\text{mol}/\text{m}^2/\text{s}$) was used in our study.

The next assay aimed at determining whether fucoxanthin is produced in a constant manner throughout the light/dark cycle, under different N concentrations.

3.5.1. Light/Dark Photoperiod Cycle

A study was carried out to follow cultures of *P. tricornutum* during the light (16 hours) and dark (8 hours) phase, evaluating cell growth and fucoxanthin concentration over 24 hours. The cultures were followed from the 4th to the 5th day of growth, which represents the initial exponential phase for the cultures under study. Given the physiology of diatom cells, the cell adaptations can be observed throughout the growth, from the exponential, stationary phase and decline/death phase (Vidoudez & Pohnert, 2012). However, the appropriated phase to assess the cell's response to stress factors in terms of pigment production is during the exponential phase (Vidoudez & Pohnert, 2012). For this purpose, biological triplicates of cultures supplemented with 1 and 10-fold NaNO₃ were used, to observe whether the availability of N could also influence the growth and concentration of fucoxanthin, throughout the

light and dark phases. Fucoxanthin was quantified using the method developed by Wang and co-workers (2018).

Through the analysis of Figure 3.19., it was observed that cultures with 1-fold NaNO_3 (0.882 mM) did not show variations in the concentration of fucoxanthin over the photoperiod. On the contrary, in cultures with 10-fold nitrate, a gradual increase was observed over the light phase, reaching a maximum of 4 hours before the dark phase, with a decrease in concentration afterwards. Four hours before the light turns on, there is a new increase in the production of fucoxanthin, following the light phase (Figure 3.19.). For both cultures, cell growth remained constant throughout the cycle, contrary to what was observed by Ragni & d'Alcalà (2007), who detected constant levels in growth during the light phase and an increase during the dark.

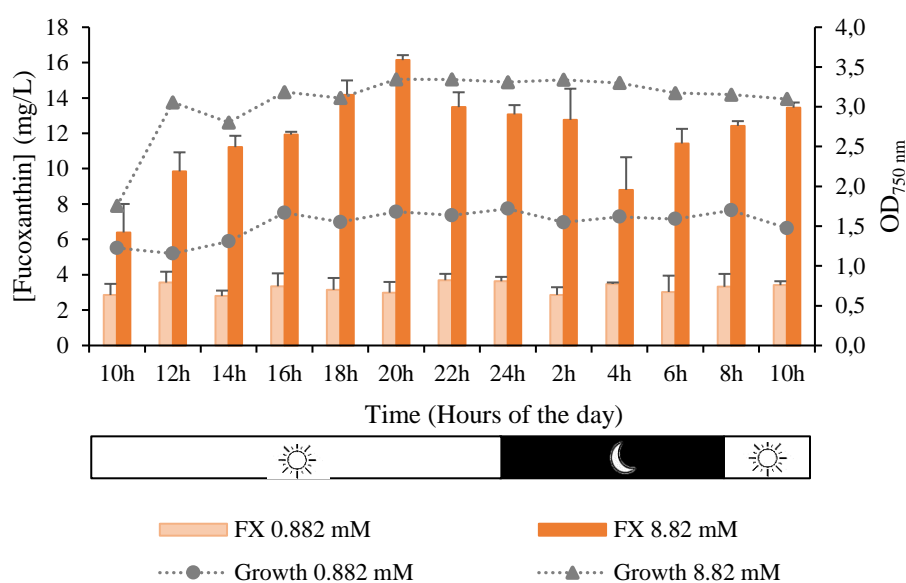


Figure 3.19. Variation of fucoxanthin concentration over the day/night cycle. The light/dark cycle was followed for 24 hours in cultures with 1-fold (0.882 mM) and 10-fold (8.82 mM) NaNO_3 . Fucoxanthin (FX) concentration is represented in mg of fucoxanthin per liter of culture. Bars indicate the concentration of fucoxanthin. Grey dashed lines indicate the growth curves by reading OD at 750 nm. Standard deviation represented by biological triplicates of each experimental condition. ($n=3$)

These variations between the light and dark phases in the fucoxanthin concentration suggest that during the night, pigment synthesis ceases, hypothesizing that throughout this period the synthesis pathways are inactive, or the components are diverged for use in other mechanisms (Ragni & d'Alcalà, 2007). A possible anticipation of the light/dark cycle was observed in our study (Figure 3.19), where it was found that 4 hours before the light phase starts, fucoxanthin synthesis begins, which suggests the activation of photoprotective carotenoid production in order to defend cells from the light damage. A similar evidence was proposed by Ashworth, *et al.* (2013), who observed that during the dark period, genes encoding photosynthetic enzymes and genes involved in protein synthesis were overexpressed,

indicating that there is an anticipation of the diurnal cycle, since there is a positive regulation of photosynthetic genes that precede the light phase (Ashworth, *et al.* 2013). Also, other studies indicate that these biological clocks seem to allow cells to anticipate abiotic variations and therefore efficiently synchronize cellular activities to survive in less favourable conditions or to limit physiological activities considering the time of day (Ragni, 2005; Ragni & d'Alcalà, 2007).

Studies dating to the 80s and 90s (Raimbault & Mingazzini, 1987; Vergara, *et al.* 1998) demonstrated, that in *P. tricornutum* cells growing in a medium with sufficient N, the extracellular nitrate content increases during the night, which seems to indicate a low assimilation of this compound during this period. During the day, the nitrate present in the medium decreases, suggesting the beginning of the nitrate reductase enzyme activity after the end of the dark period. Also was found that at the end of the dark phase and the beginning of the light phase, nitrate is accumulated by the cells, but it is not readily metabolized. Although the mechanism by which nitrogen influences pigment synthesis is unknown, it has previously been observed that nitrogen plays an important role in the production of fucoxanthin (Figure 3.18.). Thus, it is possible to hypothesize that the low assimilation of this nutrient during the dark phase may reduce pigment synthesis, leading to a reduction in the concentration of fucoxanthin during this period. Later, studies performed by Clark, *et al.* (2002) and Fábregas, *et al.* (2002), corroborate these previous results of variations in pigment production during day/night cycle, as observed by Raimbault & Mingazzini, (1987) and Vergara, *et al.* (1998).

A previous study carried out in the laboratory showed that *P. tricornutum* cultures with 0.882 mM of NaNO₃ consume half of the available nitrate when the number of cells doubles (approximately on the 2nd day of growth), and this nutrient is totally assimilated when there is a new duplication (unpublished data). Thus, the hypothesis placed is that cultures with 1-fold NaNO₃ in our study, contained very low concentration of N in the medium, promoting low assimilation and subsequent metabolization of this nutrient, not showing clear variations in the production of fucoxanthin in the different phases of the photoperiod. On the other hand, cultures with 10-fold NaNO₃, probably still had N in the medium, observing the variations in the production of fucoxanthin between day and night.

However, these results are preliminary and further studies will be needed to prove these previously mentioned hypotheses.

3.6. Gene Expression Analysis

In order to evaluate the expression variation of the key genes *PSY* and *LCYB* of the fucoxanthin synthesis pathway during the growth curve, a semi-quantitative RT-PCR study (sqRT-PCR) was performed.

One of the most important factors in the relative quantification of gene expression is the appropriate choice of endogenous control, also known as housekeeping genes or reference genes. The selection of this control must fall in the stability of the expression levels in all the tested samples (Biosystems, 2004).

Thus, it is necessary to evaluate the expression of these genes under various experimental conditions tested. The expression of the reference genes should not vary, however it is difficult to find a gene that is completely stable under the different experimental settings (Marone, *et al.* 2001, Biosystems, 2004). To this end, the following reference genes were investigated: *TATA Box Protein (TBP)* gene, which encodes a transcription factor that recognizes promoters and initiate transcription, and the *Cyclin-Dependent Kinase A (CDKA)* gene, that encodes a protein kinase which functions in the regulation of the cell cycle. Both genes were previously used as endogenous control for *P. tricornutum* by Siaux *et al.* (2007). However, it is always necessary to analyse the variation of expression of the genes, in our experimental conditions in order to assess whether they can be used as reference genes.

The target genes were *PSY*, which encodes the phytoene synthase enzyme, the first enzyme responsible for the carotenoid biosynthesis pathway (Maass, *et al.* 2009; Rodríguez-Villalón, *et al.* 2009; Meier, *et al.* 2011; Arango, *et al.* 2014; Kadono, *et al.* 2015), and the *LCYB*, which encodes lycopene beta cyclase, the first enzyme responsible for the fucoxanthin synthesis pathway in brown algae (Zhang, 2018).

A new assay was performed where 50 mL cultures of *P. tricornutum* were supplemented with basal concentration (0.882 mM) and 10-fold (8.82 mM) NaNO₃ (described in chapter 2.7. of the Materials and Methods). The growth was followed for 18 days, with the total biomass collection at days 4, 7, 11 and 18. The RNA was extracted, and the cDNA was synthesized through reverse transcriptase, normalizing the amount of RNA for all samples. The samples were tested for the reference and target genes.

Figures 3.20 and 3.21 show the agarose gels for the reference and target genes, respectively. For the *TBP* (Figure 3.20.A) and *CDKA* (Figure 3.20.B) genes, 25 cycles were initially used, however the expression was relatively low, verifying that the number of cycles was not sufficient to evaluate the expression. Thus, for the *TBP* gene it was increased to 28 cycles, verifying that the expression was more intense on day 4, than the remaining days, for both nitrate concentrations. This variation in expression levels makes the *TBP* gene a less adequate internal control, since when the experimental conditions were varied, the expression of this gene did not remain constant.

For the *CDKA* gene (Figure 3.20.B), the number of cycles was increased to 26, however the intensity of the bands was very weak, despite the slight increase compared to 25 cycles. Thus, an increase was performed to 28 cycles, observing an increment in the intensity of the bands. It was found that the expression levels were mostly constant for the two NaNO₃ concentrations during the assay. However, it was possible to notice a lower expression on the 7th day for both concentrations, which may be due to pipetting errors during the cDNA synthesis process, leading to a lower expression, due to the smaller amount of genetic material in the reaction. The bands of the gel of this last amplification with 28 cycles, were used for relative quantification of the expression of the target genes.

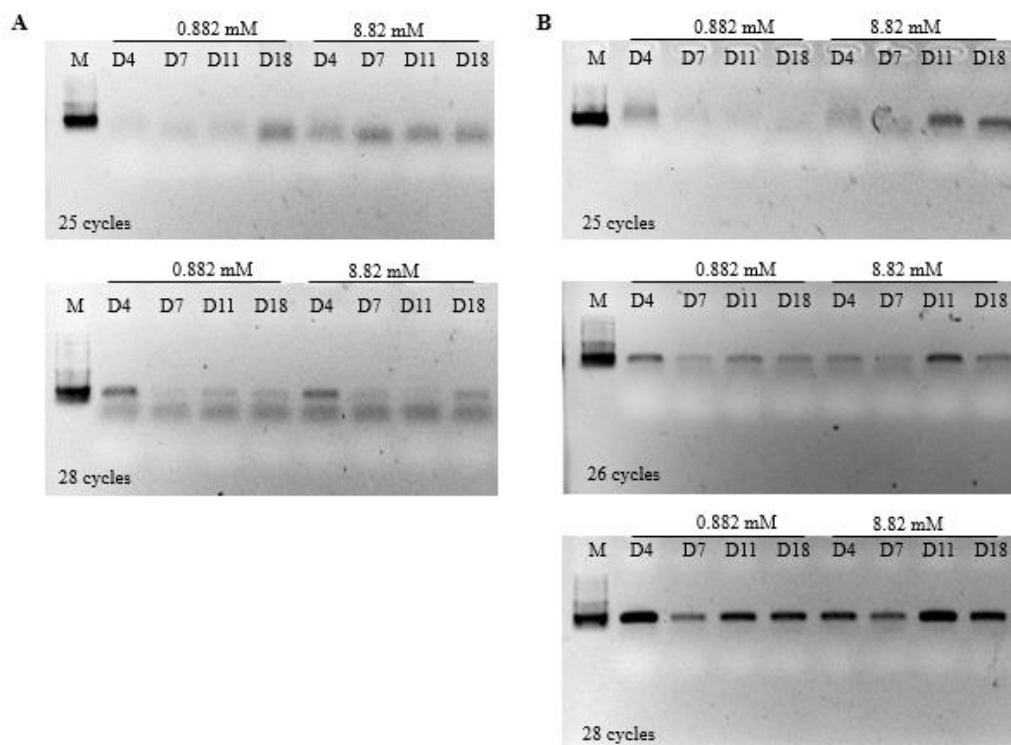


Figure 3.20. 1.2% agarose gels from the reference genes with 25, 26 and 28 cycles. (A) *TATA Box Protein (TBP)* and (B) *Cyclin Dependent Kinase A (CDKA)*. Biomass collected on days (D) 4, 7, 11 and 18 of cultures growth, for cultures supplemented with 0.882 and 8.82 mM of NaNO_3 . Marker (M) Ladder VI (NZYTech, Portugal), darker band on the marker represents the band size of 200 bp.

For the *PSY* and *LCYB* genes (Figure 3.21), 23 cycles were initially used, however for both genes, the intensity of the bands was relatively low to evaluate the expression. Thus, it was increased to 25 cycles, for the two target genes, the latter being used for expression quantification.

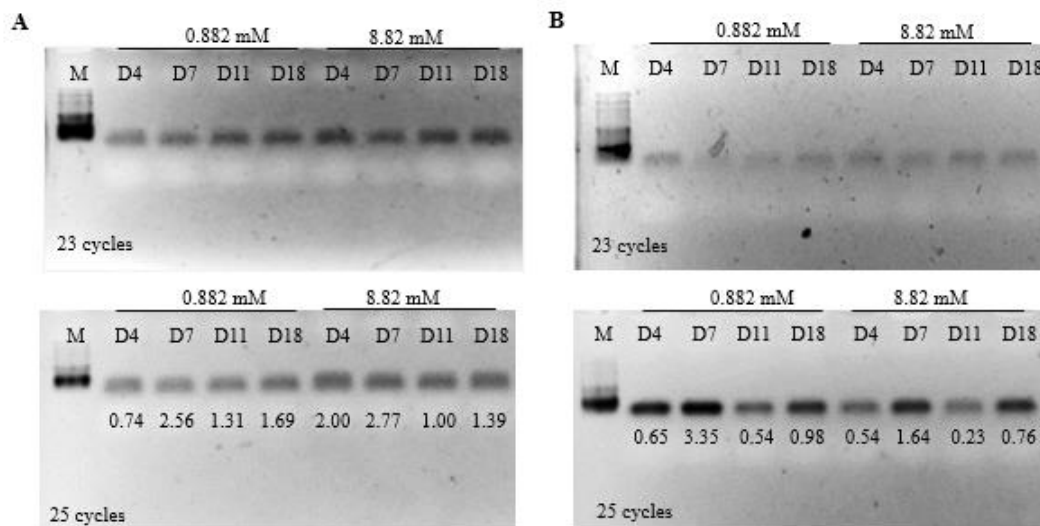


Figure 3.21. 1.2% agarose gels from the target genes with 23 and 25 cycles. (A) *Phytoene Synthase (PSY)* and (B) *Lycopene β -cyclase (LCYB)*. Biomass collected on days (D) 4, 7, 11 and 18 of cultures growth, for cultures supplemented with 0.882 and 8.82 mM of NaNO_3 . Marker (M) Ladder VI (NZYTech, Portugal), darker band on the marker represents the band size of 200 bp. The values found on the gels below each band indicate the relative expression of the target genes calculated by the ratio target/reference gene *CDKA*.

As noted earlier, the content of carotenoids, namely fucoxanthin, may vary according to the growth phase (Figure 3.18.). Thus, the hypothesis arises that the effect of this variable can also have an impact on the expression of genes involved in the synthesis pathway of this pigment.

Under non-stress conditions for algae, the gene *PSY* has relatively low levels of transcripts when compared, for example, with the enzyme geranylgeranyl diphosphate synthase that convert dimethylallyl diphosphate to geranylgeranyl diphosphate (Figure 1.3.). The conversion of this last molecule in phytoene occurs by the activity of the *PSY* enzyme (Kadono, *et al.* 2015). Regardless this evidence, the results suggests that *PSY* may be a limiting enzyme in the synthesis pathway of carotenoids (Kadono, *et al.* 2015).

Once in our study, the reference gene *CDKA* expression varied, it was not possible to take conclusions about the relative expression of the target genes (*PSY* and *LCYB*) from the Figure 3.21. In further work, new reference genes need to be analysed, like *Histone-H4 (HH4)* or *Ribosomal Protein Small (RPS)*, already used by Siaut, *et al.* (2007) as endogenous controls for *P. tricornutum*.

Nevertheless, it would be expected that the expression of the target genes may be higher at the end of the exponential phase, beginning of the stationary phase, because in this period the production of fucoxanthin is higher, for both types of supplementations. We could observe higher expression levels in these genes between days 7, maximum fucoxanthin production (Figure 3.18.) and 9, beginning of stationary phase (Figure 3.15.) for cultures with 0.882 mM of nitrate, and the days 13, maximum fucoxanthin production (Figure 3.18.) and 15, beginning of stationary phase, (Figure 3.15.) for cultures with 8.82 mM of Nitrate. For example, Kadono (2015) states that during the stationary phase, the

production of fucoxanthin may be increased with the use of precursors produced by the activation of limiting steps in the log phase. One of the limiting steps in the log phase is the catalysis of *PSY*, which is a precursor for the synthesis and accumulation of fucoxanthin (Kadono, *et al.* 2015).

Many genes that belong to the regulatory mechanism are more expressed in the exponential phase than in the stationary phase. Many of these genes are associated with cell growth. Voung *et al.* (2021) hypothesizes that fucoxanthin biosynthesis is associated with regulatory mechanisms for cell growth. In other words, the authors suggest that, unlike higher plants in which carotenoids belong to secondary metabolism, the synthesis of these pigments by microalgae could be a primary metabolic process, since it seems to be regulated in parallel with cell growth in *P. tricornutum*, more than lipid and carbohydrate metabolism (Voung, *et al.* 2021).

In addition to *PSY*, *LCYB* expression levels are very low in non-stress conditions for *P. tricornutum*, showing that this is another enzyme that may represent an important step in the fucoxanthin synthesis pathway, which suggests that this enzyme may be a limiting-rate enzyme in this process (Kadono, *et al.* 2015). There are few studies that demonstrate the role of this gene in the synthesis of pigments and how it is regulated. However, the fact that *LCYB* is the first enzyme directly responsible for the fucoxanthin biosynthesis, makes it an interesting target for studying the direct effects on this pathway.

Not all the enzymes responsible for the carotenoid biosynthetic pathway are described, so the regulation of the pigment production is not yet fully understood because of the lack of information. Besides fucoxanthin, other pigments may be produced in the biosynthetic pathway, like zeaxanthin and violaxanthin, already being described to be produced by *P. tricornutum* (Lohr & Wilhelm, 1999). The reversible interconversion of zeaxanthin and violaxanthin is an essential factor for photoprotection, allowing cells to control the pigment content depending on the light conditions (Varela, *et al.* 2015). What is not known is whether, in addition to light, if the availability of nitrogen may influence this conversion. Fontebasso (2021) observed, in our laboratory, the expression of two enzymes belonging to the carotenoid synthesis pathway in diatoms, *Zeaxanthin epoxidase* (*ZEP1* and *ZEP3*) and *Violaxanthin de-epoxidase* (*VDE*), under different N supplementation. The author observed, on the 5th day of growth, a low expression of *ZEP1* and *ZEP3* for cultures of *P. tricornutum* supplemented with 1 and 10-fold NaNO₃, which suggests that, regardless of the N concentration the expression did not vary. As for *VDE* (which acts inversely to the *ZEP* enzyme), the expression was higher for cultures with 10-fold NaNO₃, compared to cultures with 1-fold NaNO₃. These last results may suggest that with 10-fold nitrate, the fucoxanthin biosynthesis pathway is downregulated, in the early stage of the growth (unpublished results). However, it should be noted that the biomass was collected on the 5th day of the growth, and the results could be much different if analysed in the end of the exponential phase, where the fucoxanthin production is higher.

3.7. Cell viability of the *P. tricornutum* culture

A cell viability assay was performed to observe the physiological characteristics of cultures supplemented with different NaNO_3 concentrations (0.882, 8.82, 17.64 and 35.28 mM). The photographs taken under the microscope are shown in Figures 3.22. and 3.23.

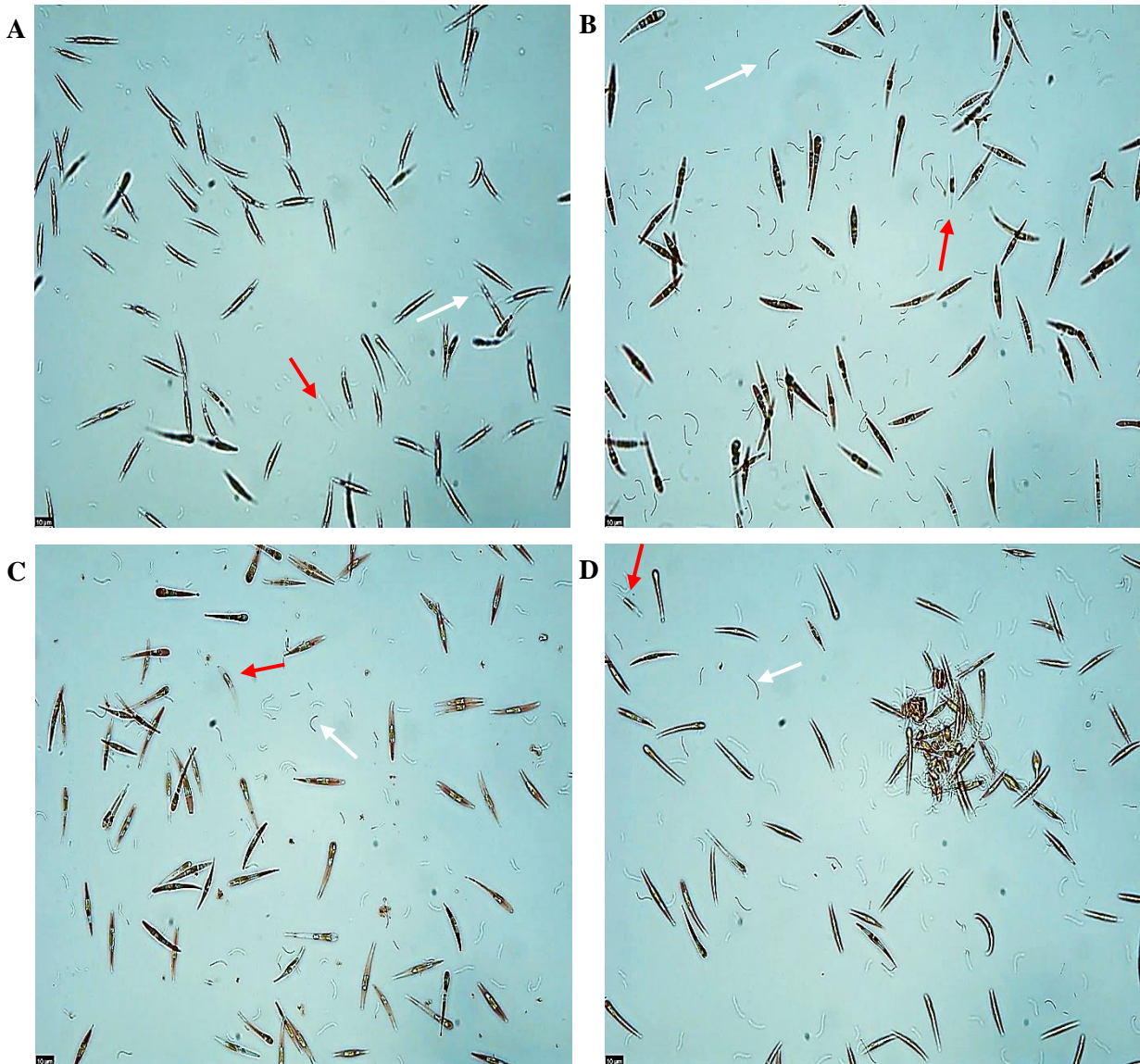


Figure 3.22. Microscopic images at the 7th day of growth, for *P. tricornutum* cultures supplemented with 0.882 mM (A), 8.82 mM (B), 17.64 mM (C) and 35.28 mM (D) of NaNO_3 . Black bar in the lower left corner represents the 10 μm ruler. White arrow indicates bacteria. Red arrow indicates dead cells.

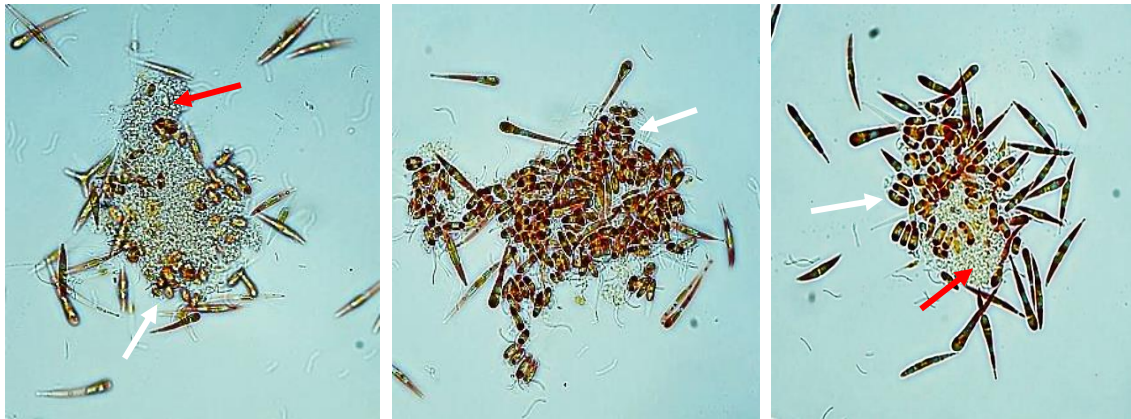


Figure 3.23. Microscopic images of cell aggregates at the 7th day of growth, of *P. tricornutum* cultures supplemented with 35.28 mM of NaNO₃. White arrow indicates round cells. Red arrow indicates matrix produced by the algae.

It was possible to observe for all cultures, that the cells were mostly alive (red colour), with a fusiform morphology, a phenotype that is characteristic of the species under study. However, it was observed that as the sodium nitrate concentration increased, the physiological characteristics of the cultures changed.

Figure 3.22.A represents the culture supplemented with a concentration of 0.882 mM of NaNO₃, considered as a basis for comparison with the other cultures. In this image, it was possible to see the presence of few bacteria in suspension. When compared to Figure 3.22.B, it appears that the addition of 10 times more nitrate (8.82 mM of NaNO₃), caused a significant increase in the amount of bacteria present.

The cultures used in this thesis were non-axenic cultures, so a previous study of peptide mapping by nanoLC-MS using Sciex TripleTOF 6600 mass spectrometer was performed, against the prokaryotic database, to identify what type of bacteria were present in culture. The sample under analysis was the supernatant culture medium where *P. tricornutum* cells were grown.

The results (mass spectrometry data was generated by the UniMS, ITQB/iBET, Oeiras, Portugal) demonstrated the existence of a large percentage of peptides produced by the family of marine bacteria Rhodobacteraceae, more specifically from the Roseobacter group. This group consists of phototrophic alphaproteobacteria, with oval morphology or small rods, and polar flagella, which attributes motility to these bacteria. These organisms have the ability to fix nitrogen, requiring sodium ions for their growth (Pujalte, *et al.* 2014). As the medium with 8.82 mM of NaNO₃ is full of sodium ions, the presence of these bacteria increased.

The algae-bacterial interaction is not yet fully known, but it was observed that the mutualism between these two organisms is the most prevalent relationship (reviewed in Ramanan, *et al.* 2016). Mutualism is an interaction between two or more organisms that benefit from each other's presence.

Studies have shown that the beneficial interaction between microalgae-bacteria occurs predominantly through the exchange of nutrients (Amin, *et al.* 2012; Fuentes, *et al.* 2016; Lian, *et al.* 2018).

In Figure 3.22.C (cultures supplemented with 17.64 mM NaNO₃) it was possible to see a reduction in the bacteria cell density, probably due to a slight increase of the toxicity environment by ammonia production during the N metabolism of the diatom. This toxicity promoted the diatom cell death, which is suggested by the appearance of cellular debris.

The concentration 35.28 mM of NaNO₃ have also previously been found to be toxic (Figure 3.15.). In Figure 3.22.D, it was possible to observe that, although the cells were alive, they formed cell aggregates, changing their morphology. This evidence seems to indicate that the formation of these aggregates is a response to environmental stress. It is known that *P. tricornutum* is a pleiomorphic diatom and changes its morphology when faced with biotic or abiotic stimuli (Song, *et al.* 2020). Under favourable culture conditions, most *P. tricornutum* variants have an elongated (fusiform) or oval morphology. On the contrary, in stressful conditions, not favourable to growth, they can change to the round morphology (reviewed in Tesson, *et al.* 2009).

The aggregates with round cells observed in our study (Figure 3.23. white arrows), were also seen in a study performed by De Martino *et al.* (2011). The authors observed the presence of cellular aggregates in unfavourable conditions of temperature and salt. The same study suggest that these round cells may be a dormancy stage of the *P. tricornutum* cell cycle, once they have similar characteristics to resting cells, with thinner cell walls, disorganized chloroplast, among others. De Martino and collaborators (2011) observed that the cells aggregate and develop biofilms, adhering to the flasks. Diatoms have the ability to produce extracellular polymeric substances, creating a matrix. The morphological change in the cells is due to the fact that only oval and round cells have the capacity to produce an extracellular mucilage, unlike fusiform and triradiated cells (Buhmann, *et al.* 2016).

Proteomic studies have shown that the proteins that compose this matrix are involved in the defence, signalling and intracellular aggregation of algae (Buhmann, *et al.* 2016). Desbois *et al.* (2010) also described for *P. tricornutum* these aggregates, with a gelatinous matrix and round cells typically alive in the centre, as observed in our study (Figure 3.23.). Curiously, the change in morphology is reversible after several subcultures in fresh medium (De Martino, *et al.* 2011).

So far, these round cells have been reported to occur in response to temperature, high salinity (De Martino, *et al.* 2007; De Martino, *et al.* 2011) and light quality (Herbstová, *et al.* 2017). Although new tests confirmation is required, our study seems to be the first to document the occurrence of these cell aggregates under conditions of nitrogen excess for *Phaeodactylum tricornutum*.

4. CONCLUSIONS

Over time, it has been shown that large-scale production of fucoxanthin from macroalgae is not beneficial due its poor sustainability. Thus, some studies have shown that microalgae are alternative platforms for the production of this pigment, since their production rate is much higher. However, switching to a new production platform tends to introduce high costs to the industry, due to the lack of information on how to implement profitable production systems. For this reason, it is necessary to invest in cellular systems with cheap requirements of nutrients and light, which is not always easy to obtain, partly due to the lack of research on the optimization processes to produce biomass, as well as by-products like the pigments in a green and affordable way, on a commercial scale. Thus, it is crucial to develop alternative cost-effective platforms for improved production of microalgal biomass and fucoxanthin.

Our study aimed to broaden the knowledge about the role of alternative sources of nitrogen and carbon in the metabolism of *P. tricornutum*, namely their influence on cell growth and fucoxanthin production, in order to optimize these two factors.

Our results suggest that the addition of a carbon source does not favour growth or fucoxanthin production. However, the addition of N, on the contrary, showed interesting results. Our study allowed to double the production of fucoxanthin, in just 7 days of growth, when 10-fold NaNO₃ (8.82 mM) was added, compared to the basal medium used for the cultivation of these diatoms (f/2 medium with 0.882 mM of NaNO₃). The maximum fucoxanthin production achieved was approximately 30 mg of fucoxanthin per liter of culture. Although the results in the growth and fucoxanthin production were similar between cultures supplemented with 8.82 and 17.64 mM of NaNO₃, the statistical analyses demonstrated that cultures with concentrations above 17.64 mM NaNO₃ represented worse results, which could mean some degree of toxicity, negatively affecting the growth and fucoxanthin production. As observed in morphological studies mentioned above, it has been reported that the alteration of some abiotic factors, either by excess or deficit, can induce physiological responses in *P. tricornutum* cells, possibly in response to stress. In our study, it was observed that the N excess in cultures supplemented with 40-fold NaNO₃ (corresponding to 35.28 mM of NaNO₃), may have caused cell aggregation and morphological changes.

Our results, under low light conditions, also suggest that the variation in fucoxanthin may depend on the photoperiod, with maximum values recorded at the end of the light phase. Cultures with high N availability seem to anticipate the light/dark phase, decreasing or increasing the synthesis of fucoxanthin, triggering photoprotection mechanisms.

At the molecular level, it was not possible to evaluate the expression levels of target genes of the fucoxanthin biosynthesis pathway, in the two types of supplementations introduced, since the reference gene used showed variations in expression under the conditions tested. Future studies are needed to better understand the role of N in the pigment production mechanism, as well as investigating other

reference genes in order to find a more stable endogenous control for *P. triornutum* supplemented with different N concentrations.

Our results confirm previous data on the influence of sodium nitrate addition by a factor of 10, to diatom cultures. They provide important information for fucoxanthin production to be further optimized. In all the tests carried out, was possible to suggest that to obtain the maximum production of fucoxanthin it was necessary to use a N source for the growth of *P. triornutum* cells. This N source should be sodium nitrate, at a concentration 10-fold higher than the basal concentration of the f/2 medium for diatoms. Furthermore, it was found that with this supplemented concentration of sodium nitrate, the culture reaches the stationary phase after 15 days, with a maximum of fucoxanthin produced after 13 days of growth, with a concentration of approximately 30 mg/L. It is also noticed that the production is maximum at the end of the light cycle, approximately 4 hours before the dark phase begins. In summary, to obtain the best fucoxanthin results it is necessary to cultivate the cells with f/2 medium supplemented with a concentration of 8.82 mM NaNO₃ and harvest the biomass for fucoxanthin extraction on the 13th day of growth, 12 hours after light onset.

These results pave the way for further investigation on the mechanism of nitrogen regulation in the fucoxanthin synthesis pathway in microalgae, as well as introduces new data on the optimizing strategy for the production of photosynthetic pigments, with a view to large-scale production through microalgae cultivation, for use of these pigments in health industry.

5. REFERENCES

- Abidov, M., Ramazanov, Z., Seifulla, R., & Grachev, S. (2010). The effects of Xanthigen™ in the weight management of obese premenopausal women with non-alcoholic fatty liver disease and normal liver fat. *Diabetes, obesity and metabolism*, 12(1), 72-81.
- Alam, M. A., Xu, J. L., & Wang, Z. (Eds.). (2020). *Microalgae biotechnology for food, health and high value products*. Singapore: Springer.
- Algatech <https://www.algatech.com/algatech-product/fucovital/> (accessed at 10/02/2021)
- Alipanah, L., Rohloff, J., Winge, P., Bones, A. M., & Brembu, T. (2015). Whole-cell response to nitrogen deprivation in the diatom *Phaeodactylum tricornutum*. *Journal of experimental botany*, 66(20), 6281-6296.
- Amin, S. A., Parker, M. S., & Armbrust, E. V. (2012). Interactions between diatoms and bacteria. *Microbiology and molecular biology reviews: MMBR*, 76(3), 667.
- Andersen, R. A. (Ed.). (2005). *Algal culturing techniques*. Elsevier.
- Apte, A., & Daniel, S. (2009). PCR primer design. *Cold Spring Harbor Protocols*, 2009(3), pdb-ip65.
- Arango, J., Jourdan, M., Geoffriau, E., Beyer, P., & Welsch, R. (2014). Carotene hydroxylase activity determines the levels of both α -carotene and total carotenoids in orange carrots. *The Plant Cell*, 26(5), 2223-2233.
- Arora, N., & Philippidis, G. P. (2021). Fucoxanthin Production from Diatoms: Current Advances and Challenges. In *Algae* (pp. 227-242). Springer, Singapore.
- ASAE <https://www.asae.gov.pt/seguranca-alimentar/aditivos-alimentares/corantes.aspx> (consulted at 18/09/2020)
- Ashworth, J., Coesel, S., Lee, A., Armbrust, E. V., Orellana, M. V., & Baliga, N. S. (2013). Genome-wide diel growth state transitions in the diatom *Thalassiosira pseudonana*. *Proceedings of the National Academy of Sciences*, 110(18), 7518-7523.
- Bauer, C. M., Schmitz, C., Corrêa, R. G., Herrera, C. M., Ramlov, F., Oliveira, E. R., Pizzato, A., Varela, L.A.C., Cabral, D.Q., Yunes, R.A., Lopes, R.G., Cella, H., Rocha, M., Rorig, L.R., Derner, R.B., Abreu, P.C. & Maraschin, M. (2019). In vitro fucoxanthin production by the *Phaeodactylum tricornutum* diatom. In *Studies in Natural Products Chemistry* (Vol. 63, pp. 211-242). Elsevier.
- Begum, H., Yusoff, F. M., Banerjee, S., Khatoon, H., & Shariff, M. (2016). Availability and utilization of pigments from microalgae. *Critical reviews in food science and nutrition*, 56(13), 2209-2222.
- Beppu, F., Niwano, Y., Tsukui, T., Hosokawa, M., & Miyashita, K. (2009). Single and repeated oral dose toxicity study of fucoxanthin (FX), a marine carotenoid, in mice. *The Journal of toxicological sciences*, 34(5), 501-510.
- Biosystems, A. (2004). Guide to performing relative quantitation of gene expression using real-time quantitative PCR. Applied Biosystems.
- Bogacz-Radomska, L., & Harasym, J. (2018). β -Carotene-properties and production methods. *Food Quality and Safety*, 2(2), 69-74.
- Bowler, C., & Falciatore, A. (2019). *Phaeodactylum tricornutum*. *Trends in Genetics*, 35 (9), 706-707.
- Borowitzka, M. A. (2018). Biology of microalgae. In *Microalgae in health and disease prevention* (pp. 23-72). Academic Press.
- Britton, G., Liaaen-Jensen, S., & Pfander, H. (2009). Carotenoids volume 5: nutrition and health (Vol. 5).
- Buhmann, M. T., Schulze, B., Förderer, A., Schleheck, D., & Kroth, P. G. (2016). Bacteria may induce the secretion of mucin-like proteins by the diatom *Phaeodactylum tricornutum*. *Journal of phycology*, 52(3), 463-474.
- Cavalier-Smith, T. (2003). Genomic reduction and evolution of novel genetic membranes and protein-targeting machinery in eukaryote-eukaryote chimaeras (meta-algae). *Philosophical Transactions of the Royal Society of London. Series B: Biological Sciences*, 358(1429), 109-134.
- Ceron, G. M., Camacho, F. G., Mirón, A. S., Sevilla, J. M., Chisti, Y., & Grima, E. M. (2006). Mixotrophic production of marine microalga *Phaeodactylum tricornutum* on various carbon sources. *Journal of microbiology and biotechnology*, 16(5), 689-694.
- Chakdar, H., & Pabbi, S. (2017). Algal pigments for human health and cosmeceuticals. In *Algal green chemistry* (pp. 171-188). Elsevier.
- Clark, D. R., Flynn, K. J., & Owens, N. J. (2002). The large capacity for dark nitrate-assimilation in diatoms may overcome nitrate limitation of growth. *New Phytologist*, 155(1), 101-108.
- Clinical Trial FucoVital, <https://clinicaltrials.gov/ct2/show/study/NCT03625284> (Consulted at 10/02/2021)
- Coesel, S., Oborník, M., Varela, J., Falciatore, A., & Bowler, C. (2008a). Evolutionary origins and functions of the carotenoid biosynthetic pathway in marine diatoms. *PLoS one*, 3(8), e2896.
- Coesel SN, Baumgartner AC, Teles LM, Ramos AA, Henriques NM, Cancela L, Varela JC (2008b) Nutrient limitation is the main regulatory factor for carotenoid accumulation and for Psy and Pds steady state transcript levels in *Dunaliella salina* (Chlorophyta) exposed to high light and salt stress. *Mar Biotechnol* 10:602–611

- Couso, I., Vila, M., Vigar, J., Cordero, B. F., Vargas, M. Á., Rodríguez, H., & León, R. (2012). Synthesis of carotenoids and regulation of the carotenoid biosynthesis pathway in response to high light stress in the unicellular microalga *Chlamydomonas reinhardtii*. *European Journal of Phycology*, 47(3), 223-232.
- Cui, H., Wang, Y., & Qin, S. (2011). Molecular evolution of lycopene cyclases involved in the formation of carotenoids in eukaryotic algae. *Plant Molecular Biology Reporter*, 29(4), 1013-1020.
- Desbois, A. P., Walton, M., & Smith, V. J. (2010). Differential antibacterial activities of fusiform and oval morphotypes of *Phaeodactylum tricornerutum* (Bacillariophyceae). *Journal of the Marine Biological Association of the United Kingdom*, 90(4), 769-774.
- De Martino, A., Bartual, A., Willis, A., Meichenin, A., Villazán, B., Maheswari, U., & Bowler, C. (2011). Physiological and molecular evidence that environmental changes elicit morphological interconversion in the model diatom *Phaeodactylum tricornerutum*. *Protist*, 162(3), 462-481.
- De Martino, A., Meichenin, A., Shi, J., Pan, K., & Bowler, C. (2007). Genetic and phenotypic characterization of *Phaeodactylum tricornerutum* (Bacillariophyceae) accessions 1. *Journal of Phycology*, 43(5), 992-1009.
- de Winter, L., Cabanelas, I. T. D., Martens, D. E., Wijffels, R. H., & Barbosa, M. J. (2017). The influence of day/night cycles on biomass yield and composition of *Neochloris oleoabundans*. *Biotechnology for biofuels*, 10(1), 1-10.
- Eilers, U., Bikoulis, A., Breitenbach, J., Büchel, C., & Sandmann, G. (2016). Limitations in the biosynthesis of fucoxanthin as targets for genetic engineering in *Phaeodactylum tricornerutum*. *Journal of applied phycology*, 28(1), 123-129.
- Fábregas, J., Maseda, A., Domínguez, A., Ferreira, M., & Otero, A. (2002). Changes in the cell composition of the marine microalga, *Nannochloropsis gaditana*, during a light: dark cycle. *Biotechnology letters*, 24(20), 1699-1703.
- Falkowski, P. G., & Chen, Y. B. (2003). Photoacclimation of light harvesting systems in eukaryotic algae. In *Light-harvesting antennas in photosynthesis* (pp. 423-447). Springer, Dordrecht.
- Fernandez, E., & Galvan, A. (2007). Inorganic nitrogen assimilation in *Chlamydomonas*. *Journal of experimental botany*, 58(9), 2279-2287.
- Fontebasso, G. (2021). Evaluation of the effect of distinct nitrogen sources in *Phaeodactylum tricornerutum* growth and fucoxanthin production. Report of Project in Cell and Molecular Biology. Faculdade de Ciências e Tecnologia, Universidade Nova de Lisboa.
- Ford, C. W., & Percival, E. (1965). 1299. Carbohydrates of *Phaeodactylum tricornerutum*. Part II. A sulphated glucuronomannan. *Journal of the Chemical Society (Resumed)*, 7042-7046.
- Fuentes, J. L., Garbayo, I., Cuaresma, M., Montero, Z., González-del-Valle, M., & Vílchez, C. (2016). Impact of microalgae-bacteria interactions on the production of algal biomass and associated compounds. *Marine drugs*, 14(5), 100.
- Francius, G., Tesson, B., Dague, E., Martin-Jézéquel, V., & Dufrière, Y. F. (2008). Nanostructure and nanomechanics of live *Phaeodactylum tricornerutum* morphotypes. *Environmental microbiology*, 10(5), 1344-1356.
- García, M. C., Sevilla, J. F., Fernández, F. A., Grima, E. M., & Camacho, F. G. (2000). Mixotrophic growth of *Phaeodactylum tricornerutum* on glycerol: growth rate and fatty acid profile. *Journal of Applied Phycology*, 12(3), 239-248.
- García, M. C., Mirón, A. S., Sevilla, J. F., Grima, E. M., & Camacho, F. G. (2005). Mixotrophic growth of the microalga *Phaeodactylum tricornerutum*: influence of different nitrogen and organic carbon sources on productivity and biomass composition. *Process Biochemistry*, 40(1), 297-305.
- Glibert, P. M., Wilkerson, F. P., Dugdale, R. C., Raven, J. A., Dupont, C. L., Leavitt, P. R. & Kana, T. M. (2016). Pluses and minuses of ammonium and nitrate uptake and assimilation by phytoplankton and implications for productivity and community composition, with emphasis on nitrogen-enriched conditions. *Limnology and Oceanography*, 61(1), 165-197.
- Gordon, H. T., Bauernfeind, J. C., & Furia, T. E. (1983). Carotenoids as food colorants. *CRC Critical Reviews in Food Science and Nutrition*, 18(1), 59-97.
- Goswami, R. K., Agrawal, K., & Verma, P. (2021). An Overview of Microalgal Carotenoids: Advances in the Production and Its Impact on Sustainable Development. *Bioenergy Research: Evaluating Strategies for Commercialization and Sustainability*, 105-128.
- Grobbelaar JU (2004) Algal nutrition: mineral nutrition. In: Richmond A (ed) Handbook of microalgal culture: biotechnology and applied phycology. *Blackwell Science*, Oxford.
- Guillard, R.R.L. 1975. Culture of phytoplankton for feeding marine invertebrates. pp 26-60. In Smith W.L. and Chanley M.H (Eds.) Culture of Marine Invertebrate Animals. *Plenum Press*, New York, USA.
- Guo, B., Liu, B., Yang, B., Sun, P., Lu, X., Liu, J., & Chen, F. (2016). Screening of diatom strains and characterization of *Cyclotella cryptica* as a potential fucoxanthin producer. *Marine drugs*, 14(7), 125.
- Gupta, V. K., Treichel, H., Shapaval, V. O., de Oliveira, L. A., & Tuohy, M. G. (Eds.). (2017). *Microbial functional foods and nutraceuticals*. John Wiley & Sons.

- Guzmán-Murillo, M. A., López-Bolaños, C. C., Ledesma-Verdejo, T., Roldan-Libenson, G., Cadena-Roa, M. A., & Ascencio, F. (2007). Effects of fertilizer-based culture media on the production of exocellular polysaccharides and cellular superoxide dismutase by *Phaeodactylum tricorutum* (Bohlin). *Journal of Applied Phycology*, 19(1), 33-41.
- Haire, T. C., Bell, C., Cutshaw, K., Swiger, B., Winkelmann, K., & Palmer, A. G. (2018). Robust microplate-based methods for culturing and in vivo phenotypic screening of *Chlamydomonas reinhardtii*. *Frontiers in plant science*, 9, 235.
- He, L., Han, X., & Yu, Z. (2014). A rare *Phaeodactylum tricorutum* cruciform morphotype: culture conditions, transformation and unique fatty acid characteristics. *PLoS one*, 9(4), e93922.
- He, Q., Yang, H., Wu, L., & Hu, C. (2015). Effect of light intensity on physiological changes, carbon allocation and neutral lipid accumulation in oleaginous microalgae. *Bioresource technology*, 191, 219-228.
- Herbstová, M., Bina, D., Kaňá, R., Vácha, F., & Litvín, R. (2017). Red-light phenotype in a marine diatom involves a specialized oligomeric red-shifted antenna and altered cell morphology. *Scientific reports*, 7(1), 1-10.
- Hosokawa, M., Wanezaki, S., Miyauchi, K., Kurihara, H., Kohno, H., Kawabata, J. & Takahashi, K. (1999). Apoptosis-inducing effect of fucoxanthin on human leukemia cell line HL-60. *Food Science and Technology Research*, 5(3), 243-246.
- Huang, W., & Daboussi, F. (2017). Genetic and metabolic engineering in diatoms. *Philosophical Transactions of the Royal Society B: Biological Sciences*, 372(1728), 20160411.
- Huete-Ortega, M., Okurowska, K., Kapoore, R. V., Johnson, M. P., Gilmour, D. J., & Vaidyanathan, S. (2018). Effect of ammonium and high light intensity on the accumulation of lipids in *Nannochloropsis oceanica* (CCAP 849/10) and *Phaeodactylum tricorutum* (CCAP 1055/1). *Biotechnology for biofuels*, 11(1), 1-15.
- Lavaud, J., Rousseau, B., & Etienne, A. L. (2004). General features of photoprotection by energy dissipation in planktonic diatoms (Bacillariophyceae) 1. *Journal of Phycology*, 40(1), 130-137.
- Lavaud, J., Materna, A. C., Sturm, S., Vugrinec, S., & Kroth, P. G. (2012). Silencing of the violaxanthin de-epoxidase gene in the diatom *Phaeodactylum tricorutum* reduces diatoxanthin synthesis and non-photochemical quenching. *PLoS One*, 7(5), e36806.
- Lian, J., Wijffels, R. H., Smidt, H., & Sipkema, D. (2018). The effect of the algal microbiome on industrial production of microalgae. *Microbial biotechnology*, 11(5), 806-818.
- Liu, X., Duan, S., Li, A., Xu, N., Cai, Z., & Hu, Z. (2009). Effects of organic carbon sources on growth, photosynthesis, and respiration of *Phaeodactylum tricorutum*. *Journal of Applied Phycology*, 21(2), 239-246.
- Lohr, M., & Wilhelm, C. (1999). Algae displaying the diadinoxanthin cycle also possess the violaxanthin cycle. *Proceedings of the National Academy of Sciences*, 96(15), 8784-8789.
- Jowers, T. P. (2019) Microalgae-derived fucoxanthin: a powerful composition for liver health. Nutraceutical Business Review. https://nutraceuticalbusinessreview.com/news/article_page/Microalgae-derived_fucoxanthin_a_powerful_composition_for_liver_health/160205 (Consulted at 10/02/2021)
- Juergens, M. T. (2016). *Analysis of carbon and energy fluxes during nitrogen deprivation in Chlamydomonas*. Michigan State University.
- Jungandreas, A., Costa, B. S., Jakob, T., Von Bergen, M., Baumann, S., & Wilhelm, C. (2014). The acclimation of *Phaeodactylum tricorutum* to blue and red light does not influence the photosynthetic light reaction but strongly disturbs the carbon allocation pattern. *PLoS one*, 9(8), e99727.
- Kadono, T., Kira, N., Suzuki, K., Iwata, O., Ohama, T., Okada, S. & Adachi, M. (2015). Effect of an introduced phytoene synthase gene expression on carotenoid biosynthesis in the marine diatom *Phaeodactylum tricorutum*. *Marine drugs*, 13(8), 5334-5357.
- Khoroshyy, P., Bina, D., Gardian, Z., Litvín, R., Alster, J., & Pšenčík, J. (2018). Quenching of chlorophyll triplet states by carotenoids in algal light-harvesting complexes related to fucoxanthin-chlorophyll protein. *Photosynthesis research*, 135(1), 213-225.
- Kosakowska, A., Lewandowska, J., Stoń, J., & Burkiewicz, K. (2004). Qualitative and quantitative composition of pigments in *Phaeodactylum tricorutum* (Bacillariophyceae) stressed by iron. *BioMetals*, 17(1), 45-52.
- Koyande, A. K., Chew, K. W., Rambabu, K., Tao, Y., Chu, D. T., & Show, P. L. (2019). Microalgae: A potential alternative to health supplementation for humans. *Food Science and Human Wellness*, 8(1), 16-24.
- Kraay, G. W., Zapata, M., & Veldhuis, M. J. (1992). SEPARATION OF CHLOROPHYLLS c1c2, AND c3 OF MARINE PHYTOPLANKTON BY REVERSED-PHASE-C18-HIGH-PERFORMANCE LIQUID CHROMATOGRAPHY 1. *Journal of Phycology*, 28(5), 708-712.
- Kromkamp, J. C., & Claquin, P. (2005). Role of the cell cycle in the metabolism of marine microalgae. Suba Rao. Kuczynska, P., Jemiola-Rzeminska, M., & Strzalka, K. (2015). Photosynthetic pigments in diatoms. *Marine drugs*, 13(9), 5847-5881.

- Kuznetsova, V., Chábera, P., Litvín, R., Polívka, T., & Fuciman, M. (2017). Effect of isomerization on excited-state dynamics of carotenoid fucoxanthin. *The Journal of Physical Chemistry B*, 121(17), 4438-4447.
- Maass, D., Arango, J., Wüst, F., Beyer, P., & Welsch, R. (2009). Carotenoid crystal formation in Arabidopsis and carrot roots caused by increased phytoene synthase protein levels. *PLoS one*, 4(7), e6373.
- Maeda, H., Hosokawa, M., Sashima, T., Funayama, K., & Miyashita, K. (2005). Fucoxanthin from edible seaweed, *Undaria pinnatifida*, shows antiobesity effect through UCP1 expression in white adipose tissues. *Biochemical and biophysical research communications*, 332(2), 392-397.
- Marone, M., Mozzetti, S., De Ritis, D., Pierelli, L., & Scambia, G. (2001). Semiquantitative RT-PCR analysis to assess the expression levels of multiple transcripts from the same sample. *Biological procedures online*, 3(1), 19-25.
- Márquez-Rocha, F. J., Palma-Ramírez, D., García-Alamilla, P., López-Hernández, J. F., Santiago-Morales, I. S., & Flores-Vela, A. I. (2019). Microalgae Cultivation for Secondary Metabolite Production. In *Microalgae-From Physiology to Application*. IntechOpen.
- Marques, A.E. & Miranda, J.R. & Batista, Ana & Gouveia, Luísa. (2013). Microalgae biotechnological applications: Nutrition, health and environment. Microalgae: Biotechnology, *Microbiology and Energy*. 1-60.
- McClure, D. D., Luiz, A., Gerber, B., Barton, G. W., & Kavanagh, J. M. (2018). An investigation into the effect of culture conditions on fucoxanthin production using the marine microalgae *Phaeodactylum tricorutum*. *Algal research*, 29, 41-48.
- Meier, S., Tzfadia, O., Vallabhaneni, R., Gehring, C., & Wurtzel, E. T. (2011). A transcriptional analysis of carotenoid, chlorophyll and plastidial isoprenoid biosynthesis genes during development and osmotic stress responses in *Arabidopsis thaliana*. *BMC Systems Biology*, 5(1), 1-19.
- Ministério da Agricultura, Pecuária e Florestas. Decreto-Lei n.º 55/2005, Diário da República n.º 44/2005, Série I-A de 2005-03-03, 1897-1900. <https://data.dre.pt/eli/dec-lei/55/2005/03/03/p/dre/pt/html>
- Mikami, K., & Hosokawa, M. (2013). Biosynthetic pathway and health benefits of fucoxanthin, an algae-specific xanthophyll in brown seaweeds. *International journal of molecular sciences*, 14(7), 13763-13781.
- Novoveská, L., Ross, M. E., Stanley, M. S., Pradelles, R., Wasiolek, V., & Sassi, J. F. (2019). Microalgal carotenoids: A review of production, current markets, regulations, and future direction. *Marine drugs*, 17(11), 640.
- Nymark, M., Valle, K. C., Brembu, T., Hancke, K., Winge, P., Andresen, K. & Bones, A. M. (2009). An integrated analysis of molecular acclimation to high light in the marine diatom *Phaeodactylum tricorutum*. *PLoS one*, 4(11), e7743.
- Nzayisenga, J. C., Farge, X., Groll, S. L., & Sellstedt, A. (2020). Effects of light intensity on growth and lipid production in microalgae grown in wastewater. *Biotechnology for biofuels*, 13(1), 1-8.
- Oryza Oil & Fat Chemical CO., Ltd. (2008). Fucoxanthin: Dietary Ingredient for Prevention of Metabolic Syndrome and Beauty Enhancement. Ver.1.0 SJ
- Pangestuti, R., & Kim, S. K. (2011). Biological activities and health benefit effects of natural pigments derived from marine algae. *Journal of functional foods*, 3(4), 255-266.
- Parjikolaie, B. R., Kloster, L., Bruhn, A., & Bo, M. (2013). Effect of light quality and nitrogen availability on the biomass production and pigment content of *Palmaria palmata* (Rhodophyta). *Chem. Eng.*, 32.
- Pereira, D. C., Trigueiro, T. G., Colepicolo, P., & Marinho-Soriano, E. (2012). Seasonal changes in the pigment composition of natural population of *Gracilaria domingensis* (Gracilariales, Rhodophyta). *Revista Brasileira de Farmacognosia*, 22(4), 874-880.
- Podevin, M., De Francisci, D., Holdt, S. L., & Angelidaki, I. (2015). Effect of nitrogen source and acclimatization on specific growth rates of microalgae determined by a high-throughput in vivo microplate autofluorescence method. *Journal of Applied Phycology*, 27(4), 1415-1423.
- Pulz, O., & Gross, W. (2004). Valuable products from biotechnology of microalgae. *Applied microbiology and biotechnology*, 65(6), 635-648.
- Pujalte, M. J., Lucena, T., Ruvira, M. A., Arahál, D. R., & Macián, M. C. (2014). The family rhodobacteraceae. *Springer*.
- Ragni, M. (2005). Circadian patterns in key physiological processes of the marine diatom *Phaeodactylum tricorutum* (Doctoral dissertation, The Open University).
- Ragni, M., & d'Alcalà, M. R. (2007). Circadian variability in the photobiology of *Phaeodactylum tricorutum*: pigment content. *Journal of plankton research*, 29(2), 141-156.
- Raimbault, P., & Mingazzini, M. (1987). Diurnal variations of intracellular nitrate storage by marine diatoms: effects of nutritional state. *Journal of experimental marine biology and ecology*, 112(3), 217-232.
- Ramanan, R., Kim, B. H., Cho, D. H., Oh, H. M., & Kim, H. S. (2016). Algae-bacteria interactions: evolution, ecology and emerging applications. *Biotechnology advances*, 34(1), 14-29.
- Ramlov, F., Souza, J., Faria, A. V., Maraschin, M., Horta, P. A., & Yokoya, N. S. (2011). Growth and accumulation of carotenoids and nitrogen compounds in *Gracilaria domingensis* (Kütz.) Sonder ex Dickie

- (Gracilariales, Rhodophyta) cultured under different irradiance and nutrient levels. *Revista Brasileira de Farmacognosia*, 21(2), 255-261.
- Ramos, A., Coesel, S., Marques, A., Rodrigues, M., Baumgartner, A., Noronha, J. & Varela, J. (2008). Isolation and characterization of a stress-inducible *Dunaliella salina* LCY- β gene encoding a functional lycopene β -cyclase. *Applied microbiology and biotechnology*, 79(5), 819-828.
- Rebelo, B. A., Farrona, S., Ventura, M. R., & Abranches, R. (2020). Canthaxanthin, a Red-Hot Carotenoid: Applications, Synthesis, and Biosynthetic Evolution. *Plants*, 9(8), 1039.
- Renhoran, M., Noviadri, D., Setyaningsih, I., & Uju, U. (2017). Extraction and Purification of Fucoxanthin from *Sargassum* sp. as Anti-acne. *Jurnal Pengolahan Hasil Perikanan Indonesia*, 20(2), 370-379.
- Rodríguez-Villalón, A., Gas, E., & Rodríguez-Concepción, M. (2009). Phytoene synthase activity controls the biosynthesis of carotenoids and the supply of their metabolic precursors in dark-grown *Arabidopsis* seedlings. *The Plant Journal*, 60(3), 424-435.
- Saini, D. K., Chakdar, H., Pabbi, S., & Shukla, P. (2020). Enhancing production of microalgal biopigments through metabolic and genetic engineering. *Critical reviews in food science and nutrition*, 60(3), 391-405.
- Satomi, Y., & Nishino, H. (2013). Inhibition of the enzyme activity of cytochrome P450 1A1, 1A2 and 3A4 by fucoxanthin, a marine carotenoid. *Oncology letters*, 6(3), 860-864
- Sevilla, J. F., Cerón García, M. C., Sánchez Mirón, A., Belarbi, E. H., Camacho, F. G., & Grima, E. M. (2004). Pilot-plant-scale outdoor mixotrophic cultures of *Phaeodactylum tricorutum* using glycerol in vertical bubble column and airlift photobioreactors: studies in fed-batch mode. *Biotechnology progress*, 20(3), 728-736
- Shimoda, H., Tanaka, J., Shan, S. J., & Maoka, T. (2010). Anti-pigmentary activity of fucoxanthin and its influence on skin mRNA expression of melanogenic molecules. *Journal of Pharmacy and Pharmacology*, 62(9), 1137-1145.
- Siaut, M., Heijde, M., Mangogna, M., Montsant, A., Coesel, S., Allen, A. & Bowler, C. (2007). Molecular toolbox for studying diatom biology in *Phaeodactylum tricorutum*. *Gene*, 406(1-2), 23-35.
- Slominski, A., Kim, T. K., Brożyna, A. A., Janjetovic, Z., Brooks, D. L. P., Schwab, L. P. & Seagroves, T. N. (2014). The role of melanogenesis in regulation of melanoma behavior: Melanogenesis leads to stimulation of HIF-1 α expression and HIF-dependent attendant pathways. *Archives of biochemistry and biophysics*, 563, 79-93.
- Skehan, J. (2019). An investigation into the optimal light conditions for the synthesis of fucoxanthin in *Phaeodactylum tricorutum*. National University of Ireland, Galway.
- Song, Z., Lye, G. J., & Parker, B. M. (2020). Morphological and biochemical changes in *Phaeodactylum tricorutum* triggered by culture media: Implications for industrial exploitation. *Algal Research*, 47, 101822.
- Stolte, W., Kraay, G. W., Noordeloos, A. A., & Riegman, R. (2000). Genetic and physiological variation in pigment composition of *Emiliania huxleyi* (Prymnesiophyceae) and the potential use of its pigment ratios as a quantitative physiological marker. *Journal of Phycology*, 36(3), 529-539.
- Tesson, B., Gaillard, C., & Martin-Jezequel, V. (2009). Insights into the polymorphism of the diatom *Phaeodactylum tricorutum* Bohlin. *De Gruyter*, 52, 104-116.
- The European Parliament and the Council of the European Union (2003). Regulation (EC) No 1831/2003 of the European Parliament and of the Council of 22 September 2003 on additives for use in animal nutrition (Text with EEA relevance). Official Journal of the European Union. <https://eur-lex.europa.eu/legal-content/EN/TXT/?uri=CELEX%3A32003R1831>
- Tran, D., Haven, J., Qiu, W. G., & Polle, J. E. (2009). An update on carotenoid biosynthesis in algae: phylogenetic evidence for the existence of two classes of phytoene synthase. *Planta*, 229(3), 723-729.
- US Food and Drug Administration. FDA 101: Dietary Supplements. <https://www.fda.gov/consumers/consumer-updates/fda-101-dietary-supplements>
- Valle, K. C., Nymark, M., Aamot, I., Hancke, K., Winge, P., Andresen, K., ... & Bones, A. M. (2014). System responses to equal doses of photosynthetically usable radiation of blue, green, and red light in the marine diatom *Phaeodactylum tricorutum*. *PLoS one*, 9(12), e114211.
- Varela, J. C., Pereira, H., Vila, M., & León, R. (2015). Production of carotenoids by microalgae: achievements and challenges. *Photosynthesis research*, 125(3), 423-436.
- Vergara, J. J., Berges, J. A., & Falkowski, P. G. (1998). Diel periodicity of nitrate reductase activity and protein levels in the marine diatom *Thalassiosira weissflogii* (Bacillariophyceae). *Journal of Phycology*, 34(6), 952-961.
- Vidoudez, C., & Pohnert, G. (2012). Comparative metabolomics of the diatom *Skeletonema marinoi* in different growth phases. *Metabolomics*, 8(4), 654-669.
- Villanova, V., Fortunato, A. E., Singh, D., Bo, D. D., Conte, M., Obata, T. & Finazzi, G. (2017). Investigating mixotrophic metabolism in the model diatom *Phaeodactylum tricorutum*. *Philosophical Transactions of the Royal Society B: Biological Sciences*, 372(1728), 20160404.

- Vuong, T. T., Choi, J., Lee, T. S., Um, J. I., Koo, S. Y., Hwang, K. T., & Kim, S. M. (2021). Fucoxanthin biosynthesis has a positive correlation with the specific growth rate in the culture of microalga *Phaeodactylum tricornutum*. *Journal of Applied Phycology*, 1-13.
- Wang, L., Zeng, Y., Liu, Y., Hu, X., Li, S., Wang, Y., & Zhang, Z. (2014). Fucoxanthin induces growth arrest and apoptosis in human bladder cancer T24 cells by up-regulation of p21 and down-regulation of mortalin. *Acta Biochim Biophys Sin*, 46(10), 877-884.
- Wang, L. J., Fan, Y., Parsons, R. L., Hu, G. R., Zhang, P. Y., & Li, F. L. (2018). A rapid method for the determination of fucoxanthin in diatom. *Marine drugs*, 16(1), 33.
- Whitmore, T. J. (2000). The Diatoms: Applications for the Environmental and Earth Sciences. *Journal of Paleolimnology*, 24(2), 241.
- Xia, S., Wang, K., Wan, L., Li, A., Hu, Q., & Zhang, C. (2013). Production, characterization, and antioxidant activity of fucoxanthin from the marine diatom *Odontella aurita*. *Marine drugs*, 11(7), 2667-2681.
- Yacobi, Y. Z. (2012). From Tswett to identified flying objects: A concise history of chlorophyll a use for quantification of phytoplankton. *Israel Journal of Plant Sciences*, 60(1-2), 243-251.
- Yang, R., & Wei, D. (2020). Improving fucoxanthin production in mixotrophic culture of marine diatom *Phaeodactylum tricornutum* by LED Light shift and nitrogen supplementation. *Frontiers in Bioengineering and Biotechnology*, 8, 820.
- Yang, Z. K., Ma, Y. H., Zheng, J. W., Yang, W. D., Liu, J. S., & Li, H. Y. (2014). Proteomics to reveal metabolic network shifts towards lipid accumulation following nitrogen deprivation in the diatom *Phaeodactylum tricornutum*. *Journal of applied phycology*, 26(1), 73-82.
- Zapata, M., Rodríguez, F., & Garrido, J. L. (2000). Separation of chlorophylls and carotenoids from marine phytoplankton: a new HPLC method using a reversed phase C8 column and pyridine-containing mobile phases. *Marine Ecology Progress Series*, 195, 29-45.
- Zaragozá, M. C., López, D., P. Sáiz, M., Poquet, M., Pérez, J., Puig-Parellada, P. & Mitjavila, M. T. (2008). Toxicity and antioxidant activity in vitro and in vivo of two *Fucus vesiculosus* extracts. *Journal of Agricultural and Food Chemistry*, 56(17), 7773-7780.
- Zhang, C. (2018). Biosynthesis of carotenoids and apocarotenoids by microorganisms and their industrial potential. *Progress in carotenoid research*, 85-105.

6. APPENDIX

1. Culture Medium F/2 Supplemented with Silica

1.1. Instant Ocean Salts

- 33.3 g of salt (Aquarium Systems, France) is added to 1 liter of medium.

1.2. Nitrogen and Carbon Sources:

- Sodium Nitrate
- Maintenance of the initial inoculum: Stock solution 1000x concentrated with the final concentration of 1x of 1.1766 mM NaNO₃ (Sigma-Aldrich, USA). Final concentration in the medium, after dilution with 25% inoculum (75% of the f/2+Si medium and 25% of inoculum), is 0.882 mM.
- Experiments with different concentrations of nitrate: Stock Solution with a concentration of 50 mM NaNO₃ (Sigma-Aldrich, USA)

All the concentrations were obtained using the different volumes of the latter stock solution above (0.183, 0.220, 0.441, 0.882, 1.176, 3.528, 7.056, 8.82, 17.64 and 35.28 mM)

Sodium nitrate was dissolved in bidistilled water and autoclaved. The solution was stored at room temperature, in the dark.

- Ammonium Chloride
- 6-well plate assay: Stock Solution with a concentration of 20 mM NH₄Cl

All the concentrations were obtained using the different volumes of the stock solution of 20 mM of ammonium chloride (0.183, 0.441, 0.882, 3.528 and 8.82 mM).

Ammonium chloride was dissolved in bidistilled water and autoclaved. The solution was stored at room temperature, in the dark.

- Urea
- 6-well plate assay: Stock Solution with a concentration of 200 mM CH₄N₂O (GE Healthcare, USA)

All the concentrations were obtained using the different volumes of the latter stock solution above (5, 10, 20, 40 and 80 mM).

Urea was dissolved in bidistilled water and autoclaved. The solution was stored at room temperature, in the dark.

➤ Glycerol

- 6-well plate assay: Stock Solution with a concentration of 200 mM C₃H₈O₃ (Scharlau, Spain)

All the concentrations were obtained using the different volumes of the latter stock solution above (25, 50, 75 and 100 mM).

Glycerol was dissolved in bidistilled water and autoclaved. The solution was stored at room temperature, in the dark.

➤ Glucose

- 6-well plate assay: Stock Solution with a concentration of 100 mM C₆H₁₂O₆ (NZYTech, Portugal)

All the concentrations were obtained using the different volumes of the latter stock solution above (3, 6, 30 and 60 mM).

Glucose was dissolved in bidistilled water and autoclaved. The solution was stored at room temperature, in the dark.

1.3. Monobasic sodium phosphate (x1000)

- 0.036 mM NaH₂PO₄·2H₂O (Sigma-Aldrich, USA)

Monobasic sodium phosphate is dissolved in bidistilled water. The solution is stored at room temperature.

1.4. Trace elements

- 11.71 mM Na₂EDTA (Sigma-Aldrich, USA)
- 13.41 mM FeCl₂·6H₂O (Merck, Germany)
- 0.04 mM CuSO₄·5H₂O (Sigma-Aldrich, USA)
- 0.08 mM ZnSO₄·7H₂O (Merck, Germany)
- 0.04 mM CoCl₂·6H₂O (Sigma-Aldrich, USA)
- 0.91 mM MnCl₂·4H₂O (Sigma-Aldrich, USA)
- 0.001 mM Na₂MoO₄·2H₂O (Sigma-Aldrich, USA)

All trace elements were dissolved in bidistilled water. The solution is stored at room temperature and wrapped in aluminium foil.

1.5. Vitamins

- 0.000369 mM Cyanocobalamin (Sigma-Aldrich, USA)
- 0.297 mM Thiamine HCl (Duchefa Biochemie, Netherlands)

- 0.002 mM Biotin (Sigma-Aldrich, USA)

The vitamins were dissolved in bidistilled water, filtered with 0.2 μm filters (VWR, USA) frozen at $-20\text{ }^{\circ}\text{C}$.

1.6. Sodium metasilicate (x1000)

- 246 mM Sodium Metasilicate (Sigma-Aldrich, USA)

Sodium metasilicate was dissolved in bidistilled water. The solution is stored at room temperature.

To prepare the basal medium (0.882 mM of sodium nitrate) was added 1 mL of each stock solution (except vitamins) to 1 liter to bidistilled water with previously dissolved salt. For all other concentrations, the base medium (salt, phosphate, trace elements and metasilicate) and a 50 mM NaNO_3 stock solution were prepared. For both, the base medium and the NaNO_3 stock solution, the pH was adjusted to 8 with 1 M of hydrochloric acid (HCl). Both were autoclaved. To prepare the media, calculations were made to add NaNO_3 and base media, in order to achieve the desired final concentration of the nitrogen source to be tested. The addition of sodium nitrate to the base medium was done under sterile conditions. The medium with a given concentration of NaNO_3 was prepared in a single container and then distributed to the several Erlenmeyer's with the necessary volume.

For solid medium, 1.2% of bacterial agar (VWR, USA) was added before autoclaving. Finally, 1 mL of filtered vitamin mixture stock solution was added. The medium is stored at room temperature. Solid cultures are plated only for maintenance of cell cultures and not for testing experimental conditions.

2. Formula Calculation - Fucoxanthin

To calculate fucoxanthin concentration, the procedure performed was as follows: From the absorbance values obtained for each wavelength of the samples, the absorbance value of the blank was subtracted (e.g. To "Sample read A445 nm the "Value at A445 nm of ethanol" is subtracted; the same applies to the remaining wavelengths). After subtracting the blank, the absorbance value was multiplied by 2 (optical path). The initial value obtained corresponds to only half of the well, since only 200 μL was added, and the well has a capacity of 400 μL . To obtain the total value of the well, it is necessary to multiply the value obtained by two. After subtraction and multiplication, the values were applied to the equations of the correlation Cuvette vs. Microplate (e.g. the "Sample value read at A445 nm" has been replaced in y, giving the value of x; the same applies to the remaining equations). The value of x obtained for 445, 663 and 750 nm was substituted in the formula. After replacing the values in the formula, the concentration of fucoxanthin in mg/L was obtained.

Note:

Negative values resulting from the calculation of the formula are indicative of concentrations not detectable using this method (below 2 mg/L), in our study conditions.

Real values of the optical density of the culture were given by replacing the y-value in the equation of the correlation line at 750 nm.

3. Agarose Gel Electrophoresis

3.1. TBE 5x Buffer (Tris / Borate / EDTA):

- 448 mM Tris-base (NZYTech, Portugal)
- 448 mM Boric acid (Merck, Germany)
- 1 mM EDTA (pH = 8)

Tris-base and boric acid solutions are prepared in bidistilled water and the EDTA solution is added at the end. The TBE buffer is stored at room temperature.

3.2. Agarose 0.8% and 1,2%

The TBE 5x solution is diluted in bidistilled water to the final concentration of 0.5 x and to which is added agarose (NZYTech, Portugal). Then, the solution is heated in the microwave until the agarose is completely dissolved. Green Safe Premium (MB13201, NZYTech) is added to the dissolved agarose and the solution is placed on a support to solidify for 30 minutes at room temperature.

3.3. Orange G 10x:

- 4.4 mM Orange G (Sigma, USA)
- 30% glycerol

Orange G is dissolved in water and glycerol is added. The solution is stored at 4 °C.

3.4. Running the samples onto a agarose gel

After preparing the solutions, the Orange G dye (10x) is applied to the reaction (1.5 µL for a 10 µL reaction), which is then loaded onto a 0.8% or 1.2% agarose gel in 0.5x TBE, with 0.4 µL of Green Safe previously added (0,4 µL to 35 mL TBE Buffer). A 100V electric field was applied to the gel for 30 or 40 minutes and the results are revealed under UV light, using a DocEZ Gel Documentation System Gel (BioRad, USA).

Table 6.1. Reaction Constituents of the GoTaq Flexi DNA Polymerase (M7805, Promega, USA)

<i>Reagents</i>	<i>Final Concentration</i>	<i>Final Volume 1x reaction</i>
<i>5X Green GoTaq® Flexi Buffer</i>	1x	1,6 µL
<i>MgCl₂ Solution</i>	2 mM	0,64 µL
<i>dNTPs mix (NZYTech)</i>	0,2 mM	0,16 µL
<i>Primer Forward</i>	0,6 mM	0,5 µL
<i>Primer Reverse</i>		
<i>GoTaq® DNA Polymerase</i>	-	0,1 µL
<i>dH₂O</i>	-	Until reach 8 µL

Constituent concentration optimized to experimental conditions tested.

Table 6.2. Reaction Constituents of the ImProm II Reverse Transcriptase System (Promega, USA)

<i>Reagents</i>	<i>Final Concentration</i>	<i>Final Volume 1x reaction</i>
<i>ImProm-II™ 5X Reaction Buffer</i>	1,3x	4 µL
<i>MgCl₂ Solution</i>	3,3 mM	2 µL
<i>dNTPs mix (NZYTech)</i>	0,5 mM	1 µL
<i>ImProm-II™ Reverse Transcriptase</i>	-	1 µL
<i>dH₂O</i>	-	Until reach 15 µL

According to the manufacturer's instructions.